Investigating chromosome pairing in bread wheat using *ASYNAPSIS I*

by

Scott Andrew Boden
B. Science (Hons.), The University of Adelaide

A thesis submitted for the degree of
Doctor of Philosophy

at

The University of Adelaide
Faculty of Sciences
School of Agriculture, Food and Wine
Discipline of Plant and Food Science
Waite Campus

July 2008

Chapter 1 - Literature Review

1.1 - Meiosis

Meiosis is a specialised cellular process that is required for the production of gamete cells that contain half of the genome content of a parental cell. This halving of genome content ensures that, upon fertilisation, the newly formed zygote contains the correct amount of genetic information, equal in quantity to that of the parents' cells. In addition, meiosis provides a means for the genetic variation that exists within a species to be accessed, *via* the processes of recombination and crossing over. Crossing over results in the production of gametes that contain a non-identical allelic combination of genes compared to the parental cells. This process is facilitated by pairing homologous chromosomes to form meiotic specific structures known as bivalents, which are a hallmark of meiosis and distinguish it from the similar process of cellular division known as mitosis. Meiosis is further distinguished from mitosis by the two rounds of chromosome segregation that follow DNA replication, compared to the one round of segregation that occurs in mitosis.

1.1.1 - Stages of meiosis

Historically, meiotic studies have involved cytological analysis of cells by light microscopy to understand key chromosomal events. Through such analysis, the meiotic cycle has been divided into stages representing various changes in chromosome morphology and cellular appearance. The meiotic cycle is preceded by interphase, which involves DNA replication and transcription of many meiotic genes required for successful completion of meiosis. Interphase is then followed by meiosis I and meiosis II, with no DNA replication occurring between the two rounds of chromosome segregation. Both meiosis I and meiosis II each include the stages

of prophase, metaphase, anaphase and telophase, with prophase I representing the most eventful and therefore most intensely studied of the stages.

Figure 1.1 – **Meiotic divisions I and II as observed in *Secale cereale* microsporocytes.** (A) Early zygotene; (B-D) early to late pachytene; (E) diplotene; (F) diakinesis; (G, H) metaphase I; (I, J) anaphase I; (K) telophase I; (L) prophase II; (M) metaphase II; (N) anaphase II; and (O) four haploid pollen mother cells. Scale bar, 5 μm. "Reprinted, with permission, from the *Annual Review of Genetics,* Volume 32 ©1998 by Annual Reviews www.annualreviews.org".

1.1.2 - Prophase I

During the first stage of prophase I, leptotene (Latin *lepto-* = spiral; Latin *tene* = ribbon), individual chromosomes are visible as long thin strands which have commenced condensing; however, alignment of homologous chromosomes is not yet visible. The late G2 phase of interphase and early leptotene are often difficult to distinguish due to the gradual transition between the stages. Nevertheless, during leptotene the chromosome cluster begins to move from a central region within the nucleus towards the nuclear periphery, which in most organisms is followed by formation of a structure known as the telomere bouquet (Bass et al., 1997; Scherthan, 2001). Recruitment of chromosomes to the nuclear periphery is thought to act as a rendezvous site for chromosomes to roughly align with their homologue (Bass, 2003; reviewed in Wilson et al., 2005). The mechanism(s) of homologue recognition is still subject to debate; however, it is recognised that the rough alignment of homologous chromosomes does occur during the transition between leptotene and zygotene (see 1.2.2) (reviewed in Zickler and Kleckner, 1998; Wilson et al., 2005).

Zygotene (Latin *zygo-* = pair) is defined as the stage when the first signs of chromosome synapsis are evident. In most organisms, chromosome synapsis involves double stranded breaks (DSBs) of DNA, associated with recombination, and the intimately involved formation of the synaptonemal complex (SC) (see 1.2.3) (Giroux et al., 1989; Keeney et al., 1997). Synapsis continues in tandem with chromosome condensation into the stage of pachytene.

During pachytene (Greek *packhus* = thick), the chromosomes appear much shorter and thicker compared to earlier prophase stages. This chromosome morphology is reflective of homologous chromosomes achieving complete synapsis, accompanied by entire formation of the SC (von Wettstein et al., 1984). Analysis of the SC by electron microscopy reveals that the SC is a tripartite proteinaceous core that runs along the entire length of chromosomes (Zickler and Kleckner, 1999). In addition to homologous chromosome interactions via the SC, interhomologue interactions via recombination are also evident at this stage. Complete synapsis is coupled by the telomeres moving out of the bouquet to become more uniformly distributed along the nuclear periphery, resulting in individual homologous chromosome pairs becoming identifiable. The distribution of bivalents is closely followed by the transition to diplotene, when bivalents open to reveal the individual sister chromatids.

Diplotene (Latin *diplo* = double) is characterised by disassembly of the SC as well as the gradual and progressive separation of homologues. Individual sister chromatids become visible as desynapsis progresses to a stage where the only physical union joining homologues are chiasmata, which represent crossover sites. Depending on the number of chiasmata joining each homologue pair, bivalents will appear in a number of different conformations. These conformations become clearer as chromosomes adopt a smoother outline through the stage of diakinesis, as chromosomes continue to condense and contract prior to the onset of metaphase I.

1.1.3 - Metaphase I to telophase II

Following diplotene and diakinesis, bivalents are arranged along the metaphase spindle in a bipolar arrangement at metaphase I. In partnership with recombination, independent assortment of one bivalent along the metaphase spindle in relation to the other bivalents ensures that the products of meiosis contain a unique combination of alleles compared to the

parental cells. Also, during metaphase I, an event known as congression occurs, whereby the centromeres of homologues move into the one plane following attachment to the spindle (Khodjakov et al., 1999). This movement facilitates destruction of chiasmata, which previous to this stage are required to hold the homologues together. However, following attachment to the spindle, chiasmata are no longer required, and the separation of homologues at anaphase I now proceeds. This separation results in the homologous chromosomes segregating to opposite poles of the cell via the process of reductional chromosome segregation. Sister chromatid connections at centromeres remain, ensuring that each sister pair will be aligned in a bipolar arrangement on the metaphase II spindle.

The events of telophase I are somewhat species dependent, but usually the separation of homologues at anaphase leads to the dyad stage in which two polar groups of chromosomes form. These two groups then prepare for the second round of segregation by partially decondensing without achieving the full interphase condition.

Metaphase II and anaphase II follow a course similar to that of mitosis, with equational segregation of chromosomes by separation of sister chromatids following arrangement of chromosomes along the metaphase spindle. Late anaphase II/telophase II cells contain the expected four groups of chromatids that represent the four haploid nuclei, which eventually undergo cytokinesis to produce four haploid gametes.

1.2 - Molecular analysis of prophase I

Many of the cytological observations that have been used to define the five sub-stages of prophase I represent the progression of three important meiotic processes: recombination, chromosome pairing and synapsis. These three processes are intimately associated with each other, with all three occurring during early prophase I. Following the alignment of homologous chromosomes during leptotene, the inter-homologue interactions of SC formation

and recombination occur. While recombination is generally recognised to initiate prior to SC formation, it is thought that the SC stabilises interactions between homologous chromosomes following the initial events of recombination to allow for resolution of recombination events into either crossovers or non-crossovers (reviewed in Kleckner, 1996; Borner et al., 2004; Page and Hawley, 2004). Recombination and SC formation have been the subject of extensive molecular analysis, and both have been implicated in the alignment and recognition of homologous chromosomes. These processes have been predominantly characterised using budding yeast as a model organism, but studies in other model organisms indicate that the processes and the proteins involved are well conserved.

1.2.1 - Recombination – from structure to functional analysis

The two roles of meiotic recombination are to generate genetically recombinant progeny and to ensure the accurate segregation of homologous chromosomes during the first meiotic division. Cytologically, recombination is observed as large multi-protein complexes called recombination nodules (RNs) (Zickler and Kleckner, 1998; 1999). These nodules are found closely associated with the SC and are divided into two categories dependent on frequency and size, known as early (ENs) and late recombination nodules (LNs) (reviewed in Anderson and Stack, 2005).

ENs are associated with axial elements of the SC and appear from leptotene until pachytene, after which they detach from the SC (Stack and Anderson, 1986b). ENs are randomly distributed along the SC, displaying no interference, and they are approximately 20 times more abundant than LNs (Stack and Anderson, 1986a). Through the use of immuno-localisation data, Anderson and Stack (2005) have assigned recombination proteins with roles in DSB formation and single end invasion (SEI) of DNA strands as components of ENs. Based on the functions of the proposed EN components and the large numbers of ENs, it is

hypothesised that ENs have roles in searching for DNA homology, chromosome synapsis, and resolving recombination events into crossovers or non-crossovers (Carpenter, 1979; 1987; 1988; Stack and Anderson, 1986a; b; Zickler and Kleckner, 1999; Anderson et al., 2001; Moens et al., 2002). An involvement in the resolution of recombination events into crossovers or non-crossovers is supported by observation that ENs are replaced by LNs at pachytene, whose number is not only much fewer then ENs (1-6 per bivalent) but also reflective of the crossover frequency per bivalent (Stack et al., 1989; Anderson et al., 2003). Unlike ENs, LNs display interference patterns consistent with crossover interference and their location correlates well with chiasmata (Stack et al., 1989; Anderson et al., 2003). These observations, combined with immuno-localisation of proteins with essential roles in DNA mismatch repair strongly indicate LNs represent crossover sites (Moens et al., 2002). The transitional relationship between ENs and LNs is unclear. However, the co-localisation of late EN proteins with LN marker proteins does indicate that a subset of ENs become LNs, most likely representing recombination events which proceed along the crossing over pathway (Anderson and Stack, 2005).

Recombination is initiated during late leptotene and early zygotene by DSBs generated by the topoisomerase protein, SPO11 (Keeney et al., 1997; McKim and Hayashi-Hagihara, 1998; Romanienko and Camerini-Otero, 2000; Grelon et al., 2001). While the decision of whether the break will lead to a crossover or non-crossover event appears to closely follow generation of the breaks, the crossover and non-crossover pathways appear to share a common sequence of events until crossover specific structures form (reviewed in Borner et al., 2004). These common events begin with the breaks being processed by DNA repair proteins RAD50 and MRE11 into a segment of DNA with 3' single stranded tails (Raymond and Kleckner, 1993; Furuse et al., 1998; Moreau et al., 1999). The single stranded DNA then penetrates and displaces a strand of DNA from the non-sister chromatid of its homologue pair with the aid of

the DNA repair protein RAD51, and in many organisms, DMC1 (Bishop, 1994; Heyer, 1994). The strand invasion is observed cytologically as single end invasions, and if the invading strand is sufficiently complementary to the target strand being invaded, then a heteroduplex DNA structure is generated (Hunter and Kleckner, 2001). It is at this stage that the crossover and non-crossover pathways display evidence of separation (Bishop and Zickler, 2004). While the events that lead to a non-crossover event are still unclear, it is known that there is differential timing of the two pathways, with non-crossovers being resolved earlier then crossovers, at the stage when crossover specific structures called double Holliday junctions appear (Allers and Lichten, 2001; Bishop and Zickler, 2004). Double holliday junctions favour crossovers, with the mismatch repair proteins MSH4, MSH5 and MLH1 displaying roles in resolving thsee junctions into crossovers through capture of the second DNA strand, branch migration and ligation (reviewed in Paques and Haber, 1999). Of interest to this project, proteins involved in crossover and non-crossover pathways have been shown to also contribute to the alignment and pairing of homologous chromosomes (Peoples-Holst and Burgess, 2005).

1.2.2 – Alignment and recognition of homologous chromosomes

The juxtaposition and alignment of homologous chromosomes during meiosis is the least well understood process of prophase I. There are many different factors that may contribute to chromosome homology recognition, which include chromosome morphology, chromatin re-modelling, regions of DNA sequence homology, and proteins that interact with chromatin (Hamant et al., 2006). However, as yet the mechanism remains unresolved. This is partially due to the difficulty in establishing whether a loss of bivalent formation in a given mutant is the consequence of defective pairing or synapsis, as deficiency in both processes could equally yield univalents. In addition, it has been difficult to establish a uniform mechanism used by

eukaryotes for chromosome homology recognition, as organisms such as *Drosophila melangastor* and *Caenorhabditis elegans* display unique methods of achieving homologous chromosome alignment (Carpenter, 1975; Goldstein and Slaton, 1982; Orr-Weaver, 1995; Fung et al., 1998; MacQueen et al., 2005).

It has been suggested that various stages of the recombination pathway contribute to homologous chromosome recognition. For example, studies in maize have shown that there is a significant decrease in the number of RAD51 foci from the beginning of zygotene compared to pachytene, and it has been proposed that the high numbers of zygotene foci represent a role for RAD51 in homology searching (Franklin et al., 1999). This has been supported by observations that maize mutants with abnormalities in the distribution and numbers of RAD51 foci during prophase I also display defects in homologous chromosome pairing (Pawlowski et al., 2003; Pawlowski et al., 2004). Similarly, it was shown that the Arabidopsis *asy1* mutant that fails to correctly synapse homologous chromosomes, displays an abrupt decline in DMC1 foci following its initial loading onto chromatin, relative to wild-type (Sanchez-Moran et al., 2007).

Another mechanism that has been suggested to facilitate homologous chromosome alignment is formation of a structure known as the telomere bouquet (reviewed in Zickler and Kleckner, 1998; Harper et al., 2004). The telomere bouquet is formed as the telomeres of each chromosome attach to the nuclear periphery and cluster together during mid-prophase I (Hiraoka, 1952; Dernburg et al., 1995; Zickler and Kleckner, 1998). It is thought that formation of the telomere bouquet may assist homologous chromosome pairing by bringing the chromosomes into close association and increasing the spatial proximity of homologous regions (Moses, 1968; Hamant et al., 2006). Studies in maize support this theory, as the *pam1* (*plural abnormalities in meiosis 1*) mutant that displayed a loss of telomere bouquet formation was also found to have a dramatic reduction in homologous chromosome pairing

(Golubovskaya et al., 2002). Having said this, there is also evidence to show that the telomere bouquet is not an essential requirement for homologous chromosome pairing, and that in a number of cases initial homologue interactions precede telomere bouquet formation (reviewed in Zickler and Kleckner, 1998; Hamant et al., 2006). Hence, while it is likely that the telomere bouquet does contribute to the alignment of homologous chromosomes, the true nature of the relationship between these processes remains to be resolved.

1.2.3 - Synaptonemal Complex – complex in structure and function

The completion of homologous chromosome alignment and pairing is observed cytologically by the formation of a structure known as the synaptonemal complex (SC). The synaptonemal complex is a tripartite protein structure that forms between non-sister chromatids of homologous chromosomes (von Wettstein et al., 1984). Its direct role in homologous chromosome interactions has been difficult to dissect. However, the evolutionary conservation of the structure across a wide range of species indicates that it does have a conserved role during meiosis (reviewed in Kleckner, 1996; Hunter, 2003).

In association with chromosome condensation that occurs through leptotene, sister chromatids become organised along structures known as axial elements. During the early stages of synapsis, the axial elements mature into lateral elements (Rockmill et al., 1995). The lateral elements of non-sister chromatids are linked through recombination-mediated induced DSBs, and become joined through the recruitment and formation of transverse filaments (reviewed in Page and Hawley, 2004). In yeast, correct localisation of transverse filament proteins requires the presence of proteins involved in chromosome condensation, indicating a coordination of chromosome synapsis with the process of chromosome condensation (Klein et al., 1999; Yu and Koshland, 2003). At pachytene, when homologous chromosomes have completely synapsed, the cell contains a complete SC complement (Albini and Jones, 1988).

The complete SC includes the lateral elements and transverse filaments, as well as a dense region at equidistance from each lateral element known as the central element (reviewed in Page and Hawley, 2004). RNs are also found in close association with the central element of the SC (reviewed in Anderson and Stack, 2005). The SC disassembles at diplotene as the chromosomes progress towards metaphase and anaphase, where chiasmata form the sole physical union between non-sister chromatids.

While the role of the SC is still unclear, recent evidence from studies in yeast, mammals and Arabidopsis indicate that formation of the SC and progression of the recombination pathway are intimately related (reviewed in Kleckner, 2006). In addition, it has been shown that the components of the SC contribute to homologue pairing by coupling chromosomes at their centromeres, which is thought to aid the homology searching process (Tsubouchi and Roeder, 2005).

Evidence for a functional relationship between recombination and the SC has been provided in the analysis of yeast mutants with decreased activity of *SPO11* (Henderson and Keeney, 2004). In addition to displaying a decreased ability to generate DSBs, these mutants showed corresponding defects in SC formation (Henderson and Keeney, 2004). It was shown that these defects were caused by a decline in the number of ZIP3 complexes, which are thought to represent sites of SC initiation through their role promoting the recruitment of the transverse filament protein ZIP1 (Agarwal and Roeder, 2000). Further evidence of a relationship between SC formation and recombination has been provided by studies of mutants from *C. elegans*, budding yeast and Arabidopsis that are defective for a component of the central element (MacQueen et al., 2002; Borner et al., 2004; Higgins et al; 2005). All of these SC-component mutants displayed reduced levels of crossover formation, and immuno-localisation studies indicated that the defects were caused by a loss of function in correct SC

nucleation during leptotene and zygotene. Therefore, these results indicate a direct link between DSB initiation and SC formation, especially during the early stages of each process.

In addition to a role in recombination, studies in yeast and Arabidopsis indicate that components of the SC may also facilitate homologous chromosome pairing (Higgins et al., 2005; Tsucouchi and Roeder, 2005). Analysis in yeast showed that the transverse filament protein, ZIP1, is required for the coupling of centromeres during early prophase I, and that homologous chromosomes failed to pair in the absence of ZIP1 (Tsucouchi and Roeder, 2005). Tsucouchi and Roeder (2005) proposed that the role for the coupling was to facilitate homologue pairing by holding chromosomes in close proximity while homology is being assessed. Further support of a role for SC-component proteins in homologous chromosome pairing was provided through analysis of ZYP1 (Arabidopsis homologue of *Sc*ZIP1) deficient Arabidopsis plants, which displayed recombination between non-homologous chromosomes (Higgins et al., 2005). Combined, these results indicate that SC-component proteins may have roles in facilitating pairing of homologous chromosomes.

1.3 - Meiosis in bread wheat – a hexaploid acting as a diploid

Allopolyploidy is an evolutionary process that is highly prevalent within the plant kingdom, with several important crop plants, such as bread and durum wheat, oat, cotton, canola, coffee and tobacco being allopolyploids (Manton, 1950; Stebbins, 1950; 1971; Grant, 1971; Feldman and Levy, 2005). Recent cytological and molecular analysis of other plants, which have previously been considered as diploids, reveals that they may in fact have been allopolyploids which have undergone diploidisation to now exist as paleopolyploids (Shoemaker *et al*, 1996; Gaut and Doebley, 1997; Gomez et al., 1998; Grant et al., 2000; Vision et al., 2000; Gaut, 2001). Such a wide-spread occurrence of this process is reflective of the potential for allopolyploid species to adapt to a wide range of environmental conditions, allowing these

plants to survive in adverse environments when compared to their diploid progenitors (reviewed in Ma and Gustafson, 2005). One of the best models for studies of allopolyploidy has been the hexaploid genome of *Triticum aestivum*, otherwise known as bread wheat.

Hexaploid bread wheat (2n = 6x = 42), sometimes referred to as dinkel, is one of three taxonomic groups within the genus *Triticum* (Schultz, 1913; cited in Feldman and Levy, 2005). The other two groups are comprised of the diploid and tetraploid wheat species. Early cytological analysis of the three groups revealed that the seven chromosome pairs of diploid wheat (genome A) plus seven additional pairs (genome B) are what constitute the 14 chromosome pairs of tetraploid wheat (Kihara, 1919; Sax, 1927). These 14 chromosome pairs plus an additional seven pairs (genome D) make up the 21 pairs found in hexaploid wheat. Studies on the origin of bread wheat have indicated that the genome formed approximately 10000 years ago, through the hybridisation of the D genome progenitor, *T. tauschii* (2n = 2x = 14), and the tetraploid containing the A and B genome, *T. turgidum* (McFadden and Sears, 1946; Feldman, 2001). While it is well recognised that the progenitor of the A genome is *T. urartu* (2n = 2x = 14), the origin of the B genome is still open to conjecture (reviewed in Feldman and Levy, 2005). Morphological, geographical, cytological, genetic, biochemical and molecular evidence does however indicate that the B genome originates from the section *Sitopsis* of the genus *Aegilops*, and more specifically *Ae. speltoides* (Feldman et al., 1995). An important behavioural characteristic of the wheat genome that ensures stabilisation of the hybrid condition is the diploid-like meiotic behaviour, with chromosome pairing occurring exclusively between homologues and not homoeologues.

Cytological diploidisation, or the diploid-like behaviour of allopolyploids, is an example of a revolutionary change which is caused by the allopolyploid condition (Feldman and Levy, 2005). Revolutionary changes occur either immediately after the hybridisation event or within one to several generations, and they are genetic or epigenetic changes that

stabilise the nascent allopolyploid to aid the establishment of the new species (Feldman and Levy, 2005). One of the central dangers to the establishment of the new species is the risk of homoeologous chromosome pairing due to the progenitor genomes usually being closely related, as this pairing would reduce fertility and therefore affect the fitness of the new species. Analysis of synthetic allopolyploids from the *Aegilops* and *Arabidopsis* genera has revealed evidence of homologous chromosome pairing representing a revolutionary change, as exclusive pairing of homologues occurs as early as three generations after their formation (Comai et al., 2003; Cunando et al., 2005). Interestingly, studies in bread wheat have also identified a number of loci that contribute to the exclusive pairing of bivalents, which could represent an evolutionary change adopted by bread wheat to ensure maintenance of homologous chromosome pairing (Riley and Chapman, 1958; Sears and Okamoto, 1958; Wall et al., 1971a; Driscoll 1972, Mello-Sampayo and Canas, 1973; Riley and Chapman, 1975; Sears, 1982). Some of these loci have been termed *Pairing homoeologous* loci (*Ph*), for their ability to suppress interactions between homoeologous chromosomes (Wall et al., 1971b). Two examples of these loci are *Ph1* and *Ph2*, which are located on chromosome arms 5BL and 3DS, respectively (Riley and Chapman, 1958; Sears and Okamoto, 1958; Driscoll, 1972; Sears, 1976).

Of the loci that contribute to the diploid behaviour of meiosis in bread wheat, the *Ph1* locus displays the strongest effect (Sears, 1976; Feldman, 1993; Moore, 2002). Since its discovery, cytological investigations of wheat mutants that lack the *Ph1* locus have shown that there are a number of defects that occur during pre-meiotic interphase and early meiosis that contribute to the homoeologous chromosome pairing observed at metaphase I (Okamoto, 1957; Riley and Chapman, 1958; Sears, 1977; Holm and Wang, 1988). Initial studies showed that synapsis is arrested in *ph1* mutants, to a level of approximately 35-40% of wild-type wheat (Holm and Wang, 1988). In addition, it was shown that multiple axial element

associations that occur during zygotene are not resolved into homologous chromosome pairs in *ph1* mutants like they are in wild-type wheat (Holm and Wang, 1988). Based on these observations, Holm and Wang (1988) proposed that the alignment of homologous chromosomes is effected in *ph1* mutants, which prevents the correction of multiple axial element associations. It is thought that the uncorrected associations are the prelude to the multivalents that are observed at metaphase I in *ph1* mutants (Holm and Wang, 1988). Similarly, it has been shown that *Ph1* is required for the synchronous remodelling of homologous chromosomes that occurs as telomeres cluster together at the telomere bouquet (Prieto et al., 2004; Colas et al., 2008). The absence of *Ph1* causes premature and asynchronous remodelling of homologous chromosomes, which leaves a chromosome just as likely to interact with a related homoeologue as with its true homologue (Martinez-Perez et al., 2001; Prieto et al., 2004; Colas et al., 2008). This has been confirmed by studies showing that *Ph1* regulates the specificity of chromosome interactions at sites of centromeres and telomeres, so that pairing only occurs between homologues (Martinez-Perez et al., 2001; Prieto et al., 2004).

In addition to the cytological investigations of meiosis in *ph1* mutants, genetic studies have been performed to identify the gene(s) responsible for the effect of the *Ph1* locus. The original *Ph1* deletion was defined to span a region of 70 Mb; however, recent studies have reduced the size of this locus to 2.5 Mb (Gill et al., 1993; Roberts et al., 1999; Griffiths et al., 2006). This refined locus was found to contain seven *Cdk*-like genes and a segment of sub-telomeric heterochromatin, with the *Cdk*-like genes shown to be closely related to *Cdk2* of human and mouse (Griffiths et al., 2006; Martinez-Perez and Moore, 2008). Interestingly, studies in mice show that deletion of *Cdk2* causes severe defects in homologous chromosome synapsis, which supports some of the *ph1* mutant phenotypes (Ortega et al., 2003). In addition, it has been shown that the *Cdk*-like genes of the 5B locus suppress the expression of the 5A

and 5D *Cdk*-like loci, which are expressed at higher than normal levels in the absence of *Ph1* (Al Kaff et al., 2007). This analysis supports genetic studies that show *Ph1* has arisen post-polyploidisation, and suggests that a possible role for *Ph1* is to regulate the overall expression of the wheat *Cdk*-like genes which would have been altered following the amalgamation of three genomes to form hexaploid wheat (Griffiths et al., 2006; Al Kaff et al., 2007). Taken together, these studies indicate that by investigating the genes and proteins that are affected by deletion of *Ph1*, it may be possible to understand the mechanism that controls the diploid-like behaviour of bread wheat meiosis.

1.4 - *ASY1* – a gene required for successful chromosome synapsis

Studies using model organisms, such as the budding yeast (*Saccharomyces cerevisiae*), have proven to be influential in understanding the factors and mechanisms regulating key cellular events such as meiosis. As meiosis is an evolutionarily conserved process performed by sexually reproducing organisms, many of the key molecular events identified in budding yeast are shared by higher eukaryotes. However, this has not necessarily meant that the amino acid sequence of proteins involved in these processes is well conserved between yeast and higher eukaryotes. Therefore, it has proven difficult to isolate key meiotic genes and proteins in plants and animals based on sequence homology alone. This has particularly been so for genes that have a role in synapsis of homologous chromosomes (Caryl et al., 2000; Higgins et al., 2005). Nonetheless, due to the apparent conservation of meiotic processes between yeast and higher eukaryotes, studies of yeast meiotic proteins have provided insight into possible roles of the analogous proteins in organisms such as Arabidopsis and rice once these proteins have been identified through alternative means (Osman et al., 2006).

1.4.1 - *ScHOP1*: A gene essential for homologous chromosome pairing in yeast

In 1989, Hollingsworth and Byers identified a yeast gene with roles in SC formation and recombination by screening yeast mutants defective for homologous chromosome pairing during meiosis (Hollingsworth and Byers, 1989). Cytological analysis of the *hop1* mutant revealed that it failed to form a SC and displayed reduced levels of recombination (Hollingsworth and Byers, 1989). Such phenotypes were consistent with the expression of the 2216 bp *ScHOP1* gene, which was restricted to sporulating cells, with the highest levels of transcripts detected during the stages of leptotene to pachytene of prophase I, when SC formation and recombination occur (Hollingsworth et al., 1990). Further evidence for a role in such processes was provided by identification of DNA interacting domains within *Sc*HOP1, as well as immuno-localisation of the protein to sites directly adjacent to the lateral elements of the SC of homologous chromosome pairs (Hollingsworth et al., 1990; Muniyappa et al., 2000; Anuradha and Muniyappa, 2004a; 2004b). It is worth noting at this stage that there is a relatively low degree of sequence identity shared between *Sc*HOP1 and the putative orthologues of interest to this project; from Arabidopsis - *At*ASY1 (17%), rice - *Os*PAIR2 (18%) and *Brassica oleracea* – *Bo*ASY1 (16%). In light of these low overall identical matches within the amino acid sequences, individual domains of *Sc*HOP1 with a known function will be described and compared to the three plant proteins of interest.

*Sc*HOP1 contains two domains which have been described to interact with DNA or chromatin associated DNA structures. The HORMA (Hop1p, Rev7p, MAD2) domain is a DNA interacting domain that is common to *Sc*HOP1 and homologues from plants as well as the nematode, *C. elegans* (*Ce*HIM-3) (Aravind and Koonin, 1998; Zetka et al., 1999; Armstrong et al., 2002; Nonomura et al., 2004). Indeed, it is only the HORMA domain within *Sc*HOP1 that displays noteworthy similarity to *At*ASY1, *Os*PAIR2 and *Bo*ASY1, and hence it

is this domain that has been suggested to be critical for the conserved function of these proteins (Armstrong et al., 2002; Nonomura et al., 2004). This domain is found in proteins that interact directly with chromatin and is proposed to mediate interactions between DNA and proteins involved in DNA repair pathways (Aravind and Koonin, 1998). Recently, it has been shown that the HORMA domain of *Sc*HOP1 contains three S[T/Q] domains that act as targets for phosphorylation by the serine/threonine kinases called *Sc*MEC1 and *Sc*TEL1 (Carballo et al., 2008). Phosphroylation of *Sc*HOP1 by *Sc*TEL1 and *Sc*MEC1 is required to promote recombination between homologues, and it is through demonstration of this that HOP1 was shown to facilitate homologous chromosome pairing (Carballo et al., 2008). *Sc*HOP1 also contains a central zinc finger motif (residues 343-378) that has been shown to bind duplex DNA and promote the synapsis of DNA double helices via the formation of guanine quartets (Hollingsworth et al., 1990; Kironmai et al., 1998; Anuradha and Muniyappa, 2004a; 2004b). The zinc finger motif has not yet been identified in any of the plant homologues.

Immuno-localisation studies and the identification of proteins that interact with *Sc*HOP1 have also provided evidence for involvement in chromosome synapsis (Hollingsworth et al., 1990; Hollingsworth and Ponte, 1997; Woltering et al., 2000). Examination of whole chromosome spreads from meiotic nuclei by electron microscopy following incubation with an anti-*Sc*HOP1 primary antibody and a colloidal gold-conjugated secondary antibody revealed that the protein is closely associated with meiotic chromosomes (Hollingsworth et al., 1990). While it was proposed that *Sc*HOP1 may serve as a component of the SC, comparisons of similar analysis with known SC components from mouse indicates that it is more likely to represent a non-SC component chromatin interacting factor (Hollingsworth et al., 1990; Schalk et al., 1998). The idea of *Sc*HOP1 representing a non-SC protein is further supported by its dissociation from chromosomes at pachytene, when SC formation becomes complete (Smith and Roeder, 1997). Having said this, analysis of protein interactions

involving *Sc*HOP1 supports a role for HOP1 in chromosome synapsis through crossing over and assembly of axial elements (Hollingsworth and Ponte, 1997; Woltering et al., 2000). One such interacting protein is *Sc*RED1, whose interaction with *Sc*HOP1 has been shown to be essential for viable spore production, wild-type levels of recombination and mature SC formation (de los Santos and Hollingsworth, 1999; Woltering et al., 2000). To date, no *Sc*RED1 orthologue has been identified in Arabidopsis, rice, wheat or any other plant. It is difficult to predict whether an analogous protein interaction to *Sc*HOP1 and *Sc*RED1 is occurring in plants, as there is little sequence conservation between the yeast and plant HOP1 homologues beyond the chromatin-interacting HORMA domain (Armstrong et al., 2002; Nonomura et al., 2004). However, the plant proteins *At*ASY1, *Os*PAIR2 and *Bo*ASY1 do contain a C-terminal SWIRM domain, which is not present within *Sc*HOP1 (Armstrong et al., 2002; Nonomura et al., 2004). The SWIRM domain is predicted to mediate specific protein-protein interactions in the assembly of chromatin-protein complexes (Aravind and Iyer, 2002). Thus, it has been proposed that the plant HOP1 homologues may achieve the same end result as *Sc*HOP1 through a series of protein interactions similar to the pathway involving *Sc*HOP1 and *Sc*RED1, albeit through a diverged mechanism (Armstrong et al., 2002).

1.4.2 - *AtASY1*, *BoASY1* and *OsPAIR2*: three genes required for synapsis of homologous chromosomes

In recent years, reverse genetics approaches have been used in Arabidopsis and rice to overcome the difficulty in identifying plant meiotic genes *via* sequence homology with yeast genes. Analysis of Arabidopsis T-DNA insertion lines for plants with reduced fertility and abnormal chromosome behaviour during meiosis led to the identification of a gene termed *ASY1* (*ASYNAPSIS 1)*, which is required for correct synapsis of homologous chromosomes (Ross et al., 1997; Caryl et al., 2000). Plants with a T-DNA disrupted *ASY1* gene display an

absence in synapsed bivalents during pachytene, with unconnected homologues appearing as univalents at diplotene and diakinesis (Ross et al., 1997). This is followed by irregular chromosome distribution at metaphase I, and multiple non-disjunction events caused by equational segregation of chromosomes at anaphase I. Such chromosome behaviour led to a reduction in fertility to approximately 10% of wild-type (Ross et al., 1997; Caryl et al., 2000). Similar analysis resulted in the identification of the rice *ASY1*/*HOP1* homologue, termed *OsPAIR2* (Nonomura et al., 2004). A mutation of *OsPAIR2* caused by insertion of the retrotransposon *Tos17* resulted in the asynapsis of homologous chromosomes with the appearance of multiple univalents at pachytene (Nonomura et al., 2004).

Expression analysis, *in situ* hybridisation and immuno-localisation studies of *AtASY1*, *BoASY1* and *OsPAIR2* have provided further evidence for a role in synapsis of homologous chromosomes. In Arabidopsis, *AtASY1* transcripts are found in meiotic and vegetative tissue; however, western blot analysis displays that protein expression is restricted to cells undergoing meiosis (Caryl et al., 2000; Armstrong et al., 2002) Unlike *AtASY1*, *OsPAIR2* transcripts are only found in meiotic tissue, and not vegetative tissue (Nonomura et al., 2004). Support for a role in chromosome synapsis by *Os*PAIR2 was shown by *in situ* hybridisation, where *OsPAIR2* expression was specifically enhanced in male and female meiocytes, but not in those at pre-meiotic S-phase or in pollen maturation stages (Nonomura et al., 2004). Furthermore, immuno-fluorescence microscopy of pollen mother cells (PMCs) that had been immunised with antibodies against *At*ASY1, *Bo*ASY1 and *Os*PAIR2, revealed that the proteins localise to chromatin associated with axial elements of chromosomes from leptotene until pachytene, and then begin to disassociate from the chromatin at diplotene (Armstrong et al., 2002; Nonomura et al., 2006). More specific localisation by electron microscopy of chromosome spreads incubated with a gold-conjugated secondary antibody strongly indicated that *At*ASY1, *Bo*ASY1 and *OsPAIR2* are proteins that associate with chromatin of SC

structures, rather than forming an integral component of the SC (Armstrong et al., 2002; Nonomura et al., 2006).

Recent analysis of recombination and SC structure formation in Arabidopsis *asy1* lines has provided evidence for *At*ASY1 promoting interactions between homologous chromosomes by facilitating DMC-dependent interhomologue recombination (Sanchez-Moran et al., 2007). It was shown that 1.39 crossovers per nucleus occur in Arabidopsis *asy1* lines, and that these crossovers are dependent on DMC1 (Ross et al., 1997; Sanchez-Moran et al., 2001; Sanchez-Moran et al., 2007). Furthermore, it was shown that these crossovers only occur in sub-telomeric regions of the chromosomes, which are thought to be facilitated by formation of the telomere bouquet that brings homologous chromosomes into close proximity (Ross et al., 1997; Sanchez-Moran et al., 2007). Based on this analysis, Sanchez-Moran et al. (2007) proposed that *At*ASY1 may function in "reeling-in" the homologous partner to each chromosome, so that DMC-mediated interactions can equally occur along the entire length of the chromosome.

1.5 – RNA interference

As discussed in 1.4.2, the identification of *AtASY1* and *OsPAIR2* emanated from reverse genetics approaches that used gene disruption events to generate a mutant phenotype (Ross et al., 1997; Nonomura et al., 2004). This approach is commonly used to investigate the function of a given gene, especially in Arabidopsis, with most of our current knowledge about plant meiosis genes having emerged from gene disruption mutants that display reduced fertility (Mercier and Grelon, 2008). However, in the analysis of *ZYP1* in Arabidopsis, it was necessary to use RNA interference (RNAi) to produce a mutant phenotype due to the presence of two functionally redundant homologues of the gene being present in the Arabidopsis genome (Higgins et al., 2005).

RNA interference is a broad term used to describe a gene silencing mechanism that is common to many eukaryotes, which is frequently used to investigate the function of a gene by reducing or silencing its endogenous expression (Novina and Sharp, 2004). The basic mechanism of RNAi is well conserved amongst eukaryotes, and begins with the cleavage of a double stranded RNA (dsRNA) molecule into short 21-26 nucleotide RNA molecules, which are known as short interfering RNAs (siRNAs) and microRNAs (miRNAs) (Hannon, 2002; Novina and Sharp; 2004). Cleavage of the dsRNA is performed by an enzyme called Dicer, which contains three RNAse III domains (Bernstein et al., 2001). The two strands of the siRNAs are then separated from each other, and the antisense strand, which is complementary to the target gene, is incorporated into the nucleotide-protein complex called RISC ((RNA induced silencing complex) (Hammond et al., 2000; Martinez et al., 2002; Gregory et al., 2005). The antisense sequence then guides the RISC complex to the target mRNA sequence, which is then catalyses the cleavage of the target mRNA (Zamore et al., 2000; Gregory et al., 2005). Thus, the expression of an endogenous gene is reduced or silenced through degradation of the mRNA transcripts produced by the gene of interest. In addition to this process, it has been shown that there are a number of other silencing mechanisms that are involved in RNAi. For example, the RNA silencing pathway is amplified in plants, nematodes and fungi by the action of RNA-dependent RNA polymerases, which pairs up with the antisense strand of the siRNA to catalyse the amplification of new long dsRNAs (Cogoni and Macino, 1999; Dalmay et al., 2000; Sijen et al., 2001). These new dsRNAs can then feed back into the RNAi mechanism described above for further degradation of mRNA molecules. Furthermore, it has been shown that RNAi in plants can inhibit transcription of the gene of interest *via* DNA and histone methylation (Wassenegger et al., 1994; Mette et al., 2000; Thomas et al., 2001; Zilberman et al., 2003).

Importantly to this study, RNAi represents a logical tool for reducing or silencing the expression of the gene of interest in hexaploid wheat. By selecting a sequence that is complementary to all three copies of a gene in the bread wheat genome, RNAi is likely to negate the compensatory effect that the homoeologous copies of a gene can have when one copy is deleted.

1.6 – Rationale of current study

As described by Riley and Chapman in 1958 with the discovery of *Ph1*, identification of the mechanisms that control homologous chromosome pairing in bread wheat would have "both theoretical and practical" implications. Firstly, studies in bread wheat, which contains three closely related genomes, may help to identify the proteins that are involved in homology searching during prophase I in a way that is not possible in diploid organisms. In addition, by understanding the mechanisms that suppress homoeologous chromosome interactions, it may be possible to manipulate this process so that homoeologous chromosomes can interact in inter-specific hybrids, which would in turn facilitate the introduction of alien genes into wheat chromosomes by normal recombination.

In association with these broader objectives, the principal aim of this project is to investigate the role of *ASY1* during meiosis in bread wheat, with special consideration for a function in chromosome pairing and/or synapsis. It is proposed that the thorough investigation of *ASY1* and its encoded protein will complement the large amount of cytological information that is available regarding bread wheat meiosis.

This investigation will begin by isolating the bread wheat homologue of *ASY1* (*TaASY1*) and analysing the expression profile of this gene a in range of tissue types. The localisation of ASY1 during prophase I will then be investigated to determine whether ASY1 is temporally and spatially associated with structures that are involved with chromosome

interactions during prophase I. In addition, the role for ASY1 in wheat and plant meiosis will be further examined by analysing the effect that reduced levels of *TaASY1* transcripts has on chromosome interactions during meiosis in bread wheat. This analysis will be complemented by investigating the expression and localisation of *TaASY1* during meiosis in the well documented bread wheat mutant, *ph1b*. Therefore, the three novel aspects of research that will be addressed in this project, which include: 1) Isolating and characterising the first gene and protein from bread wheat that has a direct role in chromosome pairing and synapsis; 2) Further understanding the role for ASY1 in plant meiosis, to dissect its function in chromosome pairing and/or synapsis; 3) Identifying whether ASY1 is a chromatin interacting protein whose function is affected by deletion of the *Ph1* locus.

Chapter 2 - Genetic and transcriptional analyses of *TaASY1*

2.1 – Introduction

While extensive research has been conducted on many meiotic genes in yeast, it has only been in the past decade that investigative research in higher eukaryotes such as Arabidopsis has commenced (Klimyuk and Jones, 1997; Doutriaux et al., 1998; Caryl et al., 2000; Armstrong et al., 2002; Higgins et al., 2004; 2005; Chen et al., 2005; Mercier et al., 2005). This was largely due to the arrival of two key resources; one being the generation of transfer DNA (T-DNA) insertion mutants in Arabidopsis and rice, and the second being the vast amount of genetic information available from many genome sequencing projects that were being completed. One gene isolated through a screen of Arabidopsis mutants displaying reduced fertility was *ASYNAPSIS 1* (*ASY1*) (Ross et al., 1997; Caryl et al., 2000). The reduced fertility in the *asy1* mutant was a result of defects that occurred during meiosis, including aberrant synapsis of homologous chromosomes that culminated in abnormal chromosome distributions during anaphase I and later stages (Ross et al., 1997). The *ASY1* gene displayed some sequence similarity to a critical meiotic gene in yeast, *HOP1*, which when deleted displayed a similar phenotype to that of *asy1* mutants (Hollingsworth and Byers, 1989; Hollingsworth et al., 1990). More recently, a null mutant from rice, *pair2*, was identified through similar screening techniques (Nonomura et al., 2004). The gene, *PAIR2*, is a homologue of *ASY1* and *HOP1*, thus showing that in a plant context, this asynaptic gene appears to be conserved across both dicotyledons and monocotyledons.

Occurring concurrently with the *ASY1* Arabidopsis research was a study using comparative genetics to identify genes that resided within a pairing homoeologous locus of bread wheat, *Ph2*. The *Ph2* locus is a region of approximately 80 Mbp on chromosome 3D

that is deleted in the bread wheat mutant, *ph2a* (Sutton et al., 2003). Through this approach, an expressed sequence tag (EST) was identified that displayed sequence similarity to *AtASY1*, which was used to isolate a full length sequence for the *ASY1* homologue in bread wheat, *TaASY1* (Chand, 2004). Chand (2004) performed complementation experiments to determine if transformation of *TaASY1* into the yeast *hop1* mutant could restore wild-type fertility levels. With those results inconclusive, it remained to be investigated whether the wheat ASY1 protein performed the same function as HOP1 does in yeast.

This chapter details all of the genetic analysis that has since been performed on *TaASY1*, which includes confirmation of the *TaASY1* cDNA and genomic sequence, as well as the *Ta*ASY1 amino acid sequence. In addition, the genome location of *TaASY1* was determined and 2.35 kb of *TaASY1* promoter sequence was obtained. This was followed by transcript expression analysis, which was performed as an initial investigation to determine whether *TaASY1* is a key meiotic gene in bread wheat as its orthologues are in other species.

2.2 – Materials and methods

2.2.1 – Plant growth conditions

Hexaploid wheat plants including wild-type (*Triticum aestivum* cv. Chinese Spring), nullisomic-tetrasomic (NT) derivatives (courtesy of Professor Adam J. Lukaszewski, University of California, Riverside, U.S.A.) and a series of 5AL deletion lines (courtesy of Professor Takashi Endo, NBRP, Kyoto University, Japan) were grown under a 14 h photoperiod in a temperature controlled glasshouse with a minimum air temperature of 15°C and a maximum temperature of 23°C (Waite Campus, Adelaide, South Australia).

2.2.2 – Staging meiotic material

Immature spikes were collected from wild-type hexaploid wheat with the distance between the flag leaf and the last leaf (stage 9 of the Feekes scale) used as an indicator to determine the stage of meiosis within the most mature spikelet. The progression of meiosis represented by this distance varied from one season to the next. Spikes were removed from plants, placed in small Petri dishes (containing a small amount of water) in preparation for dissection. Under a Leica MZ 6 stereo dissecting microscope (Leica Microsystems, New South Wales, Australia) three anthers of a primary floret from a given spikelet were removed using a scalpel (# 22, Livingstone, New South Wales, Australia), fine forceps (Proscitech, Queensland, Australia) and a needle (BD PrecisionGlide, 25 gauge, BD Biosciences, U.S.A.). One of these anthers was placed on a glass microscope slide (Livingstone) and stained with 10 μL of 2% (w/v) aceto-carmine solution for 5 min at room temperature. The anther was then cut in half longitudinally and a cover slip was placed on top of the sample. The slide was then placed in between Whatman paper and thumb pressure was applied to release the pollen mother cells (PMCs) from the anther sac. PMCs were then viewed under a Leica DM1000 compound microscope (Leica Microsystems) to determine their stage-wise progression through meiosis (Bennett et al., 1971; 1973; 1979).

Upon determining the stage, anthers were then collected in one of two ways. For experiments where a definitive and exact stage within meiosis was required, the remaining two anthers from the staged floret were placed into liquid nitrogen. With many florets being dissected through the course of these experiments, identical stages were eventually pooled under liquid nitrogen. For general experimentation that required anthers containing PMCs undergoing prophase I, the entire spike was collected and placed into liquid nitrogen.

2.2.3 – Isolation of *TaASY1* cDNA

2.2.3.1 – RNA isolation and gel electrophoresis

Unless otherwise stated, RNA for the tissue series and meiotic stage expression analysis of *TaASY1* was collected from young leaf (3 weeks old), mature leaf (8 weeks old), root tips, whole seedlings and from anthers that had been classed into one of the following groups of meiotic stages; pre-meiosis, leptotene to pachytene, diplotene to anaphase I, telophase I to telophase II, immature pollen and mature anthers.

Tissue was frozen in liquid nitrogen and ground to a powder using a pre-chilled sterilised mortar and pestle. Ground tissue (approximately 150 mg) was then mixed with 1.5 mL of Trizol reagent (Invitrogen, Victoria, Australia) and RNA was extracted following the manufacturer's recommendations. The extracted RNA was re-suspended in 50 µL of double autoclaved 10 mM Tris (pH 7.5), with concentration determined by measuring absorbance at 260 nm and quality assessed by gel electrophoresis using an ethidium bromide-stained denaturing agarose gel (1.5%, w/v), visualised under UV light. RNA was stored at -80°C until required.

2.2.3.2 – cDNA synthesis

Prior to cDNA synthesis, total RNA was treated with DNase I using the TURBO-DNA free kit, according to manufacturer's instructions (Ambion, Victoria, Australia). Synthesis of cDNA was performed using SuperScript III (Invitrogen), according to the manufacturer's instructions. Total RNA (1 µg) was used in a final reaction volume of 25 µL for the first strand cDNA synthesis.

2.2.3.3 – Isolation of full-length *TaASY1* open reading frame

Prior to commencing this project, a near full-length *TaASY1* cDNA clone had been obtained by inverse PCR (performed by Elise Tucker, reported in Boden et al., 2007). An accurate high fidelity clone of *TaASY1* was amplified using high fidelity DNA Polymerase and primers that were designed based on inverse PCR sequence results. The PCR mixture contained 10X High Fidelity Buffer (5 µL); dNTPs (10 mM, 1 µL); $MgSO_4$ (50 mM, 2 µL); primer *TaASY1F* (5' ATGGTGATGGCTCAGAAGACG 3'; 10 µM, 1 µL); primer *TaASY1R* (5' TGAACTAGGACTTCTGGCGC 3'; 10 µM, 1 µL); Chinese Spring meiotic cDNA (0.5 µL); Platinum *Taq* DNA Polymerase High Fidelity (Invitrogen) (0.25 µL, 5 U μL^{-1}) and milli-Q water (39.25 µL). The cycling conditions comprised a denaturation step at 94°C for 2 min, followed by 35 cycles of 96°C for 30 sec, 48°C for 30 sec, 68°C for 2 min, and a final extension at 68°C for 10 min. PCR products were then separated by gel electrophoresis (1.5% agarose, w/v) and visualised using ethidium bromide.

2.2.3.4 – Cloning of PCR products

2.2.3.4.1 – Purification of DNA from agarose gels

DNA fragments that had been electrophoresed in agarose gels and which were required for cloning were excised using a scalpel blade with the aid of UV light following ethidium bromide staining. The fragments were purified using the Invitrogen PureLink Quick Gel Extraction Kit, according to the manufacturer's instructions.

2.2.3.4.2 – DNA ligation

Purified *TaASY1* PCR fragments were ligated into the pGEM-T Easy vector system according to the manufacturer's instructions (Promega, New South Wales, Australia). Typically, ligation

reactions were incubated at room temperature for 2 h, followed by incubation at 4°C overnight to maximise ligation efficiency.

2.2.3.4.3 – Bacteria transformation and colony PCR

Ligation reactions were transformed into competent *Escherichia coli* DH5α cells by heat shock treatment according to the manufacturer's instructions (Promega).

Transformed competent cells were spread onto Luria Bertani (LB)/agar plates containing ampicillin (100 μg μL^{-1}) as a selective agent. In addition, 5-bromo-4-chloro-3-indolyl β-D-galactopyranoside (X-Gal, 40 μL of 20 mg mL^{-1}) and isopropyl β-D-1-thiogalactopyranoside (IPTG, 100 μL of 100 μM) were added to each plate for selection of positive colonies based on blue/white colour selection. Plates were incubated at 37°C overnight.

Single bacterial colonies were isolated the following day using a sterilised tip and placed into a PCR tube. The tip was subsequently placed into a 5 mL culture of LB broth containing 100 μg mL^{-1} ampicillin for overnight colony growth at 37°C with constant shaking (200 rpm). PCR reaction mixture (20 μL) was then added to the inoculated PCR tube, which contained 10X PCR Buffer (2 μL); $MgCl_2$ (50 mM, 0.8 μL); dNTPs (1.25 mM, 3.2 μL); primer T7 (5' TAATACGACTCACTATAGGG 3'; 10 μM, 1 μL); primer SP6 (5' ATTTAGGTGACACTATAGAA 3'; 10 μM, 1 μL), *Taq* polymerase (1.25 U, Invitrogen) and mill-Q water (11.75 μL).

The 5 mL cultures grown overnight were used for DNA plasmid mini-preparations and for generating glycerol cultures of colonies for long term storage at -80°C. DNA plasmid mini-preparations were performed using the Invitrogen PureLink Quick Plasmid Miniprep Kit, according to the manufacturer's instructions. The plasmid DNA was eluted in 50 μL of elution buffer (Invitrogen) and stored at -20°C. Glycerol cultures were prepared by combining 500 μL

of 50% glycerol with 500 µL LB/ampicillin culture, which were snap frozen using liquid nitrogen and stored at -80°C.

2.2.3.5 – Sequencing of *TaASY1* clones

All capillary separations were performed by the Institute of Medical and Veterinary Sciences (IMVS), Adelaide, Australia, using a 3700 capillary sequencer (Applied Biosystems, New South Wales, Australia). Sequencing reactions were performed in 10 µL reaction volumes using Big-Dye Terminator 3 reagent (Applied Biosystems). Each reaction comprised 1.5 µL of 5X Big-Dye buffer, 0.5 µL of Big-Dye Terminator 3 reagent, 1 µM of the appropriate sequencing primer and 0.2-0.5 µg of plasmid DNA, with the reaction volume increased to 10 µL using sterile milli-Q water. Thermal cycling parameters for the sequencing reaction were 96°C for 30 sec followed by 25 cycles of 96°C for 10 sec, 50°C for 5 sec and 60°C for 4 min. To precipitate and purify the PCR products, 75% isopropanol (40 µL) was added to the sample, which was then incubated at room temperature in the dark for 20 min. The DNA was then pelleted by centrifugation at 13000 x *g* for 20 min. The supernatant was discarded and replaced with 200 µL of 75% isopropanol followed by centrifugation at 13000 x *g* for 5 min. The wash was then carefully removed by pipette and the pellet was air-dried (in the dark) before being submitted for capillary separation. Chromatograms were analysed and assembled using the Contig Express module of Vector NTI software (Invitrogen).

2.2.4 – *TaASY1* genome location

2.2.4.1 – DNA isolation

Genomic DNA was isolated from young leaf tissue of *Triticum aestivum* (cv. Chinese Spring) using a standard protocol outlined below. Young leaf tissue (150 – 500 mg) was chilled using liquid nitrogen and ground into powder using a pre-cooled sterilised mortar and pestle. The

tissue was then placed into a 2 mL tube containing 700 µL of DNA extraction buffer (1% (w/v) sarkosyl, 100 mM Tris-HCl, 100 mM NaCl, 10 mM EDTA, 2% (w/v) PVPP, (pH 8.5) and vortexed for 5 sec. Phenol/chloroform/isoamyl alcohol (25:24:1 v/v) (700 µL) was then added to the samples, which were mixed using a multiple tube vortex machine, for 20 min. Silica gel matrix (500 µL) was then added to the inside of the lid in each tube, which was followed by centrifugation at 900 x *g* for 10 min. The upper aqueous layer was then transferred to a fresh tube and another 600 µL of phenol/chloroform/isoamyl alcohol (25:24:1 v/v) was added. The tubes were mixed again on the multiple tube vortex machine for 10 min, before being centrifuged at 900 x *g* for 5 min. The upper aqueous layer was then transferred to a fresh tube, into which 60 µL of 3 M sodium acetate (pH 4.8) and 600 µL of isopropanol were added. The DNA was then allowed to precipitate for 5 min at room temperature with constant rotation on a rotating daisy wheel. Following centrifugation at 6000 x *g* for 5 min, the supernatant was removed and replaced with 1 mL of 70 % ethanol to wash the DNA. The ethanol was then removed and the sample was air-dried for 20 min. The DNA was re-suspended in 50 µL of R40 (40 µg mL^{-1} RNase A in 1 x TE) at 4°C overnight, and then stored at -20°C. Quantification of the DNA was performed by measuring absorbance at 260 nm using a UV spectrophotometer.

2.2.4.2 – Identifying genome location

2.2.4.2.1 – Southern blot analysis

Southern blot hybridisation was performed to determine the chromosome location of *TaASY1*. This experiment was performed using membranes on which was immobilised genomic DNA from nullisomic-tetrasomic Chinese Spring wheat plants (kindly donated by Margie Pallotta, ACPFG, Australia). Genomic DNA had been digested with *Eco*RV, *Dra*I, *Bam*HI or *Xba*I.

Initially, membranes were incubated overnight in a hybridisation bottle with hybridisation solution (1.5 X HSB (0.9 M NaCl, 30 mM PIPES, 7.5 mM Na_2EDTA, pH 6.8) 30% Denhardt's III (0.6% BSA, 0.6% Ficoll 400 (Sigma-Aldrich, Australia), 0.6% PVP, 3% sodium dodecyl sulphate (SDS)), 7.5% dextran sulphate, 400 µg/mL salmon sperm DNA) at 65°C with constant rotation. The full-length cDNA clone from section 2.2.3.3 was used as template (~50 ng, 3µL) for the synthesis of the labelled probe. The template was combined with 9mer random primer mix (10 µM, 3 µL) and milli-Q water (6µL), denatured at 100°C for 10 min and immediately placed on ice for 5 min to maintain the single stranded conformation of the DNA. Oligo buffer (12.5 µL) was then added, in addition to Klenow polymerase (1 µL, GIBCO BRL, Australia) and radioactive ^{32}P (α-dCTP, Amersham, Australia) (10 mCi mL^{-1}, 4 µL). The synthesis reaction was incubated at 37°C for at least 60 min. The probe was then purified using the Machery-Nagel PCR purification kit according to the manufacturer's instructions (Machery-Nagel, Düren, Germany). The labelled probe was eluted using milli-Q (50 µL) water before being denatured in boiling water for 10 min and subsequently incubated on ice for 5 min, after which it was added to the hybridisation bottle and incubated with the membrane overnight at 65°C with constant rotation.

The following day, membranes were washed with a series of washes until the appropriate level of radioactivity was achieved for exposure to X-Ray film. Washes began with 2X standard saline citrate SSC (0.3 M NaCl, 0.03 M sodium citrate, pH 7.0), 0.1% SDS (w/v) and proceeded through to 1X SSC, 0.1% SDS (w/v), 0.5X SSC, 0.1% SDS (w/v) and 0.2X SSC, 0.1% SDS (w/v) depending on the level of activity that was present. The first wash was performed in the hybridisation bottle, while subsequent washes were performed in an incubation tray. All washes were performed at 65°C for 20 min.

Post washing, the membrane was sealed in a plastic sleeve, and placed into a X-Ray cassette with intensifying screens along with X-Ray film (Fuji HR-G-30 or Kodak Biomax).

The cassette was then stored at -80°C for an appropriate number of days determined by the radioactivity level detected on the membrane before being developed using an AGFA CP1000 Developer (Victoria, Australia).

2.2.4.2.2 – Mutant PCR analysis

PCR analysis of Chinese Spring mutants containing varying deletions of chromosome 5AL was performed to identify the location of *TaASY1* (only group 5 mutants were screened, after having identified through Southern analysis that this is where *TaASY1* resided). Eight mutants analysed were: n5AL.4-1, n5AL.12-1, n5AL14-1, n5AL14-3, n5AL14-4, n5AL14-5 and n5AL.19-5, with each mutant containing varying deletions (fraction length - FL) of 5AL, as detailed on the National BioResources Project database (courtesy of Professor Takashi Endo, Kyoto University) (Endo and Gill, 1996). Genome specific primers were designed for the A genome based on genomic DNA sequence comparisons of *TaASY1* amplified from the three nullisomic-tetrasomic lines of chromosome group 5 (TGS1AS; 5' CCACGCTCATCTTGTCATCATCA 3', TGS2S; 5' GTTATCGACAGCTGCCATCCTAGA 3'). The mutants were screened for presence or absence of the A genome specific fragment using a PCR solution that contained 10X PCR buffer (Invitrogen, 2 µL), $MgCl_2$ (50 mM, 0.8 µL), dNTPs (1.25 mM, 3.2 µL), TGS1AS (10 µM, 0.5 µL), TGS2S (10 µM, 0.5 µL), Platinum *Taq* DNA polymerase (Invitrogen, 5 U μL^{-1}, 0.25 µL) and milli-Q water (11.75 µL). Genomic DNA (50 ng, 1 µL) was used as template for the reactions. The cycling conditions included a denaturation step at 94°C for 2 min, followed by 35 cycles of 96°C for 30 sec, 55°C for 30 sec, 72°C for 1 min, and a final extension at 72°C for 10 min. PCR products were then separated by gel electrophoresis (1.5% agarose, w/v) and visualised using ethidium bromide.

2.2.5 – *TaASY1* genomic DNA and native promoter isolation

2.2.5.1 – Genomic clone isolation and sequencing

Initially, the intron/exon boundaries of the *AtASY1* and *OsPAIR2* genomic sequences were determined through the use of GenSCAN software accessed via the Massachusetts Institute of Technology's website (http://genes.mit.edu/GENSCAN.html) and the TIGR Rice Genome Annotation website (http://www.tigr.org/tdb/e2k1/osa1/), respectively. From this analysis, the sites within the *TaASY1* cDNA sequence where introns were expected to be present in the *TaASY1* genomic DNA clone were predicted. Based on these predictions, primers were designed using *TaASY1* cDNA sequence that flanked the expected intron sites (a summary of the primers used are given in Table 2.1). These primers were used in PCRs containing Chinese Spring genomic DNA as template to amplify clones of *TaASY1* genomic DNA that contained both exon and intron DNA. The PCR solution contained 10X PCR buffer (Invitrogen, 2 µL), $MgCl_2$ (50 mM, 0.8 µL), dNTPs (1.25 mM, 3.2 µL), genomic DNA (50 ng, 1 µL), Platinum *Taq* DNA polymerase (Invitrogen, 5 U μL^{-1}, 0.25 µL) and milli-Q water (11.75 µL), along with 0.25 µM of the appropriate primers. Typically, the PCR cycle conditions included denaturation at 94°C for 2 min, followed by 35 cycles of 96°C for 30 sec, annealing at the appropriate temperature (see Table 2.1) for 30 sec, extension at 72°C for the appropriate time (see Table 2.1), followed by a final extension at 72°C for 10 min.

Table 2.1 – The list of primers used to isolate the *TaASY1* genomic DNA sequence. The black numbers in parentheses represent the primer's T_m as designated by the manufacturer, and the red numbers in parentheses represent the annealing temperature used in the PCR.

Region	Sense Sequence (T_m) (Annealing Temperature)	Anti-sense Sequence (T_m) (Annealing Temperature)	Product size
Exon 1-3	CCACGCGCGCACACAACACA (66°C) (64°C)	GCAATCCGGAGCAAATTCCT (60°C) (64°C)	2.2 kb
Exon 2-3	GCTTGCTTGCTCGGTTCCATTTG (62°C) (62°C)	CCAACCAATAATCCTGCAATGTATTTG (59°C) (62°C)	1.0 kb
Exon 3-9	GGTGTCTATGATGCCTTACAAAAG (52°C) (52°C)	CTTGCTATTGACATTCCCCAC (51°C) (52°C)	1.6 kb
Exon 10-Intron 14	GCTAATGATGCTAACAGTGATGATGAC (55°C) (58°C)	GTGGACTAACACTATAAAGAAATCG (48°C) (58°C)	0.8 kb
Exon 7- 17	CGCTAGTTTCACTTATGAGGACCTTG (57°C) (58°C)	CCATCAAGCTTGCCCTGAAG (62°C) (58°C)	1.9 kb
Exon 16-Intron 20	GGAAGAGGTTGCCATGCACAAT (58°C) (58°C)	CCAAACCCAATGTGACAGAGGTAAG (58°C) (58°C)	1.2 kb
Exon 16-22	GGAAGAGGTTGCCATGCACAAT (58°C) (58°C)	GTTGCGCCGAGGCTCCTTGC (68°C) (58°C)	1.8 kb

2.2.5.2 – Native promoter isolation

2.2.5.2.1 – Production of genome walking libraries

This technique was adapted from the protocol outlined in the Clontech Universal GenomeWalker Kit (Clontech, U.S.A., Scientifix, Australia). Genomic DNA from *Triticum aestivum* was isolated as described in 2.2.4.1, and then digested using five blunt end cutting enzymes: *Dra*I; *Eco*RV; *Pvu*II; *Sca*I and *Stu*I, as per the instructions provided within the GenomeWalker Kit (Clontech, U.S.A.). The digested DNA was then purified using phenol/chloroform/isoamyl alcohol (25:24:1) and chloroform/isoamyl alcohol (24:1) as per 2.2.3.3. The DNA was then precipitated by the addition of 0.1 volume 3 M sodium acetate (pH 4.8), 20 µg of glycogen (Ambion, Victoria, Australia) and 2 volumes of ice-cold 95% ethanol. The samples were then centrifuged at 13000 x *g* for 10 min at 4°C. The DNA pellet was

washed with ice-cold 80% ethanol, before being air-dried and then resuspended in 20 µL of TE,(pH 7.5).

An adapter sequence termed GenomeWalker Adapter (Universal GenomeWalker Kit, Clontech, U.S.A.) was ligated onto the digested genomic DNA by combining genomic DNA (4 µL), the GenomeWalker Adapter (25 µM, 1.9 µL), 10X ligation buffer (1.6 µL) and T4 DNA ligase (3 U) in a reaction volume of 16 µL. Tubes were incubated overnight at 16°C and then at 70°C the following day for 5 min to cease the reaction. TE (1X, pH 7.4) (72 µL) was then added to each reaction tube and the libraries were stored at -20°C.

2.2.5.2.2 – PCR based genome walking

Amplification of promoter fragments was performed by two successive rounds of PCR, termed primary and secondary (nested), which both used Elongase components (Invitrogen). Primary PCR solutions contained Elongase buffer A (4 µL), Elongase buffer B (6 µL), dNTPs (10 mM, 1 µL), Elongase enzyme mix (1 U, 1 µL) and 1 µL of the respective genome walking library. In addition (and in each case), the forward primer for each primary PCR was Adapter primer 1 (AP1, 10 µM, 1 µL), with various reverse primers used that were specific to *TaASY1* (10 µM, 1 µL) (Table 2.2). The reaction volume was made up to 50 µL with milli-Q water. Thermal cycle conditions for the primary PCRs were as follows; denaturation at 94°C for 2 min, followed by 35 cycles of 94°C for 30 sec, 68°C for 3 min, and a final extension at 68°C for 10 min. Products from the primary PCRs were then diluted 2-fold for use in the secondary PCR.

The secondary PCR was a near replicate of the primary PCR, with primers being the major difference. The PCR solution contained Elongase buffer A (4 µL), Elongase buffer B (6 µL), dNTPs (10 mM, 1 µL), Elongase enzyme mix (1 U, 1 µL) and 3 µL of the respective diluted primary PCR product. In addition, the forward primer for each reaction was Adapter

primer 2 (AP2, 10 µM, 1 µL), with various gene specific nested primers used as the reverse primers (10 µM, 1 µL) (Table 2.2). The thermal cycling conditions were identical to those used for the primary PCR. The entire secondary PCR product was separated using a 1.5% agarose gel and visualised by ethidium bromide staining. Bands of interest were then gel-excised and purified using the Invitrogen PureLink Quick Gel Extraction Kit, according to the manufacturer's instructions.

Table 2.2 – List of primers used during genome walking experiments to isolate the *TaASY1* promoter. Primers with sequence shown in blue represent primer pairs that were used during the first round of genome walking, while primers with sequence shown in black represent primer pairs used during the second round.

Genomic Library	Primary Primer	Secondary Primer	Product size(s)
*Dra*I	CTGAGCCATCATCACCTGCATCCACC	CCTGCATCCACCGGAGAAGAGCGAC	0.33 kb
*Pvu*II	CTGAGCCATCATCACCTGCATCCACC	CCTGCATCCACCGGAGAAGAGCGAC	0.32 kb
*Eco*RV	GACAAGAAGACACGGGAGGGGTTCAC	CACTTGTGACAGCTGGAAAGTCTCGCTC	0.4 kb, 1.5 kb
*Sca*I	GACAAGAAGACACGGGAGGGGTTCAC	CACTTGTGACAGCTGGAAAGTCTCGCTC	2 kb
*Stu*I	CAGCCCCGAGGCGTGGACAAGAAG	GTGGACAAGAAGACACGGGAGGGGTT	1 kb

2.2.5.2.3 – Cloning and sequencing of genome walking fragments

Ligation of fragments into the pGEM T-Easy vector (Promega) and subsequent transformation into *E. coli* was performed as outlined in 2.2.3.4.2 and 2.2.3.4.3.

2.2.5.2.4 – Confirmation of promoter specificity to *TaASY1*

Given that the complete *TaASY1* promoter sequence was isolated through two rounds of genome walking, PCR was performed to confirm that sequence isolated through the second round remained specific to *TaASY1*. Confirmation utilised various forward primers complementary to sequence of promoter fragments amplified from unique genome walking

reactions in conjunction with reverse primers that were complementary to *TaASY1* gene sequence (primer combinations are outlined in Table 2.3).

PCR solutions contained Elongase buffer A (4 µL), Elongase buffer B (6 µL), dNTPs (10 mM, 1 µL), Elongase enzyme mix (1 U, 1 µL), forward primer (10 µM, 1µL), reverse primer (10 µM, 1 µL), Chinese Spring genomic DNA (50 ng μL^{-1}, 1 µL) and milli-Q water (up to 50 µL). PCR cycling parameters were denaturation at 94°C for 2 min, followed by 35 cycles of 94°C for 30 sec, 30 sec at the respective annealing temperatures for each primer combination, 72°C for 2 min and 30 sec, with a final extension step at 72°C for 10 min. PCR products were separated by gel electrophoresis using 1.5% (w/v) agarose gels and visualised by ethidium bromide staining.

Table 2.3 – List of primers used to confirm that the obtained promoter sequence was specific to *TaASY1*. The black numbers in parentheses represent the primer's T_m as designated by the manufacturer, and the red numbers in parentheses represent the annealing temperature used in the PCR. Reactions that involved amplification of a fragment that included a region of *TaASY1* gene sequence are designated with two asterisks, while reactions that involved confirming fragments isolated from separate rounds of genome walking overlapped with each other are designated with a single asterisk.

Fragment to confirm	**Forward primer (T_m) (Annealing Temperature)**	**Reverse primer (T_m) (Annealing Temperature)**	**Expected product size**
*Pvu*II and *Stu*I **	GGAACCAACAGAAGTCCCGTAAA (56°C) (57°C)	GCAGGAGGAAATCTGGACCGA (58°C) (57°C)	0.92 kb
*Pvu*II and *Stu*I *	GGAACCAACAGAAGTCCCGTAAA (56°C) (57°C)	ACTCACCATTTTGCCGCCCT (62°C) (57°C)	0.63 kb
*Pvu*II **	GTGTCTTCTTGTCCACGCCTCG (58°C) (57°C)	GCAGGAGGAAATCTGGACCGA (58°C) (57°C)	0.46 kb
*Dra*I and *Sca*I *	GAGTTCATCTCTGCCTCATTGGTATTG (58°C) (58°C)	AGGGGTTCACCTTTTCACTTGTG (56°C) (58°C)	1.86 kb
*Dra*I and *Eco*RV *	AGCAAACCGTATGGTAATAAAACCG (57°C) (57°C)	AGGGGTTCACCTTTTCACTTGTG (56°C) (57°C)	0.79 kb
*Dra*I and *Sca*I **	GAGTTCATCTCTGCCTCATTGGTATTG (58°C) (58°C)	TCAGGAACCGCAGGAGGAAA (62°C) (58°C)	2.34 kb

*Dra*I and *Eco*RV **	AGCAAACCGTATGGTAATAAAACCG (57°C) (58°C)	TCAGGAACCGCAGGAGGAAA (62°C) (58°C)	1.27 kb
*Dra*I **	CTCCACAATTCAAACAGAGCGAGA (57°C) (57°C)	TCAGGAACCGCAGGAGGAAA (62°C) (57°C)	0.54 kb

2.2.6 – Sequence analysis

Chromatogram files containing sequence data were uploaded into the ContigExpress program (Invitrogen, Vector NTI Advance 10, Australia) for analysis. Initially, all unnecessary sequence information including plasmid DNA sequence or adapter sequence was removed and an assembly of the files with expected overlapping sequence information was compiled. Following generation of a consensus sequence, data was uploaded into the Vector NTI 10 program (Invitrogen, Vector NTI Advance 10), whereby analysis of open reading frames (ORFs), predicted amino acid sequences and general nucleotide sequence analysis was performed. For *TaASY1* cDNA and deduced amino acid sequences, database searches were performed using BLAST (Basic Local Alignment and Search Tool) software (BLASTn, BLASTp, tBLASTn, tBLASTx and cdart) accessed via the National Centre for Biotechnology Information website to identify homologous nucleotide and amino acid sequences, as well as to determine conserved protein motifs contained within the *Ta*ASY1 protein sequence.

Consensus sequences for the *TaASY1* promoter as well as the *TaASY1* genomic DNA clone were generated through multiple rounds of cloning and sequence PCR analysis. For both of these experiments, primers for successive rounds of PCR were designed using the Vector NTI 10 program (Invitrogen, Vector NTI Advance 10) and further analysed using NetPrimer (http://www.premierbiosoft.com/netprimer/netprlaunch/netprlaunch.html) software for optimal probability of PCR success. Sequence data from successive PCRs were assembled into their respective groups using ContigExpress software (Invitrogen, Vector NTI Advance 10) to

determine regions of overlapping sequence, from which consensus sequences were generated. Consensus sequences of the promoter and genomic clone were uploaded into the Vector NTI 10 software (Invitrogen, Vector NTI Advance 10). The *TaASY1* promoter consensus sequence was analysed using the PLACE (Plant Cis-Acting Regulatory DNA Elements, http://www.dna.affrc.go.jp/PLACE/) database to identify *cis*-elements within the sequence. The *TaASY1* promoter sequence was also screened against the BLAST nucleotide (BLASTn) database to confirm that the amplified sequence was not just that of a neighbouring gene. Furthermore, the *TaASY1* genomic DNA sequence was compared to the genomic DNA sequence of *AtASY1* and *OsPAIR2* to confirm the expected intron/exon boundaries.

To determine *TaASY1* cDNA sequence that is specific to one of the three bread wheat genomes, multiple cDNA clones amplified from Chinese Spring plants nullisomic-tetrasomic for chromosome group 5 were compared to each other using AlignX software (Invitrogen, Vector NTI Advance 10). Through these comparisons, single nucleotide polymorphisms (SNPs) that existed between *TaASY1* clones from the three bread wheat genomes were identified. From this analysis, primers were designed using Vector NTI 10 (Invitrogen, Vector NTI Advance 10) and NetPrimer software to specifically isolate a clone from one of the three genomes.

2.2.7 – *TaASY1* transcriptional analysis

2.2.7.1 – RNA isolation and gel electrophoresis

Total RNA was extracted as per 2.2.3.1 from the tissue samples detailed in that section. RNA quality was assessed by gel electrophoresis and quantification performed by measuring absorbance at 260 and 280 nm.

2.2.7.2 – Northern blot analysis

Northern blot analysis was performed by Elise Tucker. Procedures for this experimentation have been reported in Boden et al., (2007).

2.2.7.3 – Microarray analysis

Microarray analysis was performed as reported by Crismani et al., (2006).

2.2.7.4 – Quantitative real time PCR (Q-PCR) analysis

Individual cDNA synthesis reactions were performed for each of the seven staged anthers (PM, LP, DA, TT, T, IP and MAN) using the same RNA that was hybridized to the wheat GeneChip® (Crismani et al., 2006). RNA (1 μg) was used as template for the cDNA synthesis reaction with Superscript III RNaseH- Reverse Transcriptase (Invitrogen) according to the manufacturer's instruction. A *TaASY1* cDNA fragment (159 bp) was amplified using primers QPCR-ASY1F (5' AGGACTCCCACAAGCAATCG 3') and QPCR-ASY1R (5' ACCTGCTGGAGGATCGGCTC 3') as described in Crismani et al., (2006). The fragment was then purified and used to prepare a dilution series covering seven orders of magnitude from a 10^9 copies/μL stock solution as detailed by Burton and colleagues (Burton et al., 2004). Three replicates of each of the seven standard concentrations were included in the Q-PCR experiment together with a minimum of three no template controls. Q-PCR experiments were assembled by a liquid handling robot, a CAS-1200 robot (Corbett Life Sciences, New South Wales, Australia). Three replicate PCRs for each of the cDNA samples were included in every run. Two μL of the cDNA solution or the diluted standard or water was used in a reaction containing 5 μL of IQ SYBR Green PCR reagent (Bio-Rad Laboratories, California, USA), 1.2 μL each of the forward and reverse primers at 4 μM, 0.3 μL of 10X SYBR Green in water and 0.3 μL of water. Reactions were performed in a RG 3000 Rotor-Gene Real Time Thermal

Cycler (Corbett Life Sciences) as follows; 3 min at 95°C followed by 45 cycles of 1 sec at 95°C, 1 sec at 55°C, 30 sec at 72°C and 15 sec at the optimal acquisition temperature (83°C). A melt curve was obtained from the product at the end of the amplification by heating from 70°C to 99°C. Using the Rotor-Gene V6 software (Corbett Life Sciences) the optimal cycle threshold (CT) was determined from the dilution series, with the raw expression data derived. The mean expression level and standard deviation of each set of three replicates for each cDNA was calculated.

Normalisation of the raw data was performed using the strategy of Burton and colleagues (Burton et al., 2004) for this time course and tissue series experiment. Four control genes were assessed (*actin*, *GAPdH*, *EFA* and *cyclophilin*). The three best control genes from this set were selected, with normalisation factors calculated using the geNorm program (Vandesompele et al., 2002). While these genes have been used in other studies the consistency of expression of the best three control genes in this case was found to be poor. A measure of consistency was obtained by examining the M value (Vandesompele et al., 2002), where a high M value indicates that a control gene has a very disparate expression with respect to other control genes. The highest M value from the best three genes in these experiments was approximately 1.7. Based on other time course experiments conducted, we anticipated M values of approximately 1.0. To address this concern, further control genes were tested until an acceptable M value was obtained. Two additional genes were selected from the microarray data (Ta.9657.1.S1_at and Ta.28350.1.S1_a_at) in addition to the four 'standard' Q-PCR control genes mentioned above. Selection criteria imposed for identifying the additional control transcripts were based on a similar strategy to Czechowski and colleagues (Czechowski et al., 2005). After re-calculating the normalization factors using geNorm, the highest M value from the three best control genes was reduced to 0.68 and the raw expression

values for *TaASY1* in the cDNA sample were divided by the normalization factor for that cDNA to produce the normalized expression data.

2.2.8 – Digital image capture

All ethidium bromide stained gel images were obtained using a UVP BioDoc-It^{TM} Imaging System (UVP, California, USA).

2.3 – Results

2.3.1 – Isolation and analysis of the *TaASY1* cDNA clone

Prior to commencing this project, a cDNA clone of *TaASY1* with a single open reading frame had been isolated from a bread wheat cDNA library (Chand, 2004). However, upon comparing sequences that had been isolated in separate reactions, differences greater than those expected between homoeologous sequences from the three bread wheat genomes were identified. As these clones would be forming the basis of all experimental work reported in this dissertation, amplification using a high fidelity *Taq* polymerase was conducted which resulted in a cDNA clone with an open reading frame of 1764 bp (see Appendix A – Figure 1). Sequence analysis and database searches using this sequence as a query revealed a high level of sequence similarity with *OsPAIR2* (84.1%), *AtASY1* (62.8%) and *BoASY1* (63.7%) (Nonomura et al., 2004; Caryl et al., 2000; Armstrong et al., 2002). While it has been reported that in both rice and Arabidopsis there are additional copies of *OsPAIR2* and *AtASY1* located within the respective genomes (Caryl et al., 2000; Nonomura et al., 2004), which are reported to be pseudo-genes, *TaASY1* and its homoeologues are not suspected to be part of a greater gene family.

The deduced amino acid sequence of *Ta*ASY1 is 588 amino acids and has a predicted molecular weight of 66.3 kDa and a pI of 5.36. BLASTp, tBLASTn, and tBLASTx searches

produced very similar results to the nucleotide based searches, revealing that *Ta*ASY1 shares sequence similarity with *Os*PAIR2, *At*ASY1, *Bo*ASY1, as well as the well characterised *Sc*HOP1 (Hollingsworth and Byers, 1990). The tBLASTx also displayed similarity between *TaASY1* and uncharacterised cDNA clones from *Vitis vinifera* (wine grape), *Physcomitrella patens* (moss) and animals such as humans, mouse, cow and chicken (Table 2.4). Domain searches revealed that *Ta*ASY1 contains a HORMA (HOP1, REV7, MAD2) domain from position 13 to 223, which is also present in the characterised homologues mentioned above (Nonomura et al., 2004; Caryl et al., 2000; Armstrong et al., 2002; Hollingsworth and Byers, 1990) (Figure 2.1). The level of identity shared between the HORMA domain of *Ta*ASY1 and homologues of other species is significantly higher then the identity values of whole protein sequences (Table 2.5). Interestingly, neither the complete amino acid sequence nor the HORMA domain sequence of *Ta*ASY1 displayed any notable sequence similarity with the HORMA domain containing protein from *Caenorhabditis elegans*, *Ce*HIM-3 (Zetka et al., 1999).

Table 2.4 - Percentage identity between the full-length *Ta*ASY1 protein sequence and characterised asynaptic proteins from other species. *Ta = Triticum aestivum*; *Os = Oryza sativa*; *At = Arabidopsis thaliana*; *Bo = Brassica oleracea*; *Sc = Saccharomyces cerevisiae*.

	***Ta*ASY1**
***Ta*ASY1**	100
***Os*PAIR2**	80
***At*ASY1**	53.8
***Bo*ASY1**	51.2
***Sc*HOP1**	16.5

Table 2.5 - Percentage identity between the HORMA domain sequence of *Ta*ASY1 and the HORMA domains of characterised asynaptic proteins from other species. *Ta = Triticum aestivum*; *Os = Oryza sativa*; *At = Arabidopsis thaliana*; *Bo = Brassica oleracea*; *Sc = Saccharomyces cerevisiae*.

	*Ta*ASY1
***Ta*ASY1**	100
***Os*PAIR2**	95.7
***At*ASY1**	78.7
***Bo*ASY1**	76.3
***Sc*HOP1**	24.5

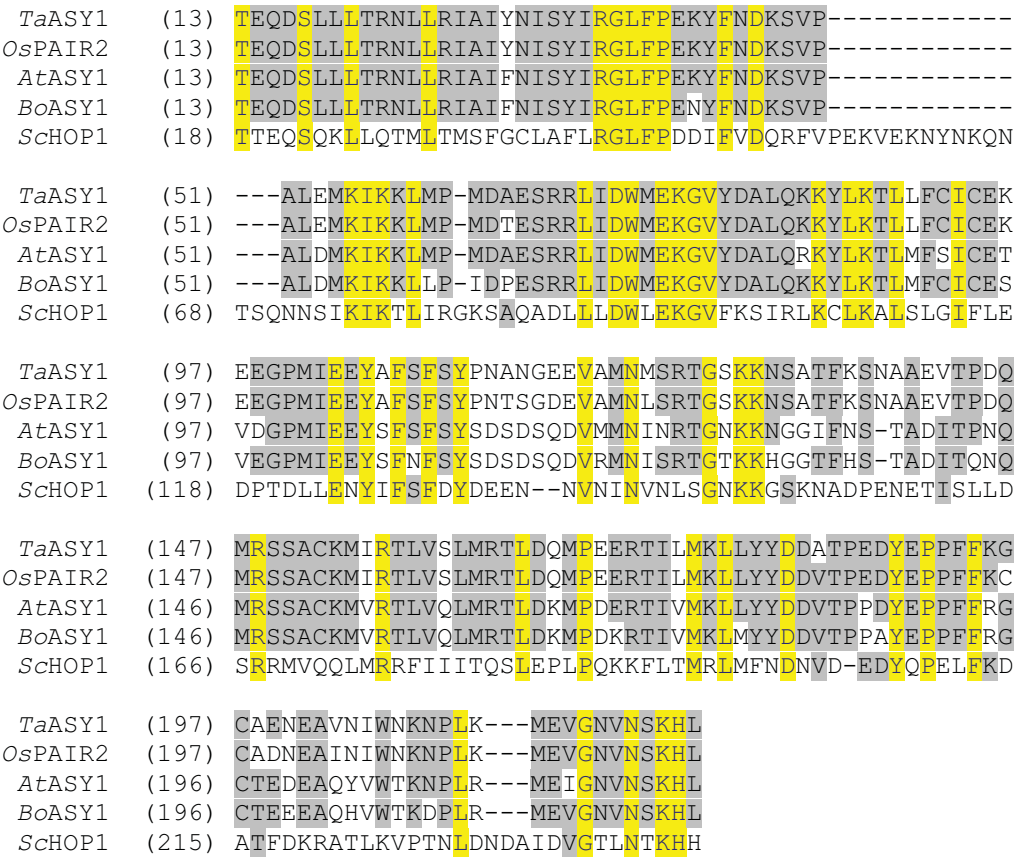

Figure 2.1 - Alignment and comparison of the deduced amino acid sequences within the HORMA domains of *Ta*ASY1, *Os*PAIR2 (*O. sativa*), *At*ASY1 (*A. thaliana*), *Bo*ASY1 (*B. oleracea*) and *Sc*HOP1 (*S. cerevisiae*). Amino acid residues conserved across all sequences are highlighted in blue with a yellow background, while residues conserved across most sequences are highlighted in black with a grey background.

2.3.2 – *TaASY1* gene structure and genome location

Comparison of *TaASY1* cDNA sequence to *OsPAIR2* genomic DNA sequence was used with *OsPAIR2* gene structure information to predict the sites within the *TaASY1* cDNA sequence where introns had been spliced during the transcription process (Nonomura et al., 2004). The complete gDNA sequence for *TaASY1* was 6924 bp in length with a direct comparison between the *OsPAIR2* genomic DNA sequence suggesting that these two genes share a very similar gene structure. *TaASY1* is composed of 22 exons and 21 introns as are *OsPAIR2* and *AtASY1* (Nonomura et al., 2004; Caryl et al., 2000) (Figure 2.2). In addition to the conserved number of exons and introns between *TaASY1*, *OsPAIR2* and *AtASY1*, there is also a level of conservation regarding the length of intron sequence amongst the three genes, including a three base pair exon (exon 1) and a 2001 bp intron between exon 2 and 3 (see Appendix A – Figure 2).

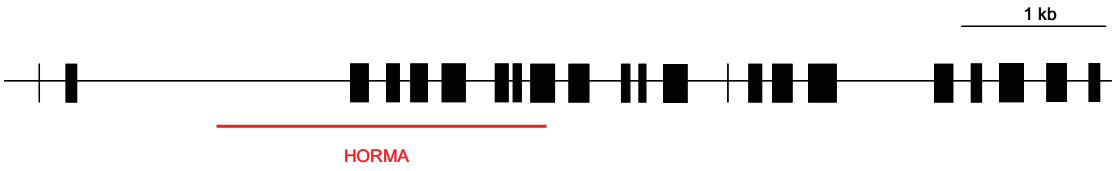

Figure 2.2 - Schematic representation of *TaASY1* gene structure with exons (indicated by solid boxes) and introns (solid lines). The red line indicates the position of the HORMA domain within *TaASY1*, and the scale bar indicates a relative length of 1 Kb.

Southern hybridisation revealed that *TaASY1* was located on chromosome Group 5 (Lanes 14 to 16, Figure 2.3) with a single copy on each of the three bread wheat genomes A, B and D. Interestingly, *OsPAIR2* has previously been mapped to rice chromosome 9 (Nonomura et al., 2004) which shows conservation of gene order with wheat chromosome Group 5. The genetic location of *TaASY1* was further refined using a PCR based approach. Firstly, the specificity of primers TGS1AS and TGS2S for the A genome was confirmed by amplification

of a 446 bp fragment from wild-type Chinese Spring and nullisomic-tetrasomic Chinese Spring lines null 5B-T5D and null 5D-T5A, but not from null 5A-T5D (Figure 2.4A). Bread wheat deletion lines that contained varying distal deletions of 5A long arm (5AL) were then screened using these primers (courtesy of Professor Takashi Endo, National Bioresource Project, Kyoto University, Japan). The fragment specific for the A genome was amplified in a deletion line that contained 0.35 fraction length (FL – see 2.2.4.2.2) of the 5AL (5AL 19-5, Professor Takashi Endo, *personal communication*), but not in a line that contained 0.32 FL of 5AL (5AL 12-1, NBRP, Kyoto University, Japan) (Figure 2.4B). This suggests that *TaASY1* is located in a region between 0.32 and 0.35 FL on 5AL when measured from the centromere.

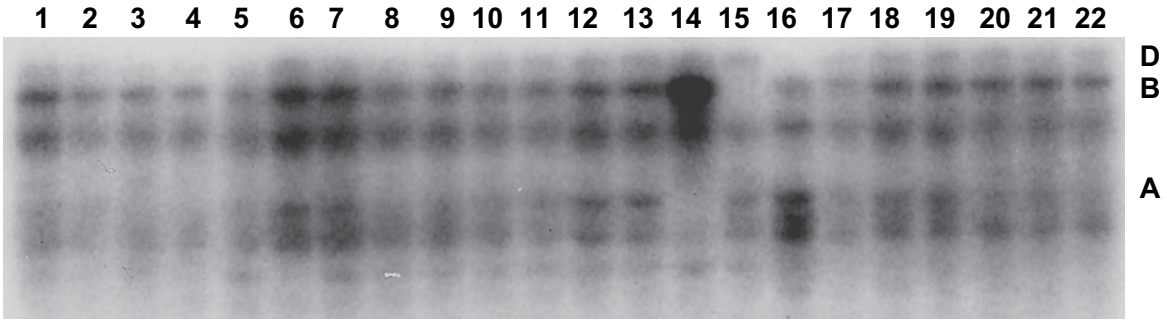

Figure 2.3 - Chromosomal location of *TaASY1* determined by Southern blot. Digested DNA from each of the 21 nullisomic-tetrasomic Chinese Spring wheat lines is shown, representing all 7 chromosome groups, which was hybridised with a full-length *TaASY1* clone labelled with α-^{32}P dCTP. Absence of hybridisation signals in lanes 14-16, which contains DNA of lines null 5A-T5B, null 5B-T5D, null 5D-T5A respectively, illustrated that *TaASY1* was located on chromosome group 5.

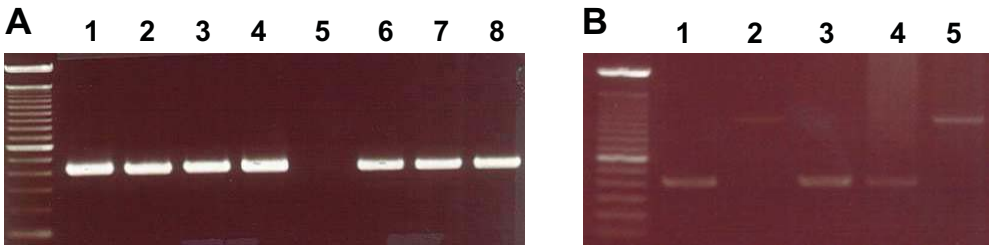

Figure 2.4 - Chromosomal location of *TaASY1* determined by PCR Analysis. (A) Amplification of a 446 bp *TaASY1* gene fragment from genomic DNA of nullisomic-tetrasomic Chinese Spring lines with lanes 1 and 5 null 5A-T5D, lanes 2 and 6 null 5B-T5D, lanes 3 and 7 null 5D-T5A, and lanes 4 and 8 wild-type Chinese Spring. Lanes 1 to 4 contain products amplified using non-genome specific primers, and lanes 5 to 8 contain products amplified using 'A genome' specific primers, as illustrated by the lack of product in lane 5 (null 5A-T5D). (B) Amplification of the 446 bp fragment from genomic DNA of wild-type and various bread wheat deletion lines (lane 1 wild-type Chinese Spring, lane 2 null 5A-T5D, lane 3 mutant 5AL 4-1 (0.55 FL), lane 4 5AL 19-5 (0.35 FL) and lane 5 5AL 12-1 (0.32 FL)). The DNA molecular weight marker in (A) and (B) is a 100 bp ladder (Invitrogen, Japan).

2.3.3 – Isolation of the native *TaASY1* promoter sequence

The native *TaASY1* promoter was isolated *via* two successive rounds of genome walking. The first round produced two fragments, including a 354 bp fragment that was amplified from the library containing *Dra*I digested DNA, and a second fragment of 316 bp amplified from a library containing *Pvu*II digested DNA (Figure 2.5A, 2.6A). Preliminary sequence analysis showed that these two fragments contained some overlapping regions. Sequence data derived from these two fragments were used to design two separate primer pairs for a second round of walking. The primers that were designed using sequence of the fragment amplified from the *Dra*I library produced multiple fragments in the second round of genome walking, with two fragments amplified from the *Eco*RV library (363 bp and 1672 bp) and one fragment from the *Sca*I library (2068 bp) (Figure 2.5B, 2.6B). Preliminary sequence analysis showed that these three fragments contained overlapping regions of sequence. Primers designed using sequence of the fragment amplified from the *Pvu*II library in the first walk produced a single fragment in the second walk from the *Stu*I library that was 921 bp in size (Figure 2.5C).

Sequence analysis of the fragments amplified using primers based on the original *Dra*I library fragment revealed that they did not match in sequence with the fragment amplified using primers based on the original *Pvu*II library fragment. This result suggested that one group of fragments was not specific to *TaASY1*. Subsequent PCR involving reverse primers that were complementary to known *TaASY1* sequence showed that it was only the fragment amplified from the *Dra*I library (and subsequent downstream amplified fragments) that were specific to *TaASY1*, as it was only in these reactions that products of the expected size were amplified (Figure 2.5D and Table 2.3). Compilation of the fragments within this group using ContigExpress software revealed that a promoter sequence of 2355 bp in length had been obtained (see Appendix A – Figure 3). A schematic summarising the genome walking is shown in Figure 2.6.

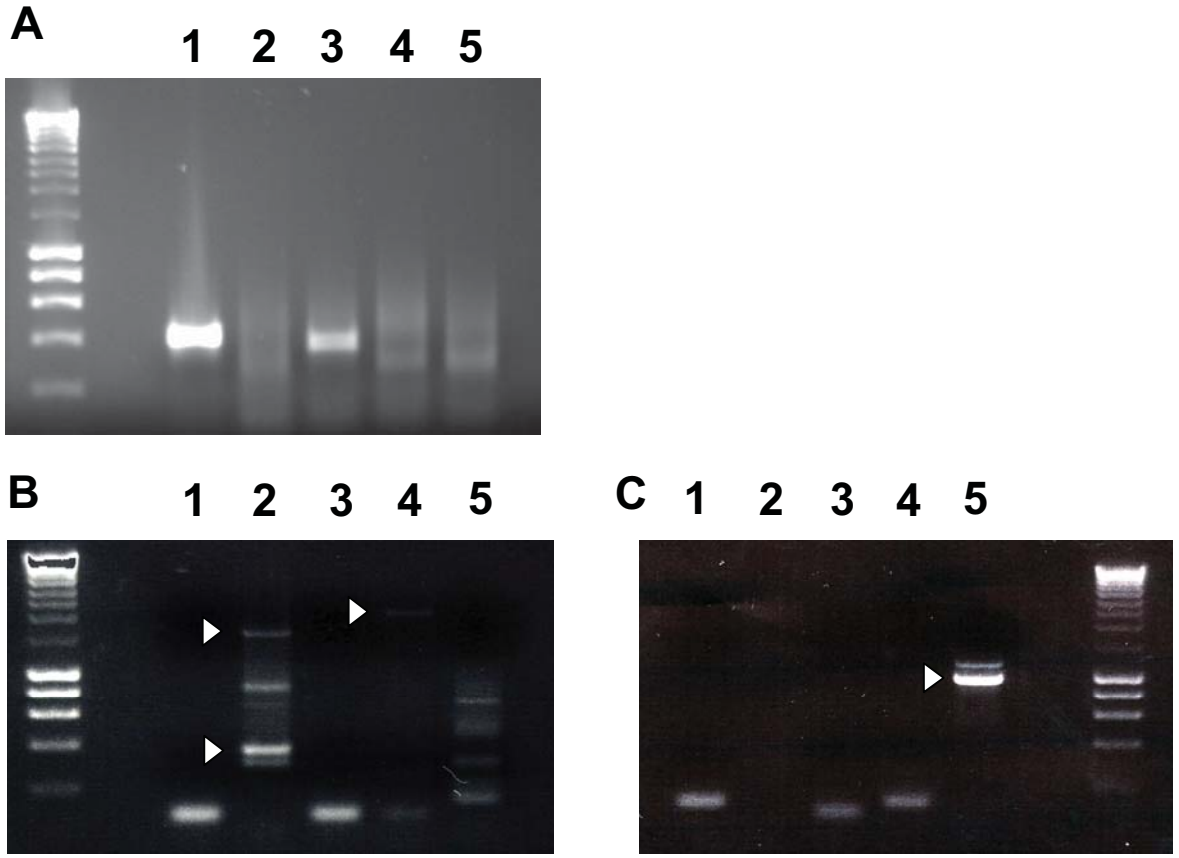

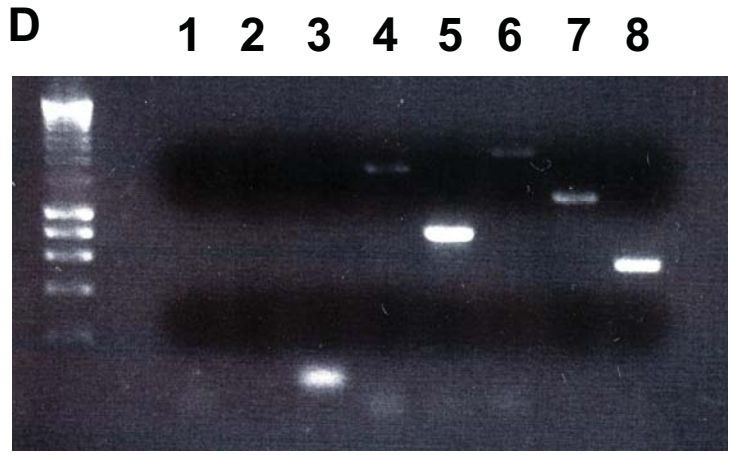

Figure 2.5 – Isolation of the *TaASY1* promoter by genome walking. (A) The first round of genome walking resulted in amplification of a 354 bp fragment amplified from the *Dra*I library and a 316 bp fragment amplified from the *Pvu*II library. (B) The second round of walking using primers complementary to the 354 bp *Dra*I library fragment resulted in amplification of multiple fragments from the *Eco*RV library and a single fragment from the *Sca*I library. (C) Second round of genome walking using primers complementary to the 316 bp *Pvu*II fragment resulted in amplification of a fragment from the *Stu*I library. Lanes 1-5 in (A), (B) and (C) represent the *Dra*I, *Eco*RV, *Pvu*II, *Sca*I and *Stu*I libraries, respectively. The arrowheads in (B) and (C) indicate fragments that were successfully cloned and sequenced. (D) Fragments amplified from the *Dra*I library in (A) and the subsequent round of genome walking in (B) are confirmed as being specific to *TaASY1*, with amplification of fragments of the expected size. Fragments amplified from the *Pvu*II library and the second round of walking in (C) were not specific to *TaASY1*. The DNA molecular weight marker was a 1 kb ladder (HyperLadder I, Bioline, Australia).

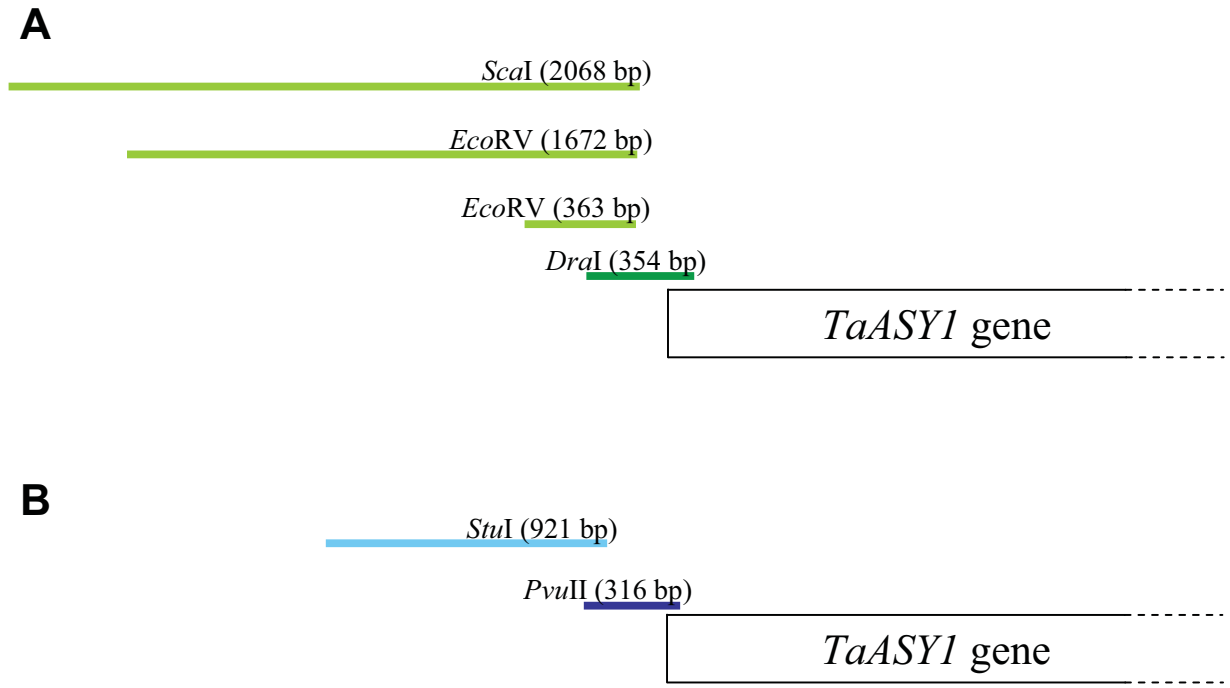

Figure 2.6 – Diagrammatic representation of products amplified *via* genome walking. (A) The dark green band represents the fragment isolated from the *Dra*I library in the first round of walking (see Figure 2.5A). The light green bands represent fragments isolated in the second round of walking using primers complementary to sequence of the *Dra*I library fragment (see Figure 2.5B). (B) The dark blue band represents the fragment isolated from the *Pvu*II library in the first round of walking (see Figure 2.5A). The light blue band represents the fragment isolated from the *Stu*I library using primers complementary to sequence of the *Pvu*II library fragment (see Figure 2.5C).

In silico analysis of the *TaASY1* promoter identified three main groups of motifs within the sequence. The first included common *cis*-elements such as TATA boxes and CAAT boxes, the second included elements responsible for gene expression during cell cycle events as well as in reproductive tissue such as pollen, endosperm and seeds, while the third included light responsive elements (Table 2.6). No meiosis specific elements were identified; however, this is more likely to represent a limitation of the database rather than the sequence lacking meiosis specific elements.

Table 2.6 – A summary of the three main groups of *cis*-elements identified within the 2355 bp *TaASY1* promoter sequence. Common *cis*-elements are found in the green shaded boxes, light-responsive elements are found within the orange shaded boxes and reproductive tissue associated elements are found within the yellow boxes. Positions of the elements are given in the direct strand (+) as well as the complementary strand (-). Nucleotide abbreviations are as follows; V = A, C or G; B = C, G or T; R = A or G; W = A or T; Y = C or T; H = A, C or T; D = A, G or T; S = G or C; N = A, G, C or T.

Motif Name	Signal Sequence	Position(s) and orientation
CAATBOX1	CAAT	334 (+), 728 (+), 845 (+), 868 (+), 1156 (+), 1310 (+), 1388 (+), 1983 (+), 2020 (+), 228 (-), 234 (-), 533 (-), 611 (-), 852 (-), 904 (-), 1104 (-), 1109 (-), 1144 (-), 1404 (-), 1641 (-), 1808 (-), 1912 (-)
CCAATBOX1	CCAAT	867 (+), 228 (-)
CGCGBOXAT	VCGCGB	1778 (+), 2205 (+), 2258 (+), 2303 (+), 369 (+), 2207 (+), 2305 (+)
CTRMCAMV35S	TCTCTCTCT	2180 (+)
EECCRCAH1	GANTTNC	1362 (+), 1382 (+), 2037 (+), 793 (-), 934 (-)
GATABOX	GATA	313 (+), 960 (+), 1138 (+), 1903 (+), 1915 (+), 99 (-), 105 (-), 145 (-), 315 (-), 435 (-), 1044 (-)
TATABOX2	TATAAAT	1646 (+)
TATABOX5	TTATTT	858 (+), 1189 (+), 1890 (+), 701 (-), 1071 (-)
BOXIIPCCHS	ACGTGGC	1744 (+)
GT1CONSENSUS	GRWAAW	260 (+), 793 (+), 934 (+), 960 (+), 967 (+), 1293 (+), 103 (-), 143 (-), 1026 (-), 1191 (-), 862 (-), 863 (-)
IBOXCORE	GATAA	104 (-), 144 (-)
LTRECOREATCOR15	CCGAC	293 (+), 340 (+), 1509 (+)
PIATGAPB	GTGATCAC	1018 (+)
PRECONSCRHSP70A	SCGAYNRNNNNNNNNNNNNNNHD	293 (+), 1509 (+), 1328 (+)
SORLIP1AT	GCCAC	1958 (+), 2107 (+), 1746 (-)
SORLIP2AT	GGGCC	1470 (+), 5 (-), 395 (-) , 1483 (-)
TBOXATGAPB	ACTTTG	682 (-)
AACACOREOSGLUB1	AACAAAC	346 (+),1316 (+)
ASF1MOTIFCAMV	TGACG	1083 (+),1776 (+), 1304 (-),2155 (-), 2317 (-)
CACGTGMOTIF	CACGTG	475 (+,-), 948 (+,-), 1691 (+, -)
CANBNNAPA	CNAACAC	328 (+), 523 (+)
CRTDREHVCBF2	GTCGAC	130 (+)
DOFCOREZM	AAAG	183 (+), 664 (+), 683 (+), 717 (+), 1218 (+), 1602 (+), 2009 (+), 2060 (+), 138 (-), 550 (-), 620 (-), 638 (-), 819 (-), 1187 (-), 1802 (-), 1860 (-), 2039 (-)
DPBFCOREDCDC3	ACACNNG	526 (+), 1233 (+), 1688 (+), 1690 (+), 2218 (+), 509 (-), 948 (-), 1006 (-) 2074 (-)
DRE2COREZMRAB17	ACCGAC	339 (+), 1508 (+)
E2FBNTRNR	GCGGCAAA	2237 (+)

GTGANTG10	GTGA	442 (+), 910 (+), 953 (+), 1018 (+), 1380 (+), 1505 (+), 1516 (+), 1843 (+), 2056 (+), 2064 (+), 2248 (+), 244 (-), 474 (-), 675 (-), 1022 (-), 1148 (-), 2050 (-), 2152 (-), 2157 (-), 2164 (-)
HEXAMERATH4	CCGTCG	2336 (+), 1 (-), 1820 (-), 1869 (-)
HEXMOTIFTAH3H4	ACGTCA	2154 (+),1083 (-)
MYBPZM	CCWACC	59 (+), 352 (+), 250 (-)
NONAMERMOTIFTAH3H4	CATCCAACG	1728 (+)
POLLEN1LELAT52	AGAAA	600 (+), 666 (+), 751 (+), 792 (+), 996 (+), 1429 (+), 1028 (-), 1654 (-), 1757 (-), 1861 (-)
QELEMENTZMZM13	AGGTCA	1492 (+)
TGTCACACMCUCUMISIN	TGTCACA	1146 (+), 2048 (+)

2.3.4 – Transcript expression analysis of *TaASY1*

TaASY1 expression was investigated using northern analysis, microarray and quantitative real time PCR (Q-PCR) technology. In the northern blot analysis, a tissue series and sub-staged meiotic anther series were completed, with *TaASY1* expression shown to be meiosis-specific (Figure 2.7A) and significantly up-regulated during pre-meiosis and leptotene to pachytene when compared to the other stages represented (Figure 2.7B).

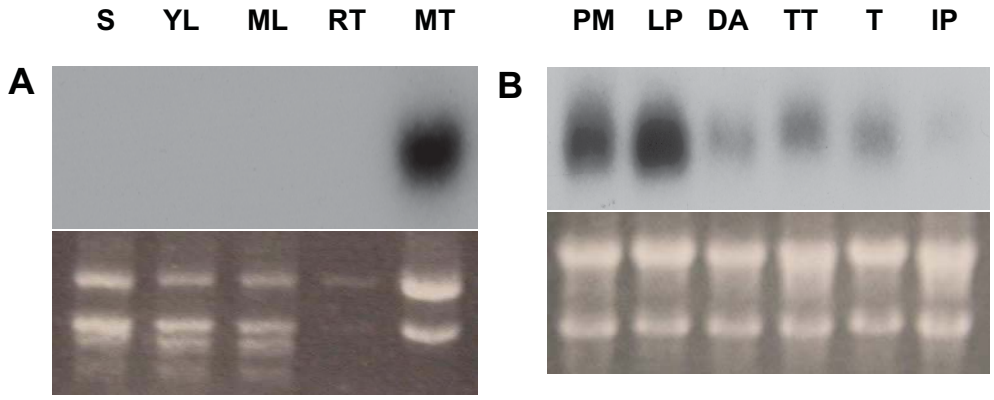

Figure 2.7 – Tissue series and meiosis stage specific northern blot analysis of *TaASY1*. (A) Tissue specific northern analysis of *TaASY1* expression in seedling (S), young leaf (YL), mature leaf (ML), root tips (RT) and meiotic tissue (MT). (B) Meiosis specific northern analysis of *TaASY1* expression during pre-meiotic interphase (PM), leptotene to pachytene (LP), diplotene to anaphase I (DA), telophase I to telophase II (TT), tetrads (T) and immature pollen (IP). For both analyses, ethidium bromide stained rRNA was used as a loading control. Figure courtesy of Elise Tucker (Boden et al., 2007).

Quantitative analysis of *TaASY1* transcript levels was initially performed by microarray using the wheat Affymetrix GeneChip®. From the 61,127 probe sets on the wheat GeneChip® which represents 55,052 transcripts, two probe sets were identical to the full length *TaASY1* cDNA sequence that was previously isolated: Ta.9186.1.S1_at and Ta.9186.2.S1_at, at positions 1591 bp to 1771 bp and 111 bp to 586 bp, respectively. The level of expression detected for the two microarray probe sets closely reflected the northern results, with *TaASY1* expression significantly elevated during pre-meiosis and leptotene to pachytene of prophase I (Figure 2.8). Detection within the mature anthers was significantly reduced (log ratio values of 6.2 and 4.7 respectively for the two transcripts identified), indicating inactivation of *TaASY1* transcription in this tissue. Ta.9186.1.S1_at displayed a significant decrease in transcript abundance, with a greater than 22-fold reduction between leptotene to pachytene of prophase I and the development of mature anthers.

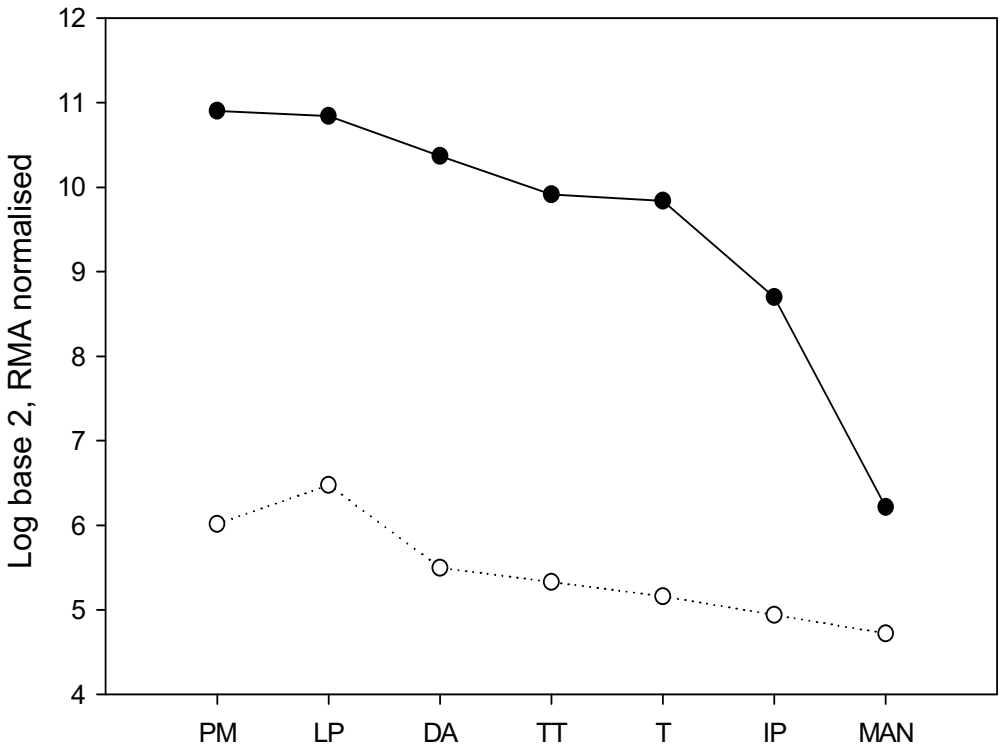

Figure 2.8 – Meiosis staged microarray analysis of *TaASY1*. Using the Affymetrix GeneChip® Wheat Genome Array, two probes were identified that matched *TaASY1*: Ta.9186.1.S1_at (1591 bp to 1771 bp – solid circles) and Ta.9186.2.S1_at (111 bp to 586 bp – open circles). While expression is considerably higher in Ta.9186.1.S1, it is evident that as meiosis concludes, transcript levels are minimal (as seen in both probes). PM, LP, DA, TT, T, IP as in (2.6B) with the addition of mature anthers (MAN).

To corroborate the microarray data, Q-PCR was also performed to investigate the transcript expression levels of *TaASY1* across a range of tissues. While low levels of expression were evident in leaf and root tips which were not detected in the tissue series northern, the results revealed significant levels of expression in anthers during the early stages of meiosis, confirming the results obtained from the other two techniques used (Figure 2.9). In parallel, the microarray and Q-PCR platforms exhibited a correlation value of 0.98 between each other suggesting that the results were highly reproducible.

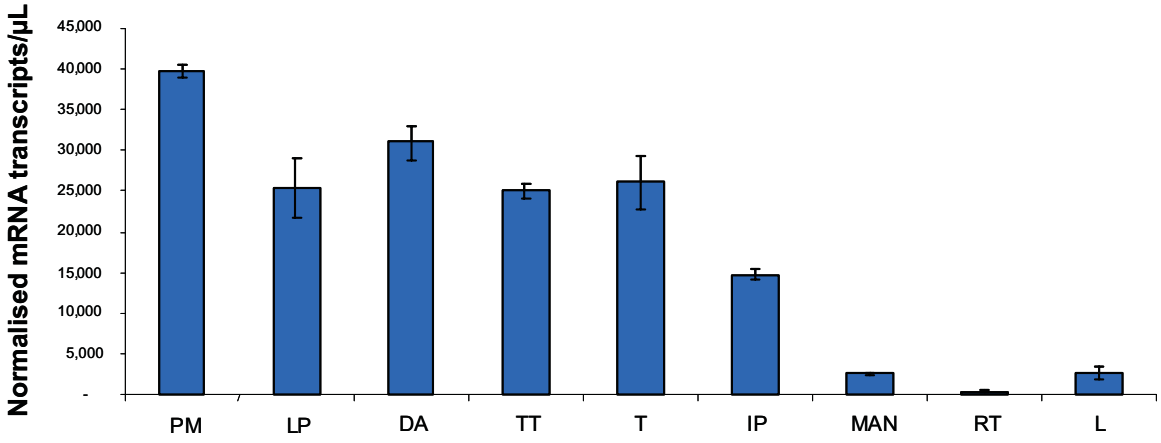

Figure 2.9 - Meiosis staged and vegetative tissue Q-PCR analysis of *TaASY1*. Quantitative analysis of *TaASY1* expression during stages of meiosis and in vegetative tissue, illustrating high levels of transcript during meiosis and basal levels in mature anthers, root and leaf tissue. PM, LP, DA, TT, T, IP, MAN as in (2.7), with the addition of root tips (RT) and leaf (L). The error bars represent the standard deviation of three replicates.

2.4 – Discussion

2.4.1 – The genetics of *TaASY1*

This chapter has established the similarities and differences at a genetic level between the isolated wheat *ASY1* gene, *TaASY1*, and many of its known orthologues. Understanding these similarities and differences enables insight into how the role of *TaASY1* may differ functionally (if at all) from related sequences of other organisms. Ultimately, through greater understanding of *TaASY1* it will be elucidated whether it too has a significant role in controlling homologous chromosome pairing, albeit, in bread wheat. More interesting will be whether *TaASY1* can be associated with the mechanism(s) that ensures chromosome associations occur between homologues and not homoeologues.

Historically in the cereal research community, a large amount of research has focussed on understanding the mechanism(s) controlling chromosome pairing in bread wheat. This research has principally involved investigating mutants with reduced restriction of chromosome associations to homologues, namely *ph1b* and *ph2a*, the loci of which are located on chromosomes 5BL and 3DS, respectively (reviewed in Sears, 1976 and Moore, 2002). Typically, investigating these mutants has followed a bipartite approach. The first has involved an extensive cytological investigation of chromosome dynamics during meiosis to identify the mechanisms that regulate homologous chromosome pairing, while the second has employed extensive genetic refinement of the loci to identify the genes that are potentially responsible for their phenotype (Roberts et al., 1999; Okamoto, 1957; Riley and Chapman, 1958; Feldmann, 1966; Wall et al., 1971a; b; Sears, 1977; Holm and Wang, 1988; Griffiths et al., 2006). Recently, the *Ph1* locus was refined to a region including seven *Cdk*-like genes and a sub-telomeric heterochromatic region that translocated from chromosome 3AL, as candidates for the *Ph1* effect (Griffiths et al., 2006; Al-Kaff et al., 2007). While this work has

dramatically increased our understanding on how *Ph1* may be regulating chromosome pairing in bread wheat, it is unlikely that any of these genes directly interact with meiotic chromatin structures and are directly involved in the chromosome pairing machinery, unlike *TaASY1*.

Sequence analysis of *TaASY1* shows that this gene represents the fourth HORMA domain containing gene to be isolated in plants, joining *ASY1* from Arabidopsis and *Brassica* as well as *PAIR2* from rice (Caryl et al., 2000; Armstrong et al., 2002; Nonomura et al., 2004). HORMA domain containing genes have also been isolated and characterised in yeast (*ScHOP1*) and *Caenorhabditis elegans* (*CeHIM3*), with a common function of these genes being that their encoded proteins form an essential component of axial elements necessary for synapsis of homologous chromosomes (Hollingsworth and Byers, 1990; Zetka et al., 1999; Armstrong et al., 2002; Nonomura et al., 2006).

The HORMA domain is a chromatin interacting domain that is able to recognise altered chromatin states, such as those that result from DNA adducts, double stand breaks and non-attachment to the spindle, which may act as an adapter for the recruitment of other proteins (Aravind and Koonin, 1998). Comparing the *Ta*ASY1 amino acid sequence to *At*ASY1, *Bo*ASY1 and *Os*PAIR2 revealed that these four proteins share significant sequence similarity. This similarity was increased further when comparing only the HORMA domains of each protein, indicating that this domain is essential for the function of these proteins. This conclusion is further supported by the alignments of the plant proteins with *Sc*HOP1, whereby it is only the HORMA domain that displays any recognisable sequence similarity (Figure 2.1). The limited sequence homology shared between *Sc*HOP1 and the plant ASY1 orthologues is not unusual, as this has been observed when comparing proteins with a role in formation of the SC, such as *ScZIP1* and *AtZYP1A/B* (Higgins et al., 2005). This lack of sequence conservation may also explain why there are no notable sequence similarities between *Ta*ASY1 and *Ce*HIM-3. The lack of sequence similarity with *Ce*HIM-3 is common with all of the plant

ASY1 homologues, with no significant homology detected between the HORMA domains of *At*ASY1 and *Ce*HIM-3 (Armstrong et al., 2002).

Analysis of the *TaASY1* gene structure revealed that it contains the same number of introns (21) and exons (22) that are found in *AtASY1* and *OsPAIR2* (Caryl et al., 2000; Nonomura et al., 2004). Interestingly, while it may be expected that the intron/exon boundaries of *TaASY1* could be determined with the aid of software that recognises conserved intron splice sites, it appears based on analysis of *TaASY1* that the splice sites of Arabidopsis, rice and also maize are not conserved in bread wheat, as the intron/exon boundaries could not be determined through the use of such software. Similar difficulties were also reported with identifying the exon/intron boundaries of *AtASY1* (Caryl et al., 2000)

Following the isolation of the *TaASY1* genomic DNA sequence, 2.35 kb of promoter sequence was obtained. The sequence was isolated *via* two successive rounds of genome walking and confirmed as being specific to *TaASY1*. Database searches for conserved *cis*-elements showed that the sequence contained many motifs common to plant promoter sequences, including TATA and CAAT boxes. These searches also showed that the promoter sequence contains a number of elements that may be responsible for the elevated expression of *TaASY1* in reproductive tissues. In addition, there were also a relatively high number of light inducible promoter elements found within the promoter sequence, which may represent a link between floral induction, which is known to be stimulated by changes in day-length, and the meiotic cycle (Baurle and Dean, 2006). While the discovery of these motifs provides support for this sequence representing an up-stream promoter region, it is worth noting that a number of the elements are only four or five base pairs in length, and are therefore relatively likely to appear by chance in a sequence of 2.35 kb. Hence, it is difficult to conclude any functional roles for this region based on sequence alone. However, functional analysis of this sequence is in progress, with stable transformed bread wheat plants containing the promoter sequence

fused to the green fluorescent protein currently being generated. In addition, ongoing work will compare this sequence to promoter sequences of other key meiotic genes that have been isolated from bread wheat to determine any common *cis*-elements that are potentially responsible for regulating gene expression in meiotic tissue.

Southern blot hybridisation indicated that *TaASY1* does not represent the *Ph2* locus, having been located on each of the Group 5 chromosomes. Further analysis based on a mutant PCR screen confirmed its position on chromosome group 5 relative to the *Ph1* locus. This analysis showed that it is located in a region more proximal to the centromere then *Ph1*, assuming that the position of *TaASY1* on 5A is reflective of its position on 5B. Therefore, while these results confirm that *TaASY1* does not represent *Ph1* or *Ph2*, they do not refute the possibility of *TaASY1* being indirectly affected by deletion of these loci.

Based on the position of *TaASY1* on the long arm of chromosome group 5, it is plausible to suggest that this candidate may represent one of the previously reported minor chromosome pairing promoters on 5AL and/or 5DL (Feldman, 1966; Riley et al., 1966; Mello-Sampayo, 1972; Feldman and Mello-Sampayo, 1967). Unfortunately, the bread wheat deletion lines in which these particular defects were originally described could not be located (after having approached several sources including the John Innes Centre, Norwich, UK). Confirming directly whether *TaASY1* is responsible for one of these phenotypes may therefore not be possible.

2.4.2 – *TaASY1* transcripts are highly abundant in meiotic tissue

The three transcript analysis procedures used in this study clearly indicated significant expression of *TaASY1* in meiotic tissue, with highest expression predominantly confined to pre-meiosis and leptotene to pachytene. As *At*ASY1 and *Os*PAIR2 load onto chromatin at the end of pre-meiotic interphase and persist through leptotene and zygotene up until pachytene, it

was expected that *TaASY1* transcripts would be at their most abundant during these stages. This result was also expected based on these stages being when synapsis occurs, which is reflected by the phenotypes of *asy1* and *pair2* mutants where chromosomes fail to synapse (Ross et al., 1997; Nonomura et al., 2004).

The Q-PCR and microarray data indicated that transcript levels of *TaASY1* remained elevated from diplotene through to the completion of telophase II. This may be due to minor asynchrony between the collection of anthers that were selected for staging and subsequent RNA isolation. In addition, as wheat meiosis takes only 24 hours to complete it is possible that the elevated expression seen later in meiosis represents the mRNA that remained in the cells as they rapidly progressed through the meiotic cycle, after the relatively lengthy prophase I period of 17 hours (Bennett and Smith, 1972).

Although the *TaASY1* transcript was not detected in vegetative tissues using northern analysis, Q-PCR and microarray analysis suggested that there were very low levels of expression (up to approximately 40,000 fold less). This relatively low level of expression in vegetative tissue is not unexpected, as there was significant detection of *AtASY1* transcripts in vegetative tissue *via* reverse transcriptase PCR (Caryl et al., 2000). In addition, given the high sensitivity of Q-PCR and microarray analysis compared to northern blot hybridisation, it is not surprising that a low level of *TaASY1* expression was detected in vegetative tissues with these two methods.

Interestingly, analysis of the microarray data revealed that there were two probes on the GeneChip® Wheat Genome Array that were identical in sequence to *TaASY1*. The first probe (Ta.9186.1.S1_at) displayed higher levels of expression then the second probe (Ta.9186.2.S1_at), despite the trend of both probes through the meiotic time-course being similar. There are several possible reasons to explain these transcriptional differences detected. First, it maybe attributed to the different recognition sites of each probe within the

TaASY1 sequence; with the first probe (Ta.9186.1.S1_at) being complementary to the 3′ region of *TaASY1*, compared to the second probe (Ta.9186.2.S1_at) which was complementary to the 5′ region. First strand cDNA synthesis was performed using an oligo-dT primer that binds to the 3' poly-adenylated end of the mRNA and marks the initiation site for reverse transcription, which then proceeds in a 3' to 5' direction relative to the template mRNA transcript. Therefore, an incomplete cDNA synthesis reaction would result in a reduced amount of sequence complementary to the 5' end of the mRNA transcript. This would result in a reduced amount of target sequence for the Ta.9186.2.S1_at probe to bind relative to the target sequence available to the Ta.9186.1.S1_at probe. This would explain the difference in the transcript levels detected by the two probes as well as the identical profile detected by the probes across the meiosis time-course. A second explanation for this difference is that the two probes may represent two of three homoeologous sequences of *TaASY1*. If this is the case, one of the copies (either A, B or D) is more highly regulated than the other copies in the genome. However, the sequence differences between the homoeologues should not be that dissimilar to see such a change in the expression profile.

Importantly, and irrespective of the two probes recognising the *TaASY1* transcript, the meiotic expression profile from the microarray analysis is in strong agreement with the profile determined using Q-PCR (with a very high correlation value of 0.98) between the two methods. This is in parallel with a recent study, which also used the GeneChip® Wheat Genome Array in conjunction with Q-PCR to analyse expression profiling during grain development (Wan et al., 2008).

Following detailed investigation of the genetics and transcript behaviour of *TaASY1*, which provided evidence of a role for this gene during meiosis in bread wheat, attention was then given to the behaviour of the protein during meiosis. This investigation would provide

information regarding the tissues that contain *Ta*ASY1, as well as the location of *Ta*ASY1 in meiotic cells.

Chapter 3 - Investigation of the *Ta*ASY1 protein

3.1 – Introduction

Following the genetic analysis of *AtASY1*, experiments were performed in Arabidopsis and *Brassica oleracea* to identify the temporal and spatial localisation of ASY1 during meiosis (Armstrong et al., 2002). Western blot analysis revealed that ASY1 protein was expressed during the early stages of both male and female meiosis, and not in vegetative tissue. Immunisation of anther sections displayed specific localisation of ASY1 to pollen mother cells (PMCs). Chromosome spreads of PMCs progressing through early meiosis showed that ASY1 localised to axial elements of pairing/synapsing chromosomes. Initially, the ASY1 signal appeared as punctate foci during pre-meiotic interphase and became increasingly continuous through leptotene and zygotene to spread along the entire length of the axial elements (excluding the telomeres). Signal continuity was maintained until pachytene, but became increasingly diffuse in regions where synapsis was complete, and disappeared during diplotene as the chromosomes de-synapsed.

Interestingly, immuno-localisation using electron microscopy revealed that while ASY1 localised to chromatin next to the axial elements, it did not form the pattern expected of a structural component of the SC (Armstrong et al., 2002). Based on these findings it was suggested that ASY1 has a role in juxtaposing homologous chromosomes during early meiosis. However, the possibility of it having a role in mediating SC formation, such as through the recruitment of SC proteins could not be discounted either (Armstrong et al., 2002). A similar role was also suggested for PAIR2 in rice, with PAIR2 reported as displaying a very similar spatial and temporal localisation as ASY1 from Arabidopsis (Nonomura et al., 2006).

The anti-ASY1 antibody has been used to study other Arabidopsis meiosis mutants, as well as mutants in rye and maize despite the ASY1 gene not having been characterised in these two organisms (Higgins et al., 2004; 2005; Mercier et al., 2005; Golubovskaya et al., 2006; Jackson et al., 2006; Kerzendorfer et al., 2006; Mikhailova et al., 2006; De Muyt et al., 2007; Vignard et al., 2007). Its common usage in studying Arabidopsis meiosis mutants is mainly due to its localisation to axial elements not being disrupted in mutants investigated thus far, meaning it represents a useful 'marker' protein in meiotic studies. This also appears to be the reason for it being used to investigate mutants in rye and maize, with observations supporting those obtained in Arabidopsis (Golubovskaya et al., 2006; Mikhailova et al., 2006). Despite the extensive characterisation of ASY1 in diploid organisms such as Arabidopsis, rice and rye, localisation of ASY1 in a polyploid has not yet been investigated.

Given the lack of knowledge in more complex genomes, this chapter describes the research findings after having investigated the *Ta*ASY1 protein in allohexaploid bread wheat, with specific attention given to its spatial and temporal localisation during meiosis. Following the development of two anti-*Ta*ASY1 antibodies, western blot analysis was performed to investigate the tissues that contain *Ta*ASY1. In addition, immuno-fluorescence and immuno-gold transmission electron microscopy (TEM) were used to determine localisation of *Ta*ASY1 during the early stages of bread wheat meiosis.

3.2 – Materials and methods

3.2.1 - Production of *Ta*ASY1 protein

3.2.1.1 - Development of protein expression vectors

The full length *TaASY1* ORF was amplified as detailed in 2.2.3.3. This clone was then inserted into pCR8/GW/TOPO, according to manufacturer's instructions (Invitrogen, Victoria,

Australia). The full length clone was then recombined into the pDEST17 vector containing a 6x histidine (6X His) repeat at the 5' end of the entry site using Gateway technology, according to manufacturer's instructions (Invitrogen) (see Appendix B – Figure 1). The pDEST17:*TaASY1* vector was transformed into BL21-A1 cells, according to manufacturer's instructions (Invitrogen), and plated onto LB/agar plates containing ampicillin (100 μg mL^{-1}) and incubated overnight at 37°C. Transformed cells were analysed by colony PCR for the presence of plasmids containing the *TaASY1* ORF as per 2.2.3.4.3, with the exception of using primers GW1 (GTTGCAACAAATTGATGAGCAATGC; 10 μM, 1μL) and GW2 (GTTGCAACAAATTGATGAGCAATTA; 10 μM, 1μL). DNA plasmid mini-preparations were performed on overnight cultures of colonies that contained the pDEST17:*TaASY1* plasmid as per 2.2.3.4.3. Sequence analysis was performed on these plasmids, as per 2.2.3.5, to confirm that the vector contained the *TaASY1* ORF in the correct orientation and frame for accurate translation.

3.2.1.2 - *Ta*ASY1 protein production in *E. coli*

Protein production in BL21-A1 cells (Invitrogen) was induced by adding L-arabinose (Sigma-Aldrich, New South Wales, Australia) to a final concentration of 0.2% in LB liquid culture, according to the manufacturer's instructions (Invitrogen). Parallel experiments were performed to collect non-induced control cultures, using the same growth conditions as the induced cultures, as per the manufacturer's instructions (Invitrogen).

3.2.1.3 – Purification and gel electrophoresis of recombinant *Ta*ASY1 protein

The recombinant protein was extracted and purified using Ni-NTA agarose under denaturing conditions, according to manufacturer's instructions (QIAGEN, Victoria, Australia). During the purification process, fractions were collected from the cell-lysis, flow through, washes and

each elution from both the induced and non-induced cultures. Aliquots (5 µL) of each fraction were loaded into a 7.5% poly-acrylamide gel for separation by SDS-PAGE (sodium dodecyl sulphate – poly-acrylamide gel electrophoresis) with SDS-PAGE loading buffer (0.09 M Tris/HCl, 20% glycerol, 2% SDS, 0.02% bromophenol blue, 0.1 M DTT) and run at 200 V for approximately 90 min in running buffer (0.3 % Tris, 1.44% glycine; 0.1% SDS, pH 8.3). The gels were stained using Coomassie Blue solution (0.03% brilliant blue, 7.5% glacial acetic acid, 50% methanol) for 3 h at room temperature with constant rotation, before being de-stained using Coomassie de-stain solution (10% glacial acetic acid, 50% methanol) for up to 36 h at room temperature with constant rotation. An image of the stained gel was obtained using an Epson Perfection 4180 Photo scanner (Epson, New South Wales, Australia).

3.2.1.4 - MS/MS analysis of recombinant *Ta*ASY1 protein

The poly-acrylamide gel containing the recombinant *Ta*ASY1 protein was sent to the Protein Core Facility, Hanson Institute, Adelaide, Australia to confirm the identity of the recombinant protein as *Ta*ASY1. The predicted *Ta*ASY1 band, at a molecular weight of 66 kDa in the lane containing protein from the elution fraction, was digested with trypsin according to standard procedures. Mass spectrometry was performed on the peptides using a $QTOF^2$ mass spectrometer. The MS/MS data were analysed using the ProteinLynx Global Server to search against the NCBI non-redundant database for peptide tag matches. This was also combined with *de novo* sequencing and BLAST analysis to confirm the identity of the *Ta*ASY1 recombinant protein.

3.2.2 - Production of anti-*Ta*ASY1 antibodies

3.2.2.1 - Production of mouse anti-*Ta*ASY1 antibody

A peptide spanning residues 486 to 499 (DRRDHQTADQEMKDC) of the *Ta*ASY1 amino acid sequence was synthesised (AusPep, Victoria, Australia). Selection of the peptide was based on its low hydrophobicity, uniqueness of sequence when used in a BLAST search against known translated sequences and protein sequences (tBLASTn and BLASTp), and its predicted structure compared to protein structures with sequence similarity to *Ta*ASY1. The peptide was initially dissolved in 200 µL of 1x PBS (10 µg μL^{-1}) and conjugated with an equal volume of the carrier molecule KLH (Keyhole Limpet Hemocyanin) (Pierce, Illinois, U.S.A.) dissolved in double autoclaved milli-Q water (10 µg μL^{-1}). For the first mouse immunisation, 50 µL of KLH-conjugated antigen was added to 50 µL of 1x PBS, and subsequently added to an equal volume of Freund's complete adjuvant (Sigma-Aldrich) prior to subcutaneous injection. For the following immunisations, which were administered at three weekly intervals, the 100 µL of KLH-conjugated antigen in 1x PBS was added to Freund's incomplete adjuvant (Sigma-Aldrich) prior to subcutaneous injection. Immune serum was extracted 68 days after the first injection.

3.2.2.2 - Production of rabbit polyclonal anti-*Ta*ASY1 antibody

The complete *Ta*ASY1 protein produced in bacteria and purified as per sections 3.2.1.2 and 3.2.1.3 was used to induce antibody production in rabbit. The protein sample was transferred from the elution buffer used in the purification of the recombinant protein into 1X PBS by dialysis. Dialysis was performed using cellulose dialysis tubing (Sigma-Aldrich), which was injected with the protein sample in elution buffer. The tubing was sealed and placed in 5 L of

1X PBS for 2 hours at 4°C with constant stirring. The 1X PBS was replaced every 2 h, with a total of 6 h incubation performed.

For the first rabbit immunisation an equal volume of Freund's complete adjuvant (Sigma-Aldrich) was added to 150 µg of *Ta*ASY1 recombinant protein in 1X PBS prior to subcutaneous injection. For the following immunisations, which were administered at three weekly intervals, an equal volume of Freund's incomplete adjuvant (Sigma-Aldrich) was added to 150 µg of *Ta*ASY1 recombinant protein in 1X PBS prior to subcutaneous injection. A final bleed was performed 74 days after the first injection, from which the immune serum was collected.

3.2.3 - *Ta*ASY1 western blot analysis

3.2.3.1 - Plant protein extraction

A phenol-based extraction, with methanol/ammonium acetate precipitation was used as described in Carpentier et al., (2005) to obtain wheat protein. Protein was collected from the following tissue: young leaf (3 weeks), mature leaf (8 weeks), root tips (2 weeks) and whole spike, with the middle floret staged at pachytene (as per 2.2.2). Tissue was frozen in liquid nitrogen and ground to a powder using a pre-chilled sterilised mortar and pestle. Ground material (150 mg) was re-suspended in chilled protein extraction buffer (500 µL; 50 mM Tris, 5 mM EDTA, 100 mM KCl, 1% DTT, 30% sucrose, 1X complete protease inhibitor cocktail (Roche, New South Wales, Australia), pH 8.5) and mixed by vortex for 30 sec. Tris-buffered phenol (500 µL; Sigma-Aldrich) was added, and the solution was mixed by vortex for 15 min at 4°C in a multiple tube vortex. Following centrifugation at 6000 x *g* for 3 min at 4°C, the phenol phase (top layer) was collected and transferred to a fresh 1.5 mL tube. Additional protein extraction buffer (500 µL) was added to the phenol phase, and the mixing and centrifugation steps above were repeated. The phenol phase was again collected and

transferred to a fresh 1.5 mL tube, to which 5 volumes of 100 mM ammonium acetate in methanol was added. The solution was incubated at -20°C overnight to precipitate the proteins.

Following overnight precipitation, the samples were centrifuged at 16000 x *g* for 30 min at 4°C. The supernatant was removed and the pellet was washed twice with ice-cold acetaone/0.2% DTT, with incubation for 60 min at -20°C between each wash. After the second wash, the supernatant was removed and the pellet was air-dried. The pellet was re-suspended in 100 µL of 1X PBS and briefly mixed by vortex at room temperature to help dissolve the protein pellet.

Protein samples were then quantified using the Bradford assay (Bradford, 1976). A Bovine Serum Albumin (BSA) dilution series was made with concentration values of 13.7 µg μL^{-1}, 10.275 µg μL^{-1}, 6.85 µg μL^{-1}, 3.425 µg μL^{-1} and 1.37 µg μL^{-1} using the BIO-RAD Protein Assay Standard II (Bio-Rad, Victoria, Australia), lyophilised BSA and milli-Q water. Triplicates of each dilution were made to ensure an accurate reading was obtained. Bradford reagent (200 µL) was added to each dilution sample (800 µL), followed by a 7 min incubation at room temperature. Bradford reagent (200 µL) was also added to 800 µL of diluted samples (1/200 in milli-Q water) of each tissue extracted protein.

After the 7 min incubation, absorbance readings at 595 nm were taken for each sample within the BSA dilution series as well as for the dilutions of each protein extraction. Measurements of the BSA dilution series were entered into Genstat software (version 8.0, Numerical Algorithms Group, Oxford, UK) to generate a standard curve. The standard curve was used with the absorbance readings of the diluted samples from each protein extraction to estimate concentrations of the undiluted samples.

3.2.3.2 - Gel electrophoresis and protein transfer to membrane

SDS-PAGE was conducted as per 3.2.1.3, with the exception of tissue protein extraction samples being used instead of fraction samples from production of recombinant *Ta*ASY1 protein. Protein (10 µg) from young leaf, mature leaf, root and meiotic tissue were loaded into the poly-acrylamide gel. Following completion of SDS-PAGE, the proteins were transferred from the gel onto a Hybond-P polyvinylidene difluoride (PVDF) membrane as per the manufacturer's instructions (Amersham Biosciences, GE Healthcare, New South Wales, Australia) using electroblotting. Electroblotting was performed using an XCELL II^{TM} Blot Module (Invitrogen), according to the manufacturer's instructions. The membrane was briefly rinsed in 1X TBS-Tween 20 and immediately used for western blot analysis.

3.2.3.3 – Western blot analysis and protein detection

The membrane was blocked with TBS-Tween 20 solution (0.137 M NaCl, 0.0027 M KCl, 0.25 M Tris, 0.05% Tween 20, pH 7.2) containing skimmed milk powder (5% w/v) for 16 h at 4°C with constant rocking. Post-incubation, the membrane was washed three times with TBS-Tween 20 solution for 5 min at room temperature with constant rocking.

The membrane was incubated with mouse anti-*Ta*ASY1 antibody diluted 1:1500 with TBS-Tween 20 solution (25 mL) for 2 h at room temperature with constant rocking. This was followed by three washes with TBS-Tween 20 as outlined above. The membrane was then incubated with anti-mouse IgG antibodies conjugated to Biotin (Sigma-Aldrich) diluted 1:1000 in TBS-Tween 20 solution (25 mL) using the same incubation conditions as those for the primary antibody.

Incubation was followed by three washes with TBS-Tween 20 as outlined above. Streptavidin conjugated to alkaline phosphatase (Sigma-Aldrich) was then added at a dilution of 1/1000 for one hour at room temperature with constant rocking. Excess alkaline

phosphatase conjugated streptavidin was removed with three 5 min washes using TBS-Tween 20 and was followed by addition of BCIP/NBT Purple Liquid Substrate System (Sigma-Aldrich) for protein detection. The enzymatic reaction was allowed to continue until the desired level of signal intensity was achieved and then quenched using ample amounts of water.

3.2.3.4 - Image capture

Once the membrane had completely dried, an image of the blot was obtained using an Epson Perfection 4180 Photo scanner (Epson).

3.2.4 - Immuno-localisation of *Ta*ASY1 by transmission electron microscopy (TEM)

3.2.4.1 - Anther fixation and sample preparation

Chinese Spring anthers were collected and staged as per 2.2.2. Partner anthers of those determined to be of the prophase I sub-stages leptotene through to diplotene were incubated in fixative solution (0.25% gluteraldehyde, 3% para-formaldehyde, 4% sucrose in 1X PBS) overnight at 4°C. Fixed anthers were washed three times with 1x PBS for 8 h each, before being dehydrated in an ethanol series of 70%, 90%, 95% and 100% consecutively, with three x 20 min incubations in each solution. Anthers were then incubated in a 50:50 mixture of 100% ethanol and LR white resin (Electron Microscopy Sciences, Pennsylvania, U.S.A) for 8 h, before being incubated three times in pure LR white resin for 8 h each. Anthers were then embedded into LR White Resin by incubation at 60°C for 60 h. Standard procedures using an ultramicrotome were used to produce tissue sections for transmission electron microscopy (TEM), which were affixed to nickel mesh grids (performed by Marilyn Henderson).

3.2.4.2 - Immunisation and counter-staining of sectioned tissue

Sectioned grids were then prepared for immunolocalisation by incubating with 0.05 M glycine for 20 min, followed by 2 incubations with incubation buffer (1 x PBS/0.15% AURION BSA-c™) (Aurion, Wageningen, The Netherlands). Sections were then incubated for 90 min with anti-*Ta*ASY1 mouse polyclonal antiserum diluted 1/400 in incubation buffer. The sections were washed 3 times with incubation buffer, before being incubated with a gold conjugated goat anti-mouse IgG serum (Aurion) diluted 1/30 with incubation buffer. This was followed with three washes using both incubation buffer and 1 x PBS, with fixation of sections using 2% glutaraldehyde in PBS. Samples were then washed two times in both PBS and distilled water. Prior to visualisation, the grids were counter-stained with uranyl acetate (50% saturated in distilled water; 10 min) and lead citrate (0.042 mol L^{-1} lead citrate trihydrate, 0.2 mol L^{-1} sodium citrate in distilled water; 5 min), with three 1 min washes in distilled water after each stain.

3.2.4.3 - Sample visualisation using TEM and image capture

Stained and labelled sections were visualised using a Philips 100 transmission electron microscope, with images recorded using a SIS Megaview II CCD camera and AnalySIS software (Soft Imaging Systems) at Adelaide Microscopy (Adelaide, Australia). The raw data images were then loaded into Adobe Photoshop Elements 2.0 software (Adobe, New South Wales, Australia) to adjust contrast, brightness and image size, and to generate schematic diagrams of the images.

3.2.5 - Immuno-localisation of *Ta*ASY1 by fluorescence microscopy

3.2.5.1 - Anther fixation

The protocol presented in this section, beginning with anther fixation and sample preparation, is essentially the same as that described by Franklin et al., (1999). Chinese Spring anthers were staged as per 2.2.2. Partner anthers of those determined to be of the stages pre-meiotic interphase through to anaphase I were dissected into filter-sterilised (0.2 μM) 1X buffer A (15 mM Pipes-NaOH (pH 6.8), 80 mM KCl, 20 mM NaCl, 0.5 mM EGTA, 2 mM EDTA, 0.15 mM spermine tetra-HCl, 0.05 mM spermidine, 1 mM DTT, 0.32 M sorbitol). The anthers were then fixed in freshly prepared 1X buffer A containing 4% para-formaldehyde (6 mL) (Electron Microscopy Sciences) for 30 min at room temperature with constant rotation. Post-fixing, anthers were washed (two times, 30 min) in 1X buffer A at room temperature with constant rotation, and then stored at 4°C in 1X buffer A (5 mL) in an air-tight container.

3.2.5.2 – Acrylamide embedding of meiocytes

Fixed anthers were placed into 60 μL of 1X buffer A on the lid of a small petri dish covered with a layer of parafilm. One anther was then removed from buffer A, and the tip was cut open using a scalpel blade (# 22, Livingstone, N.S.W., Australia). The anther was transferred to another 60 μL of 1X buffer A and the meiocytes were gently extruded from the open end of the anther using a fine needle (25 gauge, Becton Dickinson, New South Wales, Australia). The meiocytes of five anthers were collected for the preparation of each slide.

Meiocytes in 1X buffer A (10 μL) were then transferred to the surface of a poly-L-lysine coated glass cover-slip using an open cut pipette tip. This was followed by the immediate addition of activated acrylamide/bis-acrylamide solution (5 μL). The acrylamide/bis-acrylamide solution (100 μL; 30% solution, 37.5:1 acrylamide:bis-acrylamide)

(Sigma-Aldrich) was activated by the addition of 20% sodium sulfite (5 µL) and 20% sodium persulfate (5 µL). After addition of the activated acrylamide solution, a glass cover-slip (not coated with poly-L-lysine) was immediately placed on top of the solution at an angle of 45° relative to the bottom cover-slip. The meiocytes imbedded in acrylamide were incubated at room temperature for 90 min, before the top cover-slip was removed in preparation for immunisation, leaving the poly-acrylamide pad affixed to the poly-L-lysine coated cover-slip.

3.2.5.3 - Immunisation and counter-staining of poly-acrylamide pads

Following removal of the top cover-slip, the sample was immediately washed (2 times, 10 min) with 1X PBS to remove remaining polymerisation catalysts. Meiocytes were then permeabilised for 60 min in 1 mL of 1X PBS, 1% Triton X-100, 1 mM EDTA at room temperature. Cells were blocked in 1 mL of blocking solution (1X PBS, 3% BSA, 5% normal donkey serum (Sigma-Aldrich), 1 mM EDTA, 0.1% Tween-20) for 2 h at room temperature. Samples were incubated overnight in a humid chamber at room temperature with 50 µL of 1:100 dilution of rabbit anti-*Ta*ASY1 antibody in blocking solution. After 16 h, samples were washed in wash buffer (1X PBS, 0.1% Tween-20, 1 mM EDTA) for 1 h at room temperature, repeated for a total of 8 washes with the final wash performed overnight.

An AlexaFluor^{TM} 568 conjugated donkey anti-rabbit antibody (Molecular Probes, Invitrogen, Victoria, Australia) diluted in blocking buffer (50 µL, 1:100) was incubated with the sample overnight in a humid chamber in the dark. After 16 h incubation, an identical washing procedure as outlined above was performed, with the exception of all washes being performed in the dark. Samples were then washed with 1X PBS (2 times, 10 min) and stained with 10 µg µL^{-1} 4',6-diamidino-2-phenylindole (DAPI) in 1X PBS (500 µL) for 30 min at room temperature in the dark. Samples were washed in 1X PBS (3 times, 10 min) and rinsed three times with DABCO anti-fade reagent (2.5% 1,4 diazabicyclo-[2,2,2] octane (Sigma-

Aldrich), 50 mM Tris/HCl (pH 8.0), 90% glycerol). Excess anti-fade solution was removed, and the sample was placed onto a glass microscope slide. A cover-slip was placed on top of the sample, which was then sealed with nail polish and stored at -20°C.

3.2.5.4 - Sample visualisation and image capture

All images were obtained using a Leica TCS SP5 Spectral Scanning Confocal Microscope (Leica Microsystems, Wetzlar, Germany) with a water immersion HCX Plan Apochromat 63x/1.2 lens. A computer controlled stage and photomultipliers were used to collect 90 – 100 optical sections per nucleus, 180 - 220 nm apart. A 405 nm pulsed laser was used to obtain the DAPI signal, and a Diode-Pumped Solid State (DPSS) 561 nm laser was used to obtain the signal from the AlexaFluor^{TM} 568 conjugated antibody, corresponding to ASY1. Optical sections were combined and processed using Leica Application Suite Advanced Fluorescence (LAS-AF; version 1.8.2, build 1465, Leica Microsystems, Germany) software to generate maximum intensity projections of each nucleus. LAS-AF software was also used to overlay the signals from the 405 nm pulsed laser (DAPI) and the DPSS 561 nm laser (ASY1) to obtain merged maximum intensity projections.

3.3 – Results

3.3.1 – Production of *Ta*ASY1 recombinant protein

Coomassie staining of the poly-acrylamide gel containing protein samples from both the induced and non-induced cultures displayed the presence of a band in the induced sample at approximately 70 kDa that was not in the non-induced sample (Figure 3.1). Based on the calculated theoretical mass, this band was at the predicted weight for *Ta*ASY1, as the 6X His-repeat was expected to add 2.7 kDa to the 66.3 kDa protein. A band at the same weight was

present in the cell-lysis lane but not in the flow-through or wash lanes, indicating that it represented the protein containing the 6X His-repeat.

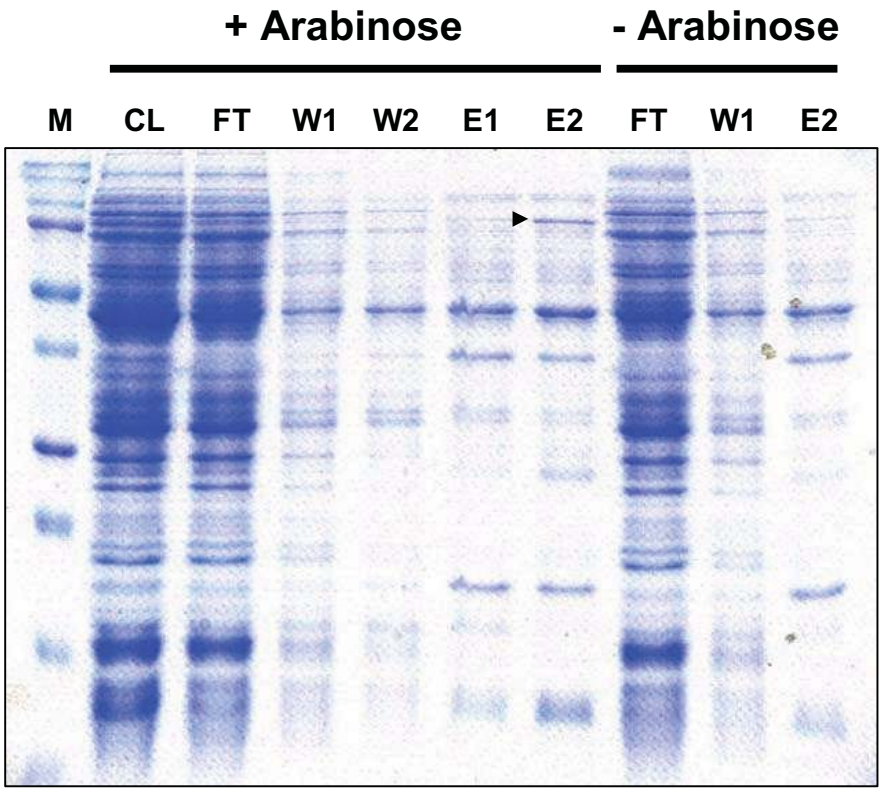

Figure 3.1 – Production of recombinant *Ta*ASY1 in *E coli*. A Coomassie Blue stained SDS-PAGE gel containing the bacterially expressed *Ta*ASY1 protein at a molecular weight of 70 kDa in the E2 lane of Arabinose induced culture (see band adjacent to arrow-head). CL = cell lysis, FT = flow-through, W = wash, E = elution. The marker (M) used was the Precision Plus Dual Color marker (Bio-Rad, Victoria, Australia).

MS/MS analysis of the band at 70 kDa confirmed its identity as being *Ta*ASY1 (see Appendix B – Figure 2). Searches using data of five individual peptides from the MS/MS analysis resulted in a single strong match to an "essential protein for meiotic synapsis *Oryza sativa* japonica cultivar group" (Acc # 37999050), which corresponds to *Os*PAIR2 (Nonomura et al., 2004) (see Appendix B – Figure 2).

3.3.2 – Western blot analysis

Immunisation of the western blot containing protein extracted from four tissue types (young leaf, mature leaf, root tip and meiotic tissue) using the mouse anti-*Ta*ASY1 antibody resulted in the detection of a single band at approximately 70 kDa (Figure 3.2). High levels of *Ta*ASY1 protein were detected in meiotic tissue, as expected from the transcript analyses. A faint signal was also detected in the lanes containing protein extracted from the vegetative tissues (young leaf, mature leaf and root tip).

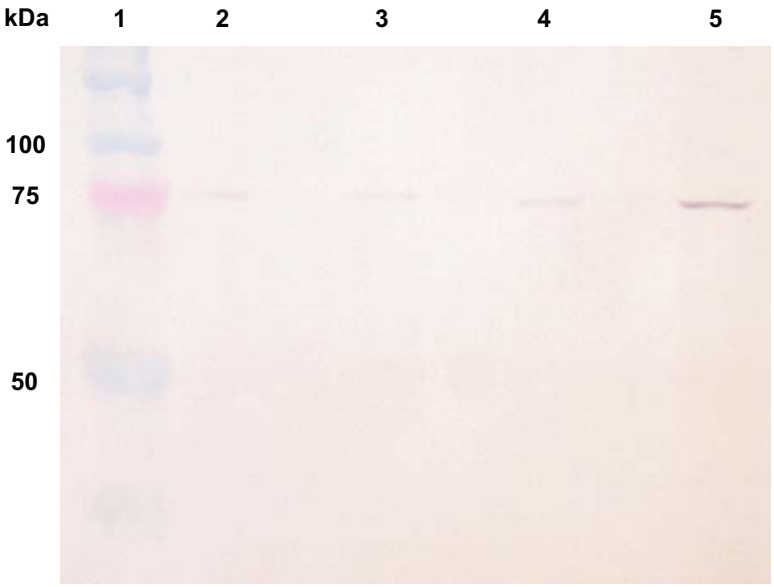

Figure 3.2 – Western blot analysis of *TaASY1*. Western blot analysis using anti-*Ta*ASY1 antibody shows high levels of protein in meiotic tissue (lane 5), with very low levels also detected in young leaf (lane 2), mature leaf (lane 3) and root tissue (lane 4). Lane 1 contains the marker (Precision Plus Dual Color, Bio-Rad).

3.3.3 – Immuno-gold localisation of *Ta*ASY1 using TEM

TEM was used to visualise sections of anthers containing cells undergoing meiosis to localise *Ta*ASY1 via detection of gold particle-conjugated secondary antibodies. *Ta*ASY1 localised to the nucleus of meiotic cells, and specifically to structures that form part of the SC. During leptotene and early zygotene, *Ta*ASY1 was found to associate with chromatin adjoining axial

elements (Figure 3.3A, 3.4A). Upon complete SC formation in pachytene nuclei, *Ta*ASY1 was found to interact with axis-associated chromatin, with labelling present amongst dense chromatin adjacent to lateral elements of the tri-partite SC (Figure 3.3B, C, 3.4B). The pattern of *Ta*ASY1 labelling within the chromatin regions appeared random, with no consistent distance between individual foci detected, nor were there any clusters of *Ta*ASY1 protein such as those observed with proteins that localise to recombination nodules. Labelling was not observed in nuclei of cells that were progressing through diplotene and diakinesis, suggesting that the protein is degraded or removed upon disassociation of the SC (Figure 3.3D). The two negative controls including grids without primary antibody (Figure 3.3E) and grids labelled with a goat anti-rabbit secondary antibody (see Appendix B – Figure 3) displayed no labelling. These observations are consistent with those made in *B. oleracea* and rice (Armstrong et al., 2002; Nonomura et al., 2006).

Figure 3.3 – Immuno-gold localisation of *Ta*ASY1 *via* electron microscopy. (A) During early zygotene, *Ta*ASY1 was found to localize to axial elements (bar = 0.5 μm). (B) A low magnification image of a meiotic cell at late zygotene to early pachytene, containing formed SCs, as illustrated by the SC within the boxed area, which is shown in (C) (bar = 2 μm). (C) During late zygotene/early pachytene, *Ta*ASY1 localised to chromatin regions associated with lateral elements of a formed SC (bar = 0.5 μm). (D) A meiocyte at diplotene, displaying absence of *Ta*ASY1 (bar = 1 μm). (E) A negative control excluding the primary antibody (bar = 0.1 μm). In (C) and (E), arrows indicate the chromosome axes (lateral elements), and arrow heads represent the central element. All sections were counterstained with uranyl acetate and lead citrate.

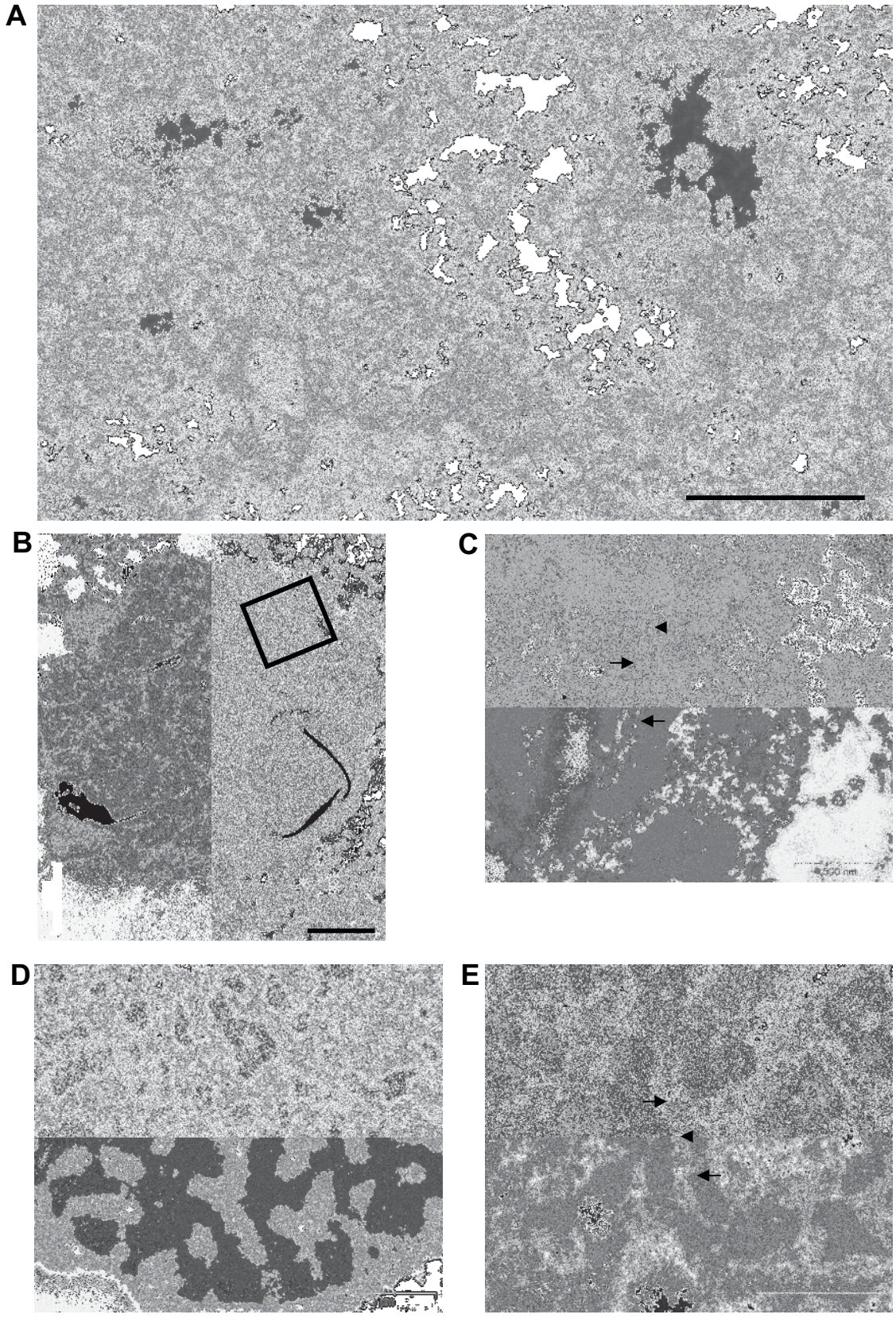
A
B
C
D
E

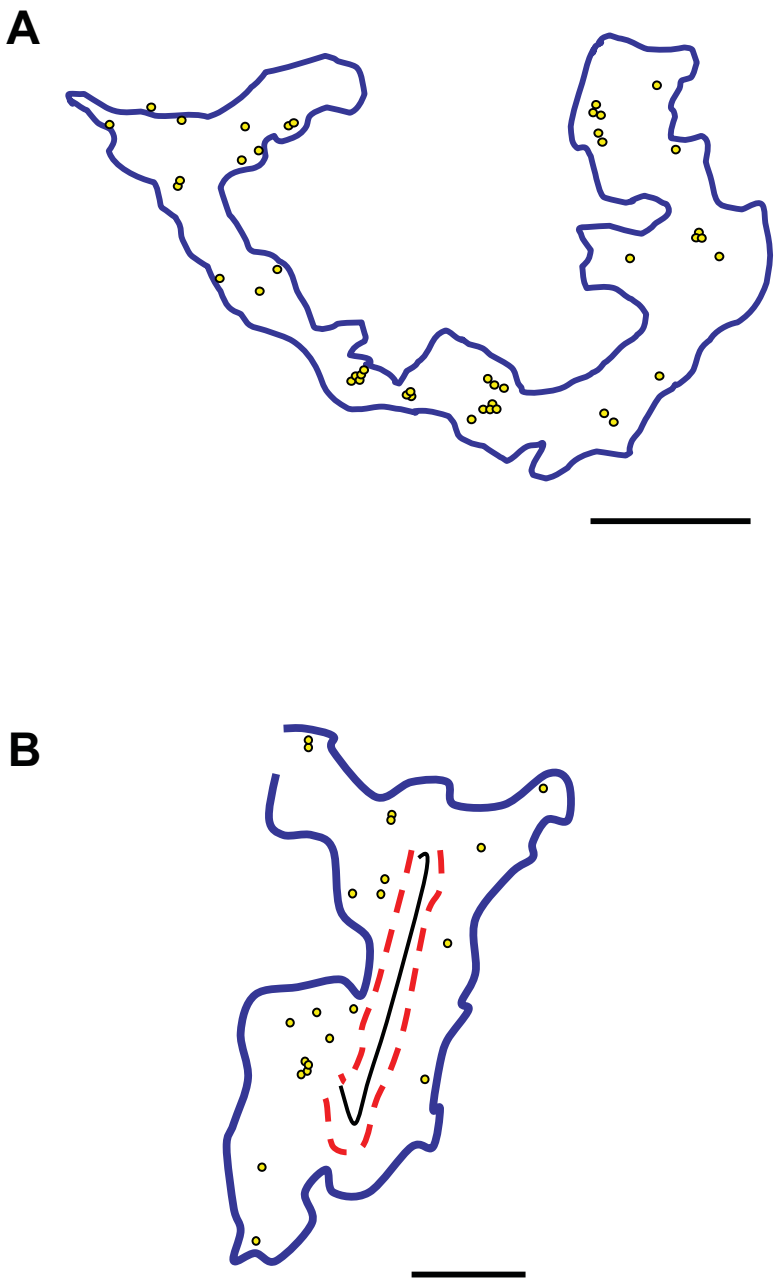

Figure 3.4 – Schematic diagrams of *Ta*ASY1 localisation as detected by electron microscopy. (A) A schematic diagram of Figure 3.3A, displaying localisation of *Ta*ASY1 to chromatin of axial elements prior to synapsis (bar = 0.5 µm). (B) A schematic diagram of Figure 3.3C, displaying localisation of *Ta*ASY1 to chromatin associated with lateral elements of a formed SC (bar = 0.5 µm). In each diagram, the yellow dots represent detected *Ta*ASY1 foci, the blue lines are the outer boundaries of the chromatin, the red lines indicate the chromosome axes, and the black line is the central element.

3.3.4 – Immuno-fluorescence localisation of *Ta*ASY1

Immunisation of meiocytes maintained in their three-dimensional state was performed to determine the spatial and temporal localisation of *Ta*ASY1 during meiosis in bread wheat. Initial observations of cells extruded from anthers revealed that *Ta*ASY1 specifically localises to meiocytes that were progressing through early meiosis I (Figure 3.5). *Ta*ASY1 first appeared during pre-meiotic interphase as punctuate foci that were confined to the nucleoplasm, which did not form a discernable pattern amongst chromatin regions (Figure 3.6A). As the cell progressed into leptotene, a continuous signal began to emerge from the punctate foci, which appeared to represent the formation of axial elements. This signal was confined to the regions of the nucleoplasm containing chromatin, as shown by the merged image of the ASY1 signal with that of DAPI (Figure 3.6B).

The ASY1 signal became more continuous and structurally defined as the condensing chromosomes began to synapse and pair during zygotene, extending along the entire length of the axial elements (Figure 3.6C, D). In addition, progression of synapsis was visible by the presence of ASY1 labelled synapsis forks (Figure 3.6D). The ASY1 signal did not localise to the nucleolus, which was readily observable during zygotene, when it is positioned towards a corner of the nuclear periphery. Through late-zygotene and pachytene, the ASY1 signal thickened concurrently with the progression of synapsis, appearing to define the lateral elements of homologous chromosomes in regions where synapsis was complete (Figure 3.6E). This was followed by the gradual removal of ASY1 from the lateral elements at the completion of synapsis, with protein detected as foci found throughout the nucleoplasm (Figure 3.6F, G). These foci were not confined to regions containing chromatin, but were instead localised more towards the nuclear periphery. No ASY1 signal was detected at late-diplotene or diakinesis, as individual chromosomes became more readily distinguishable

(Figure 3.6H). Absence of an ASY1 signal persisted throughout the remaining stages of meiosis examined (see Appendix B – Figure 4).

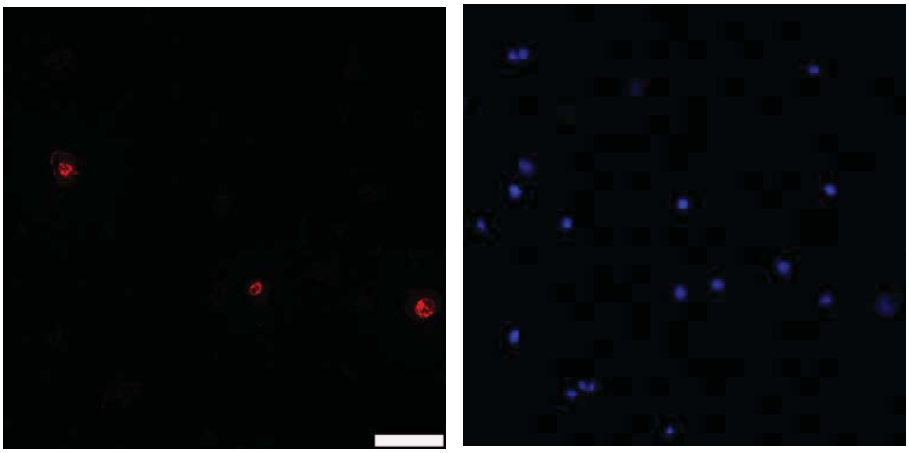

Figure 3.5 – Immuno-fluorescence localisation using anti-*Ta*ASY1 immune sera detected *Ta*ASY1 only in meiocytes during prophase I. Of meiotic and mitotic cells extruded from anthers, *Ta*ASY1 (shown in red) was detected only in meiotic cells during prophase I, and not in cells of later meiotic stages or in mitotic cells. The blue signal represents DAPI counter staining of DNA (bar = 100 μm).

Figure 3.6 – Immuno-fluorescence localisation of *Ta*ASY1 during pre-meiotic interphase and throughout prophase I. (A) Pre-meiotic interphase, (B) leptotene, (C) early-zygotene, (D) late-zygotene, (E) pachytene, (F) early-diplotene, (G) late-diplotene, (H) diakinesis. Panels on the top display *Ta*ASY1 in white, and panels on the bottom show merged ASY1 (red) with DAPI (blue) (bar = 10 μm). The white arrow heads in (D) indicate synapsis forks, displaying active sites of synapsis.

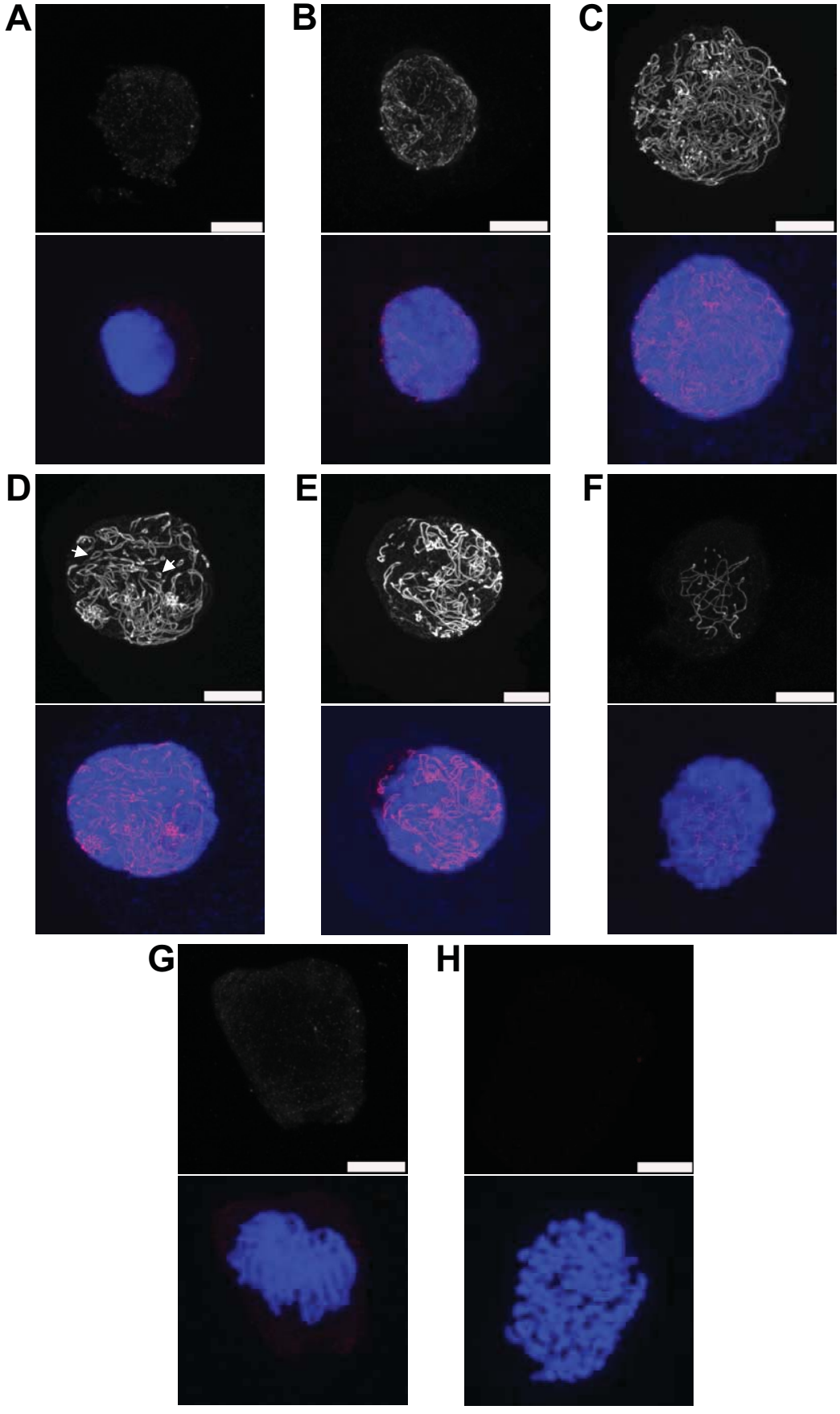
A
B
C
D
E
F
G
H

3.4 – Discussion

3.4.1 – Using localisation studies to understand the role of *Ta*ASY1

Results presented in this chapter have shown the spatial and temporal localisation of *Ta*ASY1. While such experiments have been performed previously in diploid plant species such as Arabidopsis, *B. oleracea*, rice and rye, localisation of an ASY1 homologue has not been investigated in a polyploid organism such as bread wheat. As such, the aim of the work presented in this chapter was to identify similarities and differences between these observations and those already reported in diploid species.

Initial localisation of *Ta*ASY1 protein was performed using western blot analysis to identify tissue types that contain *Ta*ASY1. This result largely supports the *TaASY1* transcript expression analyses that were presented in Chapter 2, with a high level of *Ta*ASY1 protein found in meiotic tissue. While this result is supported by observations of ASY1 homologues in Arabidopsis, *B. oleracea* and rice, the very low levels of *Ta*ASY1 detected in vegetative tissues contrasts western analysis of ASY1/PAIR2 in these other species (Armstrong et al., 2002; Nonomura et al., 2006). This difference may be attributed to alternative experimental procedures used, such as the protein extraction procedure or the higher concentration of primary antibody used in this study. Either way, as localisation of *Ta*ASY1 was restricted to meiotic prophase I cells within a collection of both meiotic and mitotic cells extruded from anthers (Figure 3.5), it appears that the low level signal detected is unlikely to represent an active role for *Ta*ASY1 in vegetative tissue.

Localisation of *Ta*ASY1 in meiocytes was initially performed using immuno-gold based electron microscopy. However, this work was expanded upon using immuno-fluorescence microscopy at a later date. The benefit of using these two techniques in conjunction is that the electron microscopy provided very detailed spatial localisation of the

protein, while the fluorescence microscopy allowed stage-wise activity (with reference to time and position) of *Ta*ASY1 to be monitored. The combined data reported here has clearly provided insight into the role of *Ta*ASY1 during prophase I, especially in relation to chromosome pairing and synapsis.

Firstly, sections of cells stained with uranyl acetate and lead citrate displayed well defined SC structures (Figure 3.3). All of the structures one would expect to see within a SC were present; including the chromatin of each chromosome within the pair, the chromosome axes which are also known as lateral elements, and the central region which contained examples of recombination nodules. Further examination of the labelled SCs revealed that *Ta*ASY1 specifically localised to the chromatin associated with the lateral elements, and appeared to be randomly distributed throughout the chromatin. While these results do not necessarily define a role for *Ta*ASY1 in either pairing or synapsis, they do suggest that it does not form a structural component of the SC, nor is it likely to have a role in recombination.

Support for these conclusions comes from previous observations of proteins that do have roles in such processes. Immuno-gold localisation of proteins that form a component of the lateral element typically results in a more linear pattern than that observed with *Ta*ASY1, with the proteins found to closely juxtapose the chromosome axes (Anderson et al., 1994; Higgins et al., 2005). In addition, proteins with a role in recombination are typically found in clusters that localise to recombination nodules within the central region of the SC, which was not found to be the case with *Ta*ASY1 (Anderson and Stack, 2005; Lhuissier et al., 2007).

To further investigate the possible role of *Ta*ASY1, axial elements were observed to determine whether *Ta*ASY1 localised to chromatin prior to formation of the SC. Axial elements represent the chromosome axes prior to formation of the SC (which later become lateral elements), and therefore represent the observable structure of a chromosome that is involved in chromosome pairing and the initial stages of synapsis. Indeed, *Ta*ASY1 was found

to localise to the chromatin next to the axial elements in a random distribution, thus supporting a role for the protein in pairing and the initial stages of synapsis. These two sets of results support previously reported observations of ASY1 in *B. oleracea* and PAIR2 in rice (Armstrong et al., 2002; Nonomura et al., 2006). Furthermore, the immuno-fluorescence experiments provide greater insight into the temporal activity of *Ta*ASY1. With no ASY1 detected in diplotene cells following the completion of synapsis, this clearly indicates that the role for the protein is complete once the SC begins to disassemble.

Immuno-fluorescence microscopy was conducted primarily to investigate the activity of *Ta*ASY1 during pre-meiotic interphase and prophase I. Both the timing of ASY1 appearance and disappearance, as well as the positioning of ASY1 at each of the stages correlates well with previous observations in Arabidopsis, *B. oleracea*, rice, rye and limited analysis in maize (Armstrong et al., 2002; Golubovskaya et al., 2006; Mikhailova et al., 2006; Nonomura et al., 2006). However, it was noted that the 'spiral' conformation adopted by ASY1 during diplotene in rye was not observed in bread wheat (which was also the case for ASY1/PAIR2 in Arabidopsis, *B. oleracea* and rice) (Mikhailova et al., 2006). This is perhaps a little surprising given that rye is a close relative to wheat, at least when compared to other organisms in which ASY1 has been investigated. This difference may not reflect a change in function of ASY1, but instead may represent a difference in the chromatin remodelling that occurs in rye compared to the other organisms (Fedotova et al., 1989). It is also possible that this discrepancy is an artefact of the experimental procedure used, as different reports have used slightly different techniques, including the para-formaldehyde concentration used in the fixative solution, which has previously been shown to cause differences in the detection of ASY1 (Golubovskaya et al., 2006).

In comparing the localisation of *Ta*ASY1 to known homologues from other species, it would be remiss not to mention *Sc*HOP1. Despite the weak amino acid sequence similarity

shared between *Sc*HOP1 and the characterised plant homologues, *Sc*HOP1 displays very similar spatial localisation to *Ta*ASY1, as well as *At*ASY1, *Bo*ASY1, and *Os*PAIR2 (Hollingsworth et al., 1990, Smith and Roeder, 1997; Armstrong et al., 2002; Nonomura et al., 2006). However, it has been reported that there are minor temporal differences in the localisation of *Sc*HOP1 compared to *At*ASY1 and *Os*PAIR2, with *Sc*HOP1 reported to be removed from the chromosomes immediately after the completion of synapsis, compared to *At*ASY1 and *Os*PAIR2 which appear to partially maintain their association with chromatin during diplotene (Smith and Roeder, 1997; Hamant et al., 2006). However, given the similar phenotypes of the *asy1*, *pair2* and *hop1* mutants, it is unlikely that this minor difference represents a functional divergence between *Sc*HOP1 and the plant homologues (Hamant et al., 2006).

Taken together, the immuno-gold and immuno-fluorescence localisation of *Ta*ASY1 have provided significant insight into its possible function. While it has already been discussed that *Ta*ASY1 is unlikely to form a component of the SC or have a role in recombination, its localisation to chromatin associated with axial and lateral elements prior to and at the complete formation of the SC suggests a role in pairing and/or synapsis. Given that *Ta*ASY1 first appears during pre-meiotic interphase, and begins to form defined structures during leptotene as axial elements are forming, it is possible that ASY1 has a role in axial element formation and/or elongation. However, results from analysis of the *pair2* mutant in rice suggest that ASY1 does not have a role in either of these processes, as it was shown that dense axial elements still form in this mutant, and that the axial elements are normal in size compared to those of wild-type meiocytes (Nonomura et al., 2006). Secondly, the localisation of *Ta*ASY1 to chromatin associated with axial and lateral elements supports a role for *Ta*ASY1 in synapsis. This is further supported by the detection of *Ta*ASY1 at sites where synapsis is occurring, as seen in Figure 3.6D, which were also observed in rye (Mikhailova et

al., 2006). Furthermore, Mikhailova et al. (2006) showed that in a rye mutant that failed to correctly synapse homologous chromosomes, ASY1 and ZYP1 (a known SC component) still load correctly onto chromosome axes without formation of the tripartite SC (Higgins et al., 2005). Therefore, it is plausible that localisation of *Ta*ASY1 to axial elements prior to synapsis may represent a role in recruiting components of the SC, such as ZYP1, to the axial elements in preparation for SC formation.

It is also possible that the localisation of *Ta*ASY1 represents a role for this protein in chromosome pairing. It has been shown that the Arabidopsis *asy1* mutant displays near normal centromere and telomere clustering behaviour during pre-meiotic interphase and leptotene. However, subsequent stages are atypical, with non-recognisable pairing and synapsis of homologues (Armstrong et al., 2001). This indicates that ASY1 is active between the time point where telomeres and centromeres first associate and homologues correctly synapse. In addition, it has been shown in bread wheat that centromeres of homoeologous chromosomes cluster together to form seven distinct groups during pre-meiotic interphase, before being resolved into 21 bivalents during prophase I (Martinez-Perez et al., 2003). Therefore, it is possible based on these observations and the localisation of *Ta*ASY1 presented in this chapter, that this protein has a role in chromosome pairing, perhaps in the resolution of homologues from the related homoeologues.

To provide a more definitive answer on the role(s) of the *Ta*ASY1 protein, several lines of experimentation could be investigated. This would include at least two main approaches, which are the focus of the following chapter. Firstly, through the generation and subsequent analysis of transgenic wheat plants that are defective for the *TaASY1* transcript, and secondly through the study of this gene/protein in known bread wheat pairing mutants (such as the *ph1* mutants) that have been previously characterised cytogenetically. In fulfilling

these objectives, a specific role for this protein in pairing and synapsis of homologous chromosomes would be obtained.

Chapter 4 - Investigating meiosis in *Taasy1* and *ph1b* mutants

4.1 – Introduction

Studies of *ASY1* and *PAIR2* in Arabidopsis and rice emanated from the identification of mutants that displayed reduced fertility, which in both cases, was shown to be caused by reduced synapsis of homologous chromosomes (Ross et al., 1997; Caryl et al., 2000; Nonomura et al., 2004). The reduced synapsis causes the appearance of univalents at metaphase I, which in turn leads to unequal segregation of homologous chromosomes at anaphase I (Ross et al., 1997; Nonomura et al., 2004). In rice, it was shown that the reduced synapsis is not caused by defects in axial element elongation, sister chromatid cohesion at centromeres or kinetochore assembly during meiosis I (Nonomura et al., 2006). In addition, the Arabidopsis *asy1* mutant displays near normal telomere pairing during pre-meiotic interphase and leptotene, indicating reduced synapsis is not caused by a pre-meiotic interphase/leptotene defect in the early stages of meiotic chromosome arrangements (Armstrong et al., 2001).

When combined with the localisation data presented in Chapter 3, these results suggest that ASY1/PAIR2 has a role in either homologous chromosome pairing or synaptonemal complex formation (Armstrong et al., 2002; Nonomura et al., 2004). However, defining a precise role for ASY1/PAIR2 in either pairing or synapsis is difficult, because the intimacy of the two events implies that a defect in one process is as likely as the other to cause reduced synapsis. Nevertheless, recent results from work investigating the function of *Sc*HOP1 provide evidence for a role for in chromosome pairing rather then chromosome synapsis (Carballo et al., 2008). Inter-homologue recombination is an essential meiotic event, as it ensures that homologous chromosome interactions are maintained until metaphase I, so that at anaphase I there is an equal segregation of chromosomes to each pole of the cell (Jones, 1987). This

process relies on a mechanism that promotes repair of DNA double-strand breaks *via* inter-homologue interactions rather then sister chromatid interactions, and it has been recently shown that *Sc*HOP1 facilitates this process (Carballo et al., 2008). Thus, while demonstration of a role for ASY1/PAIR2 in either chromosome pairing or synapsis is not yet resolved, these results from yeast imply a role for this protein in chromosome pairing, by promoting inter-homologue interactions rather then sister chromatid interactions.

One class of mutants that do display a definite defect in homologous chromosome pairing are the *pairing homoeologous* mutants from bread wheat (reviewed in Sears, 1976). It has been shown that deletion of the *Ph1* and *Ph2* loci, as well as a number of other loci throughout the bread wheat genome, results in homoeologous chromosome interactions in bread wheat and inter-specific hybrids (Okamoto, 1957; Riley and Chapman, 1958; Driscoll, 1972; Sears, 1977; Sears, 1982, Miller et al., 1983). Deletion of *Ph1* causes the strongest effect on chromosome pairing, which is displayed by the presence of multivalents at metaphase I (Okamoto, 1957; Riley and Chapman 1958; Sears 1977). Furthermore, subsequent research has shown that deletion of *Ph1* causes multiple defects in chromosome behaviour during pre-meiotic interphase and prophase I, including an arrest in synapsis at zygotene (Holm and Wang, 1988; Aragon-Alcaide et al., 1997; Martinez-Perez et al., 1999; 2001; Prieto et al., 2004; Colas et al., 2008). These observations further implicate synapsis with chromosome pairing, and indicate that the polyploid genome of bread wheat may provide insight into the relationship between synapsis and chromosome pairing that cannot be observed in a diploid organism. Interestingly for this study, it implies that bread wheat mutants with reduced activity of *TaASY1* may cause disruptions in chromosome pairing different from the observations of univalents at metaphase I in *asy1* and *pair2*.

This chapter presents the results of experiments that were performed to gain a greater understanding for the role of ASY1 during meiosis in bread wheat. More specifically,

experimentation was targeted to define whether or not ASY1 in bread wheat has a role in ensuring integrity of homologous chromosome interactions. As such, experimentation includes the analysis of both transgenic RNAi bread wheat mutants during meiosis that have reduced *TaASY1* activity, and the investigation of *TaASY1* activity and *Ta*ASY1 localisation during meiosis in the *Ph1* mutant, *ph1b.*

4.2 – Materials and methods

4.2.1 – Plant material and growth conditions

Hexaploid wheat plants including wild-type (*Triticum aestivum* cv. Bob White MPB26), the *ph1b* mutant, and *Taasy1* RNA interference (RNAi) mutants were grown under a 14 h photoperiod in a temperature controlled glasshouse with a minimum air temperature of 15°C and a maximum temperature of 23°C (Waite Campus, Adelaide, South Australia).

For the T_1 generation of the *Taasy1* mutant plants, a total of twelve lines were selected for germination. For lines that did not germinate using standard techniques, seed were vernalised to stimulate germination, which involved imbibing the seed in water for 16 h, followed by incubation at 4°C for 7 days on moist filter paper. Of the lines that successfully germinated (6 in total), 4-12 individual plants were grown for analysis (refer to Table 4.1).

For the T_2 generation, a total of eight lines were selected for analysis, with five originating from the T_1 generation line SB1525, and three selected from the T_1 line NW2804. In six of the T_2 lines, 10 plants were planted for genotype and phenotype analysis, while the two remaining lines (which had very low seed numbers) only had 3 and 1 seed planted for analysis (refer to Table 4.2).

Table 4.1 – A summary of selected T_1 *Taasy1* mutant plant lines. The two lines with allele names are those which contained plants used for analysis in the T_2 generation. An additional six lines failed to germinate (lines not shown in Table).

Selected lines for T_1 generation (allele name)	Number of germinated plants
SB1525 (asy1-1)	12
NW2804 (asy1-2)	12
SB1687	12
SB1984	10
SB1753	12
SB1534	4

Table 4.2 – A summary of selected T_2 *Taasy1* mutant plant lines. Seed for lines SB1525.6 and SB1525.12 was very limited based on seed set from the preceding generation. The allele names used in this study are shown in red.

Selected lines for T_2 generation (allele name)	Parental line	Number of germinated plants
SB1525.7 (asy1-1.7)	SB1525	10
SB1525.9 (asy1-1.9)	SB1525	10
SB1525.11 (asy1-1.11)	SB1525	10
SB1525.6 (asy1-1.6)	SB1525	1
SB1525.12 (asy1-1.12)	SB1525	3
NW2804.2 (asy1-2.2)	NW2804	10
NW2804.4 (asy1-2.4)	NW2804	10
NW2804.9 (asy1-2.9)	NW2804	10

4.2.2 – Generating *Taasy1* mutant plants

4.2.2.1 – Construction of the RNA interference (RNAi) vector

Using the backbone construct that is present in all biolistic transformations conducted in the laboratory or Prof. German Spangenberg (a collaborator within Molecular Plant Breeding Co-operative Research Centre (MPB CRC)) (refer to Figure 4.1 and Appendix C – Figure 1), an RNA interference construct was designed and made that contained sequence complementary and specific to the *TaASY1* cDNA clone (see Appendix A – Figure 1). This sequence corresponded to nucleotides 1057-1317 of the *TaASY1* open reading frame, with the sense and anti-sense sequences being separated by an intron of 397 bp. Transcription of the RNAi cassette was controlled by the *Actin* promoter, with the construct also containing the *bar* gene (enabling resistance to the herbicide Basta) to act as a selectable marker for transformed plants. Activity of the *bar* gene was controlled by the *Ubiquitin* promoter. This construct was generated in the laboratory of Prof. Spangenberg.

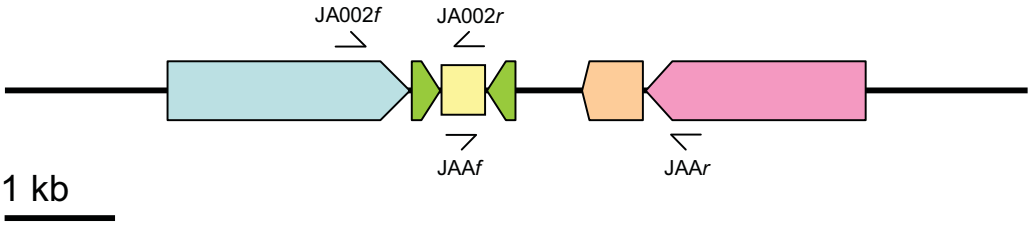

Figure 4.1 – Schematic diagram of the construct used to generate the *Taasy1* RNAi lines. The blue arrow represents the *Actin* promoter used to promote the activity of the RNAi cassette which contains sequence complementary to the *TaASY1* open reading frame (green arrows) (nucleotides 1057-1317), separated by an intron (yellow). The orange arrow represents the selection gene (*bar* – enabling resistance to the herbicide Basta) used to identify positive transformed plants. The pink arrow represents the *Ubiquitin* promoter.

4.2.2.2 – Transformation of Bread Wheat (Bob White MPB26)

Transformation of bread wheat plants (cv. Bob White MPB26) was conducted in the laboratory of Prof. German Spangenberg at the Victorian AgriBiosciences Centre, La Trobe University, Victoria, Australia. Transformation was performed *via* microprojectile particle bombardment of immature wheat embryos (15 to 20 days post-anthesis) as previously reported (Pellegrineschi et al., 2002). The T_0 generation was grown at the Victorian AgriBiosciences Centre, and seed collected from these plants were delivered to the Waite Campus of the University of Adelaide, where T_1 and T_2 analysis was conducted.

4.2.3 – Genotype analysis

4.2.3.1 – Identification of positive transgenic plants *via* PCR

Positive transgenic plants of both the T_1 and T_2 generation were identified using PCR. In both cases, PCR was performed using two sets of primers. The first primer pair was designed to amplify a fragment from the transformed construct to identify positive transgenic plants, while the second amplified a fragment from the bread wheat genome to ensure genomic DNA integrity. For both the T_1 and T_2 generation, DNA samples were obtained using the REDExtract-N-Amp Plant PCR Kit (Sigma-Aldrich, Missouri, U.S.A.) according to manufacturer's instructions, with the following exceptions. To each leaf sample, 40 µL of extraction buffer was added prior to incubation at 95°C for 10 min, which was followed by the addition of 40 µL of dilution buffer. The extractions were performed in PCR strip tubes (Astral Scientific, New South Wales, Australia).

4.2.3.1.1 – Identification of positive T_1 transgenic plants

PCR analysis was performed on all T_1 plants with the REDExtract-N-Amp PCR ReadyMix, according to manufacturer's instructions (Sigma-Aldrich). The primers used to confirm the

integrity of the extracted DNA samples were eASY1*f* (5' – GCTAATGATGCTAACAGTGATGATGAC - 3') and eASY1*r* (5' – GTGGACTAACACTATAAAGAAATCTG - 3'), which were expected to amplify a fragment of 762 bp. The primers used to identify positive transgenic plants were primers JAA*f* (5' – CTATTCATCATGTGACATACTTCCCCA - 3') and JAA*r* (5' – GCCCTGCCTTCATACGCTATTT - 3'), which were expected to amplify a fragment of 1749 bp. These two primer sets were included within the one reaction. The primer annealing temperature used in the reaction was 56°C, and the extension time was 2 min. PCR products were separated by gel electrophoresis using 1.5% (w/v) agarose gels and visualised by ethidium bromide staining.

4.2.3.1.2 – Identification of positive T_2 transgenic plants

PCR analysis was performed on all plants within each of the T_2 lines, using the DNA samples extracted in 4.2.3.1. As per the T_1 PCR analysis, primers eASY1*f* and eASY1*r* were used to confirm the integrity of the extracted DNA samples. Primers JA002*f* (5' – GAATGGGGCTCTCGGATGTAGAT - 3') and JA002*r* (5' – GCATTTTTTTCCATGTCACCTGC - 3'), which were expected to produce a fragment of 788 bp, were used to identify positive transgenic plants. Separate reactions were performed for each primer set. The annealing temperature and extension time used in each reaction were 56°C and 1 min, respectively. PCR products were separated by gel electrophoresis using 1.5% (w/v) agarose gels and visualised by ethidium bromide staining.

4.2.3.2 – Southern blot hybridisation

Southern blot analysis was performed to determine the number of transgene insertions in each line. This was performed using DNA from plants of the T_1 generation.

4.2.3.2.1 – DNA extraction

DNA was extracted from positive transgenic plants identified within each of the T_1 generation lines that were analysed. DNA was also extracted from one null-transgenic plant of each line, which was to be used as a negative control in the hybridisation experiments. DNA was isolated and quantified as per 2.2.4.1.

4.2.3.2.2 – Genomic DNA digestion and transfer to membrane

Genomic DNA of the selected T_1 plants was digested using the restriction enzyme *Nco*I. Digestion reactions contained genomic DNA (15 µg), *Nco*I (30 U; Roche, New South Wales, Australia), 10X Restriction Enzyme Buffer H (1.5µL; Roche) and milli-Q water in a total volume of 15 µL. Reactions were incubated at 37°C for 16 h, followed by enzyme inactivation at 65°C for 15 min. Products of the digestion reactions, as well as an undigested sample of plasmid DNA from 4.2.2.1 (to be used as a positive control), were separated *via* gel electrophoresis on a 1% (w/v) agarose gel run at 33 V overnight (approximately 16 h). The DNA was then transferred onto Biodyne® B membranes (0.45 µm) (Pall Life Sciences, Florida, U.S.A.) using a standard capillary transfer blotting technique (Sambrook et al., 1989).

4.2.3.2.3 – Southern blot analysis

Southern blot analysis was performed as per 2.2.4.2.1, except that the probe used to hybridise the membranes was amplified using primers JA002*f* and JA002*r* (see 4.2.3.1.2). The PCR solution used to amplify the probe contained 10X PCR Buffer (2 µL); $MgCl_2$ (50 mM, 0.8 µL); dNTPs (1.25 mM, 3.2 µL); primer JA002*f* (10 µM, 1 µL); primer JA002*r* (10 µM, 1 µL), *Taq* polymerase (1.25 U, Invitrogen, Victoria, Australia), plasmid DNA (as per 4.2.2.1; 50 ng) and milli-Q water (12.25 µL). The PCR cycle conditions were denaturation at 94°C for 2 min, followed by 35 cycles of 96°C for 30 sec, 56°C for 2 min, extension at 72°C for 1 min,

followed by a final extension at 72°C for 10 min. Following gel electrophoresis of the PCR product on a 1.5% (w/v) agarose gel and visualisation using ethidium bromide, the probe fragment (788 bp) was excised and gel purified as per 2.2.3.4.1.

4.2.4 – RNA and protein analysis

RNA samples were extracted from all positive transgenic plants of the T_1 generation, as well as a null-transgenic plant from each line. In addition, RNA samples were collected from the following: all plants of lines *asy1-1.9*, *asy1-2.2*, *asy1-1.12* and *asy1-1.6* from the T_2 generation, the *ph1b* mutant, and wild-type bread wheat (cv. Bob White MPB26 and Chinese Spring) for use as a control. Protein samples were also collected from the *ph1b* mutant and wild-type bread wheat (cv. Chinese Spring).

4.2.4.1 – Collection of meiotic tissue from *Taasy1* mutants

Whole spikes of the *Taasy1* mutants (for both T_1 and T_2 generation) and the wild-type Bob White MPB26 controls were collected when the anthers of the central spikelet were at the stage of prophase I (as per 2.2.2). Whole spikes were placed in 2 mL tubes, and immediately frozen using liquid nitrogen, before being stored at -80°C.

4.2.4.2 – Collection of meiotic tissue from *ph1b*

Using the procedure outlined in 2.2.2, staged anthers were collected from the *ph1b* mutant for RNA and protein extraction. Anthers were immediately frozen using liquid nitrogen and stored at -80°C. Anthers were pooled into one of four groups according to the determined meiotic stage. The four groups were pre-meiotic interphase (PM), leptotene to pachytene (LP), diplotene to anaphase I (DA) and immature pollen (IP). This was performed to replicate the collection of wild-type anthers performed in 2.2.3.1, with the exception of no anthers having been collected for the stages of telophase I to telophase II, tetrads and mature anthers.

4.2.4.3 – RNA and protein extraction

RNA and protein extractions were performed using Trizol reagent (Invitrogen), according to manufacturer's instructions. RNA samples were prepared and quantified as per 2.2.3.1. Protein samples of the *ph1b* mutant were re-suspended in 50 µL of protein re-suspension buffer (10 M Urea, 50 mM DTT),. The protein samples were incubated at room temperature for 1 h, followed by incubation at 50°C for 10 min to facilitate re-suspension. Protein concentrations were determined using the Bradford assay, as per 3.2.3.1.

4.2.5 – *TaASY1* expression analysis in *Taasy1* and *ph1b*

Quantitative real time PCR (Q-PCR) was performed using cDNA synthesised from RNA samples extracted in 4.2.4. In the *Taasy1* mutants, Q-PCR was performed to determine levels of *TaASY1* transcript relative to wild-type plants (cv. Bob White MPB26). Q-PCR using cDNA from *ph1b* was performed to determine whether the levels of *TaASY1* transcripts across a meiotic time-course were altered in this mutant. Western blot analysis was performed as a semi-quantitative assay to determine the levels of *Ta*ASY1 protein in the *ph1b* mutant relative to wild-type plants (cv. Chinese Spring).

4.2.5.1 – Q-PCR analysis of *Taasy1* mutants

Individual cDNA synthesis reactions were performed for each of the *Taasy1* mutants from the T_1 and T_2 generation, as well as the wild-type controls, as described in 2.2.7.4. Q-PCR analysis was performed as per 2.2.7.4, with the following exceptions. Firstly, rather then comparing levels of *TaASY1* transcripts across different stages of meiosis, comparisons of *TaASY1* transcripts were made between each of the mutants and the wild-type controls to determine relative levels of *TaASY1* transcripts in the mutants. Secondly, for analysis of the T_1 cDNA samples, normalisation of the *TaASY1* transcripts was performed using the three control genes

Ta.28350.1.S1_a_at, *TaGAPdH* and *TaActin1*. The control genes used to normalise the data from the T_2 mutant plants included Ta.9657.1.S1_at, Ta.28350.1.S1_a_at and *TaEFA*.

4.2.5.2 – Q-PCR analysis of *ph1b*

Individual cDNA synthesis reactions were performed for each of the four staged anthers (PM, LP, DA and IP) using cDNA that was extracted in 4.2.4.3, as per 2.2.7.4. Q-PCR analysis was performed as per 2.2.7.4, with the following exception. Not all of the stages used in 2.2.7.4 were used in this analysis, with no comparisons made between *ph1b* and wild-type at the stages telophase I to telophase II, tetrads or mature anthers. The levels of *TaASY1* transcripts detected in *ph1b* were normalised using control genes Ta.9657.1.S1_at, Ta.28350.1.S1_a_at and *EFA* (as per wild-type in 2.2.7.4), and were compared to the wild-type data obtained in 2.2.7.4.

4.2.5.3 – Western blot analysis of *ph1b* mutants

SDS-PAGE and western blot analysis was performed as described in 3.2.3.2 and 3.2.3.4, with the following exceptions. NuPAGE® Novex® Bis-Tris Gels (Invitrogen) were used for protein separation, as per manufacturer's instructions (Invitrogen). Each lane was loaded with 2 μg of extracted protein, which was subsequently transferred onto NitroBind pure nitrocellulose membranes (0.22 micron; GE Water and Process Technologies, Pennsylvania, U.S.A.), as per 3.2.3.2. Membranes were immunised with rabbit anti-*Ta*ASY1 antibody diluted 1:1500 with TBS-Tween 20 solution (25 mL), and subsequently immunised using an anti-rabbit alkaline phosphatase conjugated secondary antibody diluted 1:1000 with TBS-Tween 20 solution (25 mL). Following the washes to remove excess antibody, BCIP/NBT Purple Liquid Substrate System (Sigma-Aldrich) was added to the membranes for protein detection, with the enzyme reaction inactivated by addition of excess water, as per 3.2.3.3.

4.2.6 – Fertility analysis of *Taasy1* mutants

Fertility analysis was performed on *Taasy1* mutants of both the T_1 and T_2 generations, as well as wild-type bread wheat (cv. Bob White MPB26). Fertility analysis within the T_1 generation included analysis of null-transgenic plants.

4.2.6.1 – Analysis of whole plant morphology

Observations of germination rate, leaf development, plant height and flowering time were recorded for each of the T_2 generation *Taasy1* mutants. Following complete emergence of spikes from the sheaths (stage 10.5 of the Feekes scale), images were captured of whole plant and spike morphology, using representative plants from each line. These images were obtained using a Canon EOS 300D digital camera (Canon, New South Wales, Australia), equipped with a Canon EF-s 18-55mm lens (Canon) (for whole plant images) or a Tamron SP AF Di90mm 1:2.8 macro lens (Tamron, New York, U.S.A.) coupled to the Canon macro ring lite MR-14Ex flash unit (Canon) (for spike images).

4.2.6.2 – Analysis of pollen viability

Pollen abortion rates of *Taasy1* mutant plants (T_2 generation) were assessed using Alexander stain (Alexander, 1969). Anthers were collected prior to dehiscence (stage 10.54 of the Feekes scale) and mounted onto a glass microscope slide and immersed in Alexander stain. The Alexander stain contained 95% ethanol (10 mL), 1% malachite green in 95% ethanol (5 mL), 1% acid fuchsine in milli-Q water (5 mL), 1% Orange G in milli-Q water (5 mL), glacial acetic acid (2 mL), glycerol (2 mL), phenol (5 g) and milli-Q water (to a total volume of 100 mL). Pollen grains were released by gently tapping the anthers with a needle. Following release of the pollen, the empty anther debris was removed and a cover-slip was placed over the solution. The samples were incubated at 50°C for 3 h, and visualised using a Leica

DM1000 compound microscope (Leica Microsystems, New South Wales, Australia). Aborted (green) and non-aborted (red) pollen grains were counted for three plants from each of the lines *asy1-1.9* and *asy1-2.2*, as well as for three wild-type plants (cv. Bob White MPB26).

4.2.6.3 – Analysis of seed set in *Taasy1* mutants

Total seed numbers were detailed for each plant of the T_1 and T_2 generation to determine fertility levels of the *Taasy1* mutants relative to wild-type plants (cv. Bob White MPB26).

4.2.6.3.1 – Seed collection from T_1 and T_2 generation plants

For each T_1 generation plant, including both positive and null transgenics, the total number of seeds and spikes were recorded. For each T_2 generation plant, the total number of seeds, spikes and florets per spike were recorded. Seeds were primarily collected from the primary and tertiary tiller (seed were collected from additional tillers only if adequately developed). Post-harvest, seeds were dried at 37°C for 7 days before being stored at 4°C. An identical procedure was used for the collection of seed from wild-type plants.

4.2.6.4 – Data analysis

Statistical analysis of the variation in seed per head, seed per floret and pollen viability between T_2 generation *Taasy1* mutants and wild-type wheat was performed using a Student's two-tailed t-test assuming unequal variances (Microsoft© Office Excel Professional Edition, 2003).

4.2.7 – Analysis of chromosome morphology during meiosis

The morphology of chromosomes during prophase I, metaphase I and anaphase I were assessed in the *Taasy1* (T_2 generation) and *ph1b* mutants, and compared to wild-type plants (cv. Bob White MPB26 and Chinese Spring), using a protocol adapted from Sharma and

Sharma (1980). *Taasy1* plants used in this analysis were from the T_2 generation, including plants from line *asy1-1.9*, *asy1-1.12* and *asy1-2.2*.

4.2.7.1 – Collection of staged anthers

Anthers from the same floret as those staged at prophase I, metaphase I and anaphase I (as per the procedure outlined in 2.2.2) were placed in a 1.5 mL tube containing Carnoy's fixative (75% ethanol, 25% acetic acid), and incubated at room temperature for 48 h. Post-fixation, the anthers were washed in 70% ethanol (5 x 5 min). Washed anthers could be stored for up to a week; however, anthers were typically stained immediately after the completion of washes.

4.2.7.2 – Analysis of chromosome morphology using Feulgen's stain.

Following completion of the washes, supernatant was removed and replaced with 1 M hydrochloric acid (500 µL). Anthers were incubated at 60°C for precisely 13 min, followed by immediate removal of the hydrochloric acid. Feulgen's stain (500 µL; 0.4% Basic Fuschin, 1.8% sodium sulphate, 0.15 M hydrochloric acid) was immediately added to the samples to stain the anthers during incubation at room temperature for 3 h. Once stained, the anthers were briefly rinsed in 45% acetic acid, before being placed on a glass microscope slide in a drop of 45% acetic acid (2 anthers per slide). The meiocytes were then extruded from the anthers using a needle, with the anther debris then removed. A cover-slip was placed over the solution, and thumb pressure was applied to spread the chromatin/chromosomes. The underside of the slide was gently heated using an alcohol burner, and the cover-slip removed by dipping the slides in liquid nitrogen and then flicking it off using a scalpel blade. Once air-dried, a drop of Crystal Mount™ Aqueous Mounting Medium (Sigma-Aldrich) was applied to each sample, which was evenly distributed over the chromosome spreads by placing a new cover-slip on top of the sample.

4.2.7.3 – Image capture

The chromosome spreads were visualised using a Leica AS-LDM microscope (Leica Microsystems, Wetzlar, Germany) equipped with a HCX PL Fluotar 63X/0.70 Lens (Leica Microsystems). Images were captured using a Hitachi HV-C20A CCD camera (Hitachi Kokusai Electric Inc., Japan) and processed using LMD system software (v. 4.3.1, Leica Microsystems). As the stain was susceptible to fading, images were captured immediately after sample preparation.

4.2.8 – Immuno-localisation of *Ta*ASY1 in *Taasy1* and *ph1b* mutants

Localisation of *Ta*ASY1 during pre-meiotic interphase and meiosis I was assessed in the *Taasy1* and *ph1b* mutants using immuno-fluorescence microscopy. *Ta*ASY1 localisation in the *Taasy1* mutants was visualised in plants of the T_2 generation, specifically from individuals of line *asy1-1.9*, *asy1-1.12* and *asy1-2.2*.

4.2.8.1 – Collection of staged anthers

Anthers were staged and fixed as described in 3.2.5.1. For the *Taasy1* T_2 lines *asy1-1.9* and *asy1-2.2*, anthers of four plants were fixed for immuno-localisation, while anthers of two plants were fixed from line *asy1-1.12*. For analysis of the *ph1b* mutant, anthers were collected from multiple spikes of two separate plants.

4.2.8.2 – Sample preparation and immunisation

Meiocytes were extruded from anthers, embedded in poly-acrylamide pads, immunised with the rabbit anti-*Ta*ASY1 antibody and the Alexafluor^{TM} 568 anti-rabbit antibody, and counter-stained with DAPI as described in 3.2.5.2 and 3.2.5.3. For each plant, three slides were prepared, with each slide containing meiocytes from five anthers.

4.2.8.3 – Sample visualisation and image capture

The samples were visualised and images were captured as described in 3.2.5.4.

4.3 – Results

4.3.1 – *Taasy1* mutant analysis – T_1 generation

Analysis of the *Taasy1* mutants from the T_1 generation was performed to identify transgenic lines that could be used in the T_2 generation to provide reliable and accurate mutant phenotype data. For this reason, it was decided to keep the data for each T_1 transgenic line separate, to ensure that any variations in transformation events could be minimised. This decision is of particular importance when interpreting the fertility analysis of plants from the T_1 generation, due to the unexpected numbers of negative transgenic plants obtained in some lines, even though a sample size of 12 was analysed.

4.3.1.1 – Genotype analysis

Using fertility and plant development observations of the T_0 generation, 12 lines were chosen for T_1 generation analysis. Of these 12 lines, six failed to germinate, even after vernalisation. Within the six lines that did successfully germinate, four had 12 plants that germinated (SB1525, NW2804, SB1687, SB1753), while the remaining two had 10 and 4 plants (SB1984 and SB1534, respectively) (Table 4.3). PCR analysis was performed on each line to determine which plants were positive for the transgene, and positive plants were analysed *via* Southern blot hybridisation to determine the transgene copy number for each line (Figure 4.2; see Appendix C - Figures 2 and 3). Three of the lines (SB1525, SB1984 and SB1534) were found to have multiple insertions of the transgene within their genomes, while line NW2804 was found to contain a single copy of the transgene (Table 4.3). In each of the lines analysed using Southern blot hybridisation, all positive plants displayed the same banding pattern.

While both positive and negative transgenic plants were identified within each line, the expected segregation ratio of 3:1 was not observed in any of the lines. Both PCR analysis and Southern blot hybridisation provided inconclusive results for line SB1753, and hence no further work was performed on this particular line. A summary of the T_1 generation genotype analysis is shown in Table 4.3.

Table 4.3 – A summary of genotype analysis performed on *Taasy1* mutants from the T_1 generation. Genotype analysis revealed that of the six lines germinated, four contained multiple transgene copies, while one contained a single copy of the transgene. Ratios of positive to negative transgenic plants (based on the seed examined only) are given for each line (except for SB1753). The allele names of lines used for analysis at the T_2 generation are provided (lines SB1525 and NW2804). * n.d. (not determined) denotes information where genotype analysis was inconclusive.

Line name (allele)	# Plants Germinated	Transgene insertions	Positive transgenics	Segregation ratio
SB1525 (asy1-1)	12	5	10	5:1
NW2804 (asy1-2)	12	1	8	2:1
SB1687	12	7	5	1:1.4
SB1984	10	n.d.	5	1:1
SB1753	12	n.d.	n.d.	n.d.
SB1534	4	2	1	1:3

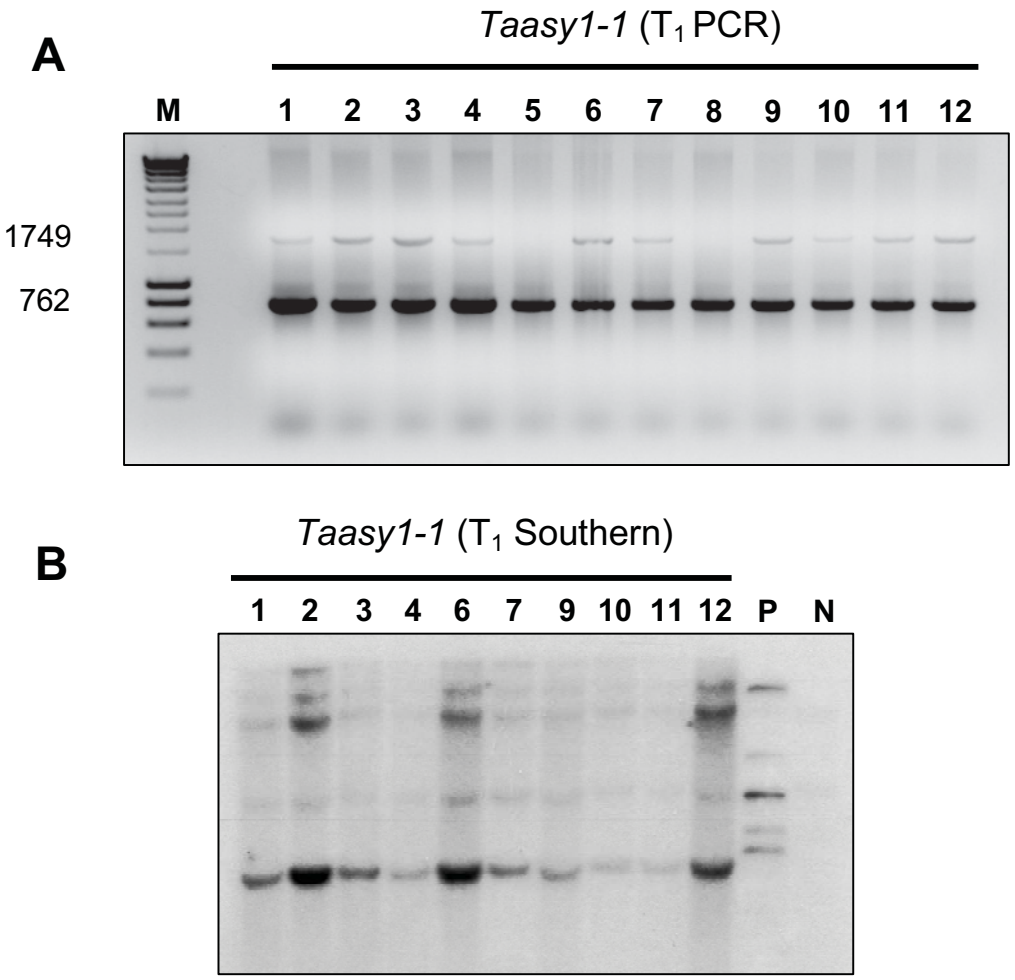

Figure 4.2 – Genotype analysis of T_1 generation *Taasy1* mutants. (A) Gel image of PCR analysis used to identify positive plants of line SB1525 (*asy1-1*) (lanes 1-12). The fragment at 1749 bp represents the transgene fragment amplified in positive transgenic plants, while the band at 762 bp represents the endogenous *TaASY1* gene fragment conferring genomic DNA integrity. Lanes 1-4, 6-7, 9-12 are positive transgenic plants. (B) Southern blot analysis of positive transgenic plants identified in (A) show that there are five (5) copies of the transgene inserted in SB1525 (*asy1-1*). The marker (M) used in (A) was the Bioline Hyperladder I (Bioline, New South Wales, Australia).

4.3.1.2 – Q-PCR analysis of T_1 generation *Taasy1* mutants

Q-PCR analysis of positive plants from the T_1 generation indicated that the abundance of *TaASY1* transcript was reduced (Figure 4.3). While positive plants within each line displayed varying levels of *TaASY1* transcript, the majority of positive transgenic plants were found to contain less *TaASY1* transcript then wild-type wheat. Transgenic plants of lines SB1525 (*asy1-*

1) and NW2804 (*asy1-2*) displayed the lowest levels of *TaASY1* transcript, with many individuals of these two lines displaying a two-fold reduction in normalised transcript copy numbers relative to the wild-type controls. To a lesser extent, reduced levels of *TaASY1* transcript were also observed in line SB1687. In addition, two transgenic plants of line SB1984 (SB1984.3 and SB1984.5) contained reduced levels of *TaASY1* transcripts; however, there were also three positive transgenic plants that contained levels comparable to wild-type wheat.

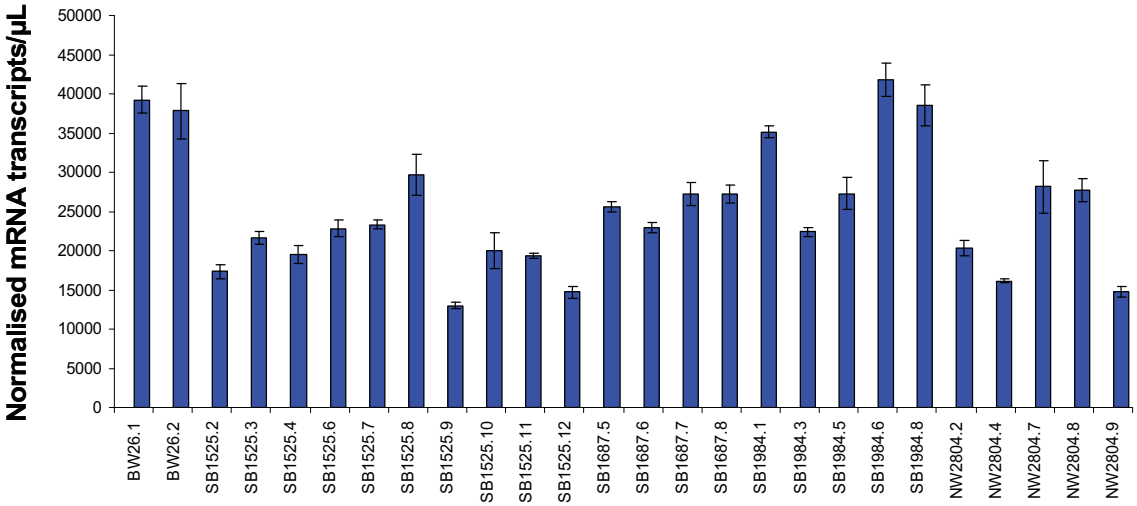

Figure 4.3 – Q-PCR analysis of T_1 generation *Taasy1* mutants. Q-PCR analysis of positive transgenic plants from lines SB1525, SB1687, SB1984 and NW2804 show that a number of plants contain reduced levels of *TaASY1* transcripts relative to wild-type wheat (BW26.1 and BW26.2). Error bars represent the standard deviation of three replicates.

4.3.1.3 – T_1 generation *Taasy1* plants display reduced fertility

Transgenic plants of the T_1 generation were assessed for fertility by performing seed counts of both positive and negative transgenic plants. High degrees of variability were observed between positive transgenic plants within each line and between positive plants of different lines (see Appendix C – Table 1). However, for all lines except SB1984, all positive transgenic plants were less fertile then the wild-type controls, and in the majority of cases,

positive transgenic plants were less fertile then negative transgenic plants. Lines SB1525 (*asy1-1*) and NW2804 (*asy1-2*) displayed the lowest levels of fertility, with examples of plants from both lines being completely sterile (*asy1-1.2*, *asy1-1.3* and *asy1-2.6*). The only difference in vegetative growth that was observed between transgenic plants and wild-type plants was that the transgenic plants produced fewer tillers. However, this was observed in both positive and negative transgenic plants and hence it is likely to be an effect of the transformation process.

4.3.2 – *Taasy1* mutant analysis – T_2 generation

Based on the results of the T_1 generation, a total of eight lines were selected for T_2 generation analysis, with five lines selected from SB1525 and three from NW2804. It was here that lines SB1525 and NW2804 were re-named *asy1-1* and *asy1-2*, respectively. The five lines selected from *asy1-1* included: *asy1-1.6*, *asy1-1.7*, *asy1-1.9*, *asy1-1.11* and *asy1-1.12*. Lines *asy1-1.6* and *asy1-1.12* were selected because they originated from T_1 generation plants with very low seed numbers (1 and 3, respectively). The three lines selected from *asy1-2* included: *asy1-2.2*, *asy1-2.4* and *asy1-2.9*.

4.3.2.1 – Genotype analysis

PCR analysis was performed to identify positive transgenic plants for phenotype analysis (Figure 4.4; see Appendix C – Figure 4). This included identifying T_2 generation lines that were likely to have originated from a T_1 individual that was homozygous for the transgene. All 10 offspring of *asy1-1.9* and *asy1-2.2* were positive for the transgene, indicating that the parental plants of these lines were more than likely homozygous for the transgene. Lines *asy1-1.7*, *asy1-1.11*, *asy1-2.4* and *asy1-2.9* contained both positive and negative plants, in a ratio that approached that expected for the offspring of a heterozygous T_1 individual (3:1) (Table 4.4). All plants from lines *asy1-1.6* (1) and *asy1-1.12* (3) were positive for the transgene.

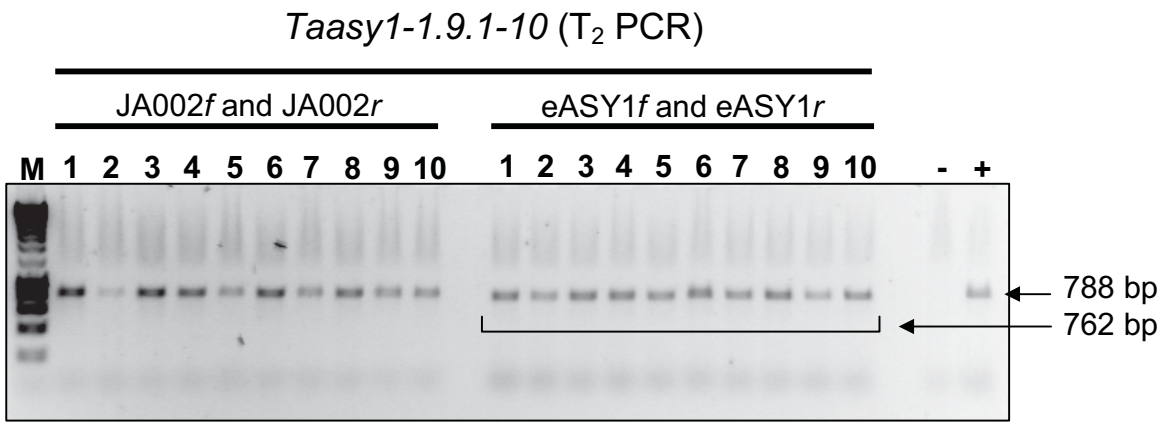

Figure 4.4 – Genotype analysis of T_2 generation *Taasy1* mutants *via* PCR. T_2 PCR analysis using primers JA002*f* and JA002*r* (788 bp product) confirmed the presence of the transgene in all 10 *Taasy1-1.9* plants (lanes 1-10), indicating that the positive plant from lane 9 in Figure 4.2A was homozygous for the transgene. Primers eASY1*f* and eASY1*r* (762 bp product) were used to confirm the genomic DNA integrity in these samples. Primers JA002*f* and JA002*r* were also used to ensure no amplification signal was obtained with the negative control template DNA (wild-type Bob White MPB26). Positive control DNA template used in the PCR was the vector shown in Figure 4.1, and resulted in amplification of the expected 788 bp product using primers JA002*f* and JA002*r*. The marker (M) used was the Bioline Hyperladder I (Bioline).

Table 4.4 – A summary of genotype analysis performed on *Taasy1* mutants from the T_2 generation. Genotype analysis revealed that of the six lines for which ten seed germinated, two were comprised of only positive transgenic plants (*asy1-1.9* and *asy1-2.2*). Ratios of positive to negative transgenics are given for those that contained negative plants (N/A is used for lines that did not contain negative plants).

Line name	# Plants Germinated	Positive transgenics	Segregation ratio
asy1-1.7	10	8	4:1
asy1-1.9	10	10	N/A
asy1-1.11	10	8	4:1
asy1-2.2	10	10	N/A
asy1-2.4	10	8	4:1
asy1-2.9	10	6	1.5:1
asy1-1.6	1	1	N/A
asy1-1.12	3	3	N/A

4.3.2.2 – Q-PCR analysis of T_2 generation *Taasy1* mutants

Q-PCR analysis was performed to determine whether T_2 generation *Taasy1* mutants had reduced levels of *TaASY1* transcripts, relative to wild-type controls. The results showed that while there was a degree of variation in transcript copy number between samples, all *Taasy1* plants had at least a 2-fold reduction of *TaASY1* transcript when compared to wild-type wheat (Figure 4.5). In general, plants of line *asy1-1.9* were found to contain higher levels of *TaASY1* transcript than lines *asy1-2.2*, *asy1-1.6* and *asy1-1.12*. Irrespective, as all 10 plants from lines *asy1-1.9* and *asy1-2.2* displayed reduced levels of *TaASY1* transcript relative to wild-type, these plants were used for the majority of the phenotype analysis. Plants from lines *asy1-1.6* and *asy1-1.12* also displayed reduced levels of *TaASY1* transcript, but they were only used for some of the phenotype analysis due to the limited sample sizes.

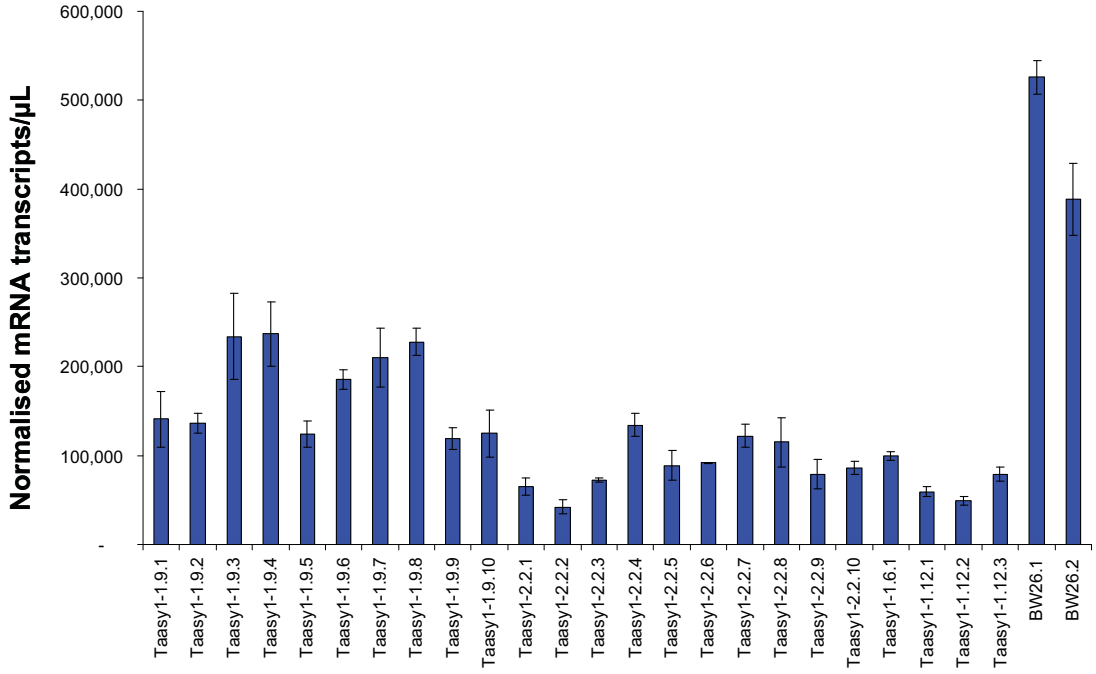

Figure 4.5 – Q-PCR analysis of T_2 generation *Taasy1* mutants. Q-PCR analysis of positive transgenic plants from lines *asy1-1.9*, *asy1-2.2*, *asy1-1.6* and *asy1-1.12* shows that all plants have reduced levels of *TaASY1* transcripts, relative to wild-type wheat (BW26.1 and BW26.2). Error bars represent the standard deviation of three replicates.

4.3.2.3 – *Taasy1* mutants display significant reduction in fertility

Phenotype analysis of the *Taasy1* mutants and wild-type plants was performed during stages of vegetative and reproductive development to identify changes in whole plant morphology caused by disrupted activity of *TaASY1*. After examining germination rate, leaf development, plant height and flowering time in the *Taasy1* mutants, it was concluded that there were no significant vegetative development differences (Figure 4.6A-D, whole plant phenotype panels only). However, observable differences in fertility were detected when comparing the reproductive structures of the *Taasy1* mutants with those of wild-type plants (Figure 4.6A-E, spike panels). Empty spikelets were often found towards the top half of spikes from the *Taasy1* mutants (Figure 4.6A-D, spike panels). These empty spikelets were later found to be devoid of seed following completion of plant ripening (stage 11.4 of Feekes scale).

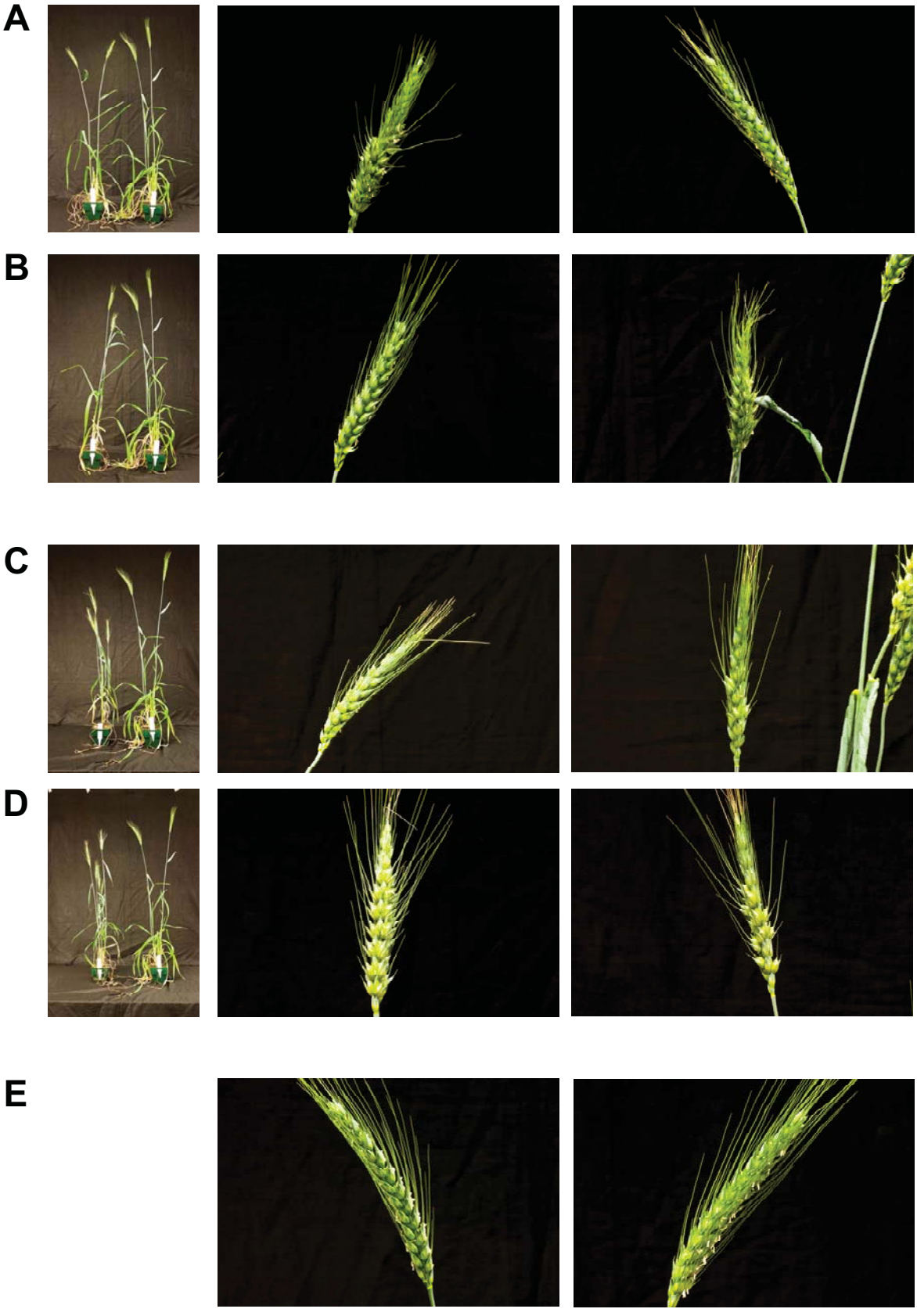
A
B
C
D
E

Figure 4.6 - Phenotype of *Taasy1* mutants (T_2 generation) compared to wild-type wheat during vegetative and reproductive development. (A-D) Whole plant images are shown with *Taasy1* mutants on left and control plants on right, with corresponding head images from those mutants shown in (A) *Taasy1-1.9.2*, (B) *Taasy1-1.9.5*, (C) *Taasy1-2.2.3*, (D) *Taasy1-2.2.8*. Images of heads from wild-type wheat controls are also shown (E). A distinct reduction of seed set in the mutant lines close to the top of each head when compared to the wild-type controls is evident as has been reported previously in *ph1b* (Sears, 1977).

Pollen viability was assessed in the *Taasy1* mutants using Alexander stain (Alexander, 1969), which stains aborted pollen green and non-aborted pollen red (Figure 4.7). Pollen counts from three plants of both *asy1-1.9* and *asy1-2.2* revealed a significant difference ($P < 0.001$) in pollen abortion relative to the wild-type plants, with a mean of 22.26% aborted pollen compared to a mean 9.06% for wild-type plants (Table 4.5).

Seed counts were also recorded for the *Taasy1* mutants and compared to those from wild-type plants. These comparisons provided further evidence of reduced fertility in the *Taasy1* plants, with a significant difference ($P < 0.001$) observed in the seeds per floret and seeds per head relative to those of wild-type wheat (Table 4.5).

Table 4.5 - Statistics of the number of seeds per floret, seeds per head and pollen abortion in RNAi *Taasy1* transgenic wheat plants (T_2) compared to wild-type wheat plants (Bob White MPB26). The standard deviation is given in parentheses. Student's t-test was used to test the null hypothesis that the two means in the presence or RNAi knock-down of *TaASY1* are the same. Null hypotheses can be discounted in all comparisons. Seeds/floret is expressed as the fraction of seeds observed from the total number of florets on any given head. Pollen abortion is expressed as a %.

	Transgenics	**Wild-type**	**t-test**
Seeds/floret	0.59 (0.27)	0.99 (0.02)	P <0.001
Seeds/head	24.5 (11.92)	48.13 (2.49)	P <0.001
Pollen viability	22.26 (0.04)	9.06 (0.01)	P <0.001

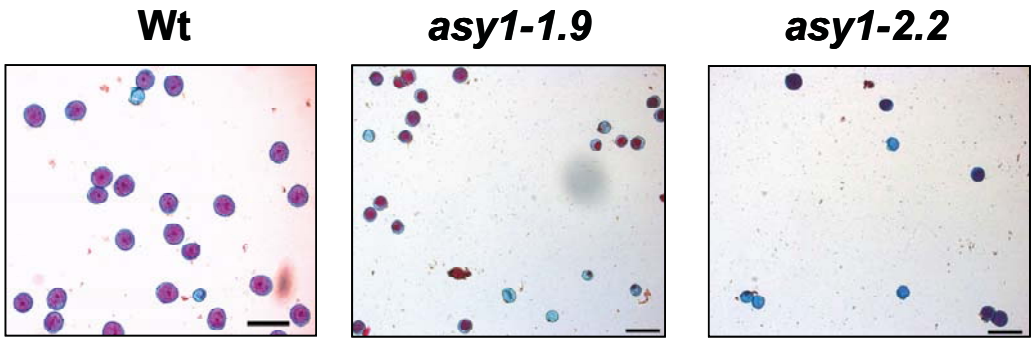

Figure 4.7 – Alexander stain shows increased pollen abortion in *Taasy1* mutants (T_2 generation). Aborted pollen cells are stained green and non-aborted pollen cells red. In addition, pollen size and shape were used to determine viability, with aborted pollen cells often appearing smaller in size and deflated in comparison to viable pollen cells. Scale bar, 500 µm.

4.3.2.4 – Meiotic chromosome morphology is disrupted in the *Taasy1* mutants

Parallel observations of meiotic chromosomes from the *Taasy1* mutants and wild-type plants were performed using Feulgen's stain to identify differences in chromosome morphology and distribution during prophase I, metaphase I and anaphase I (Figure 4.8). Analysis of chromosome morphology during prophase I showed that reduced bivalent formation and a lack of chromosome spreads representing a true pachytene cell were typical of numerous *Taasy1* mutants (Figure 4.8A, B). Differences in chromosome morphology were also evident during metaphase I, with *Taasy1* mutants displaying signs of homoeologous chromosome interactions (Figure 4.8C). In contrast to the 21 bivalents observed during metaphase I of wild-type wheat, *Taasy1* metaphase I spreads often contained multivalents as well as univalents. In addition, *Taasy1* mutants displayed more bivalents in a rod-like structure than observed in wild-type metaphase I, which typically contained ring-bivalents. During anaphase I, most *Taasy1* cells appeared regular, often displaying equal distribution of chromosomes to the opposite poles of the cell (Figure 4.8D). However, a number of cells did display abnormal chromosome arrangements, either through unequal segregation of chromosomes, chromosome "stickiness", or presence of a "lagging" chromosome (Figure 4.9).

These observations were consistent of multiple plants from the two independent transgenic lines that were investigated in this study (*asy1-1* and *asy1-2*) (Figure 4.10B-F). Furthermore, confirmation that the metaphase I phenotype observed in the *Taasy1* mutants was not an artifact of the transformation procedure was obtained by analysing plants (cv. Bob White MPB26) that had been transformed with a construct that did not contain any sequence complementary to *TaASY1*. Metaphase I chromosome preparations from these plants were identical to those of wild-type plants (Figure 4.10A).

Following the observation of chromosome arrangements in the *Taasy1* mutants being synonymous with homoeologous chromosome interactions, comparisons in chromosome morphology were made with the *pairing homoeologous* mutant, *ph1b* (Figure 4.8A-D). During zygotene, the chromosome morphology of the three genotypes was very similar. However, pachytene chromatin did adopt a different conformation in *ph1b* to that observed in wild-type plants, and a comparable stage for the *Taasy1* mutants (Figure 4.8A, B). During pachytene, the chromatin appeared to cluster towards the centre of the nucleus, with filamentous structures extending towards the nuclear periphery (Figure 4.8B). Metaphase I chromosome spreads were very similar to those of the *Taasy1* mutants, with multivalents, univalents and an increase in rod-like bivalents observed in multiple cells (Figure 4.8C). Finally, as was observed with the *Taasy1* mutants, most anaphase I cells of *ph1b* displayed regular chromosome segregation. However, there were a number of cells that displayed unequal patterns of chromosome segregation (Figure 4.8D). These observations of *ph1b* meiocytes are consistent with previous reports (Riley and Chapman, 1958; Sears 1977; Holm, 1988).

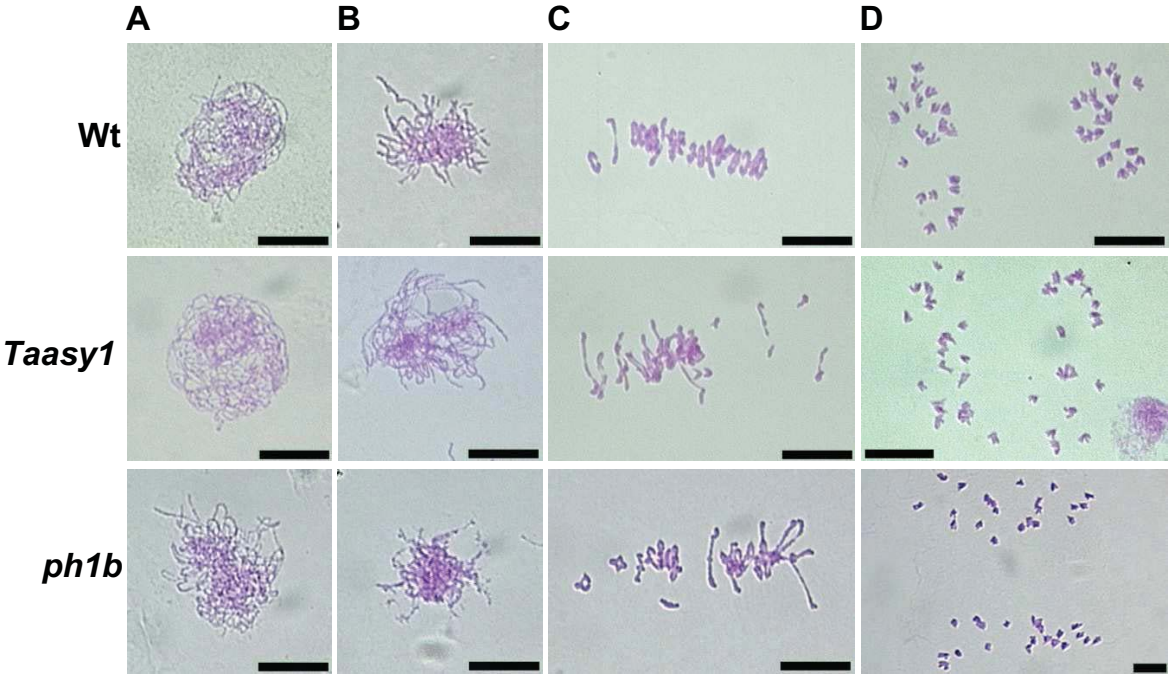

Figure 4.8 – Feulgen's-stained chromosome preparation of *Taasy1* mutants (T_2 generation) and *ph1b*. (A) At zygotene very few differences in chromosome morphology are observed between chromosome spreads from the three genotypes. (B) At pachytene differences in synapsis and chromosome morphology are clearly visible when comparing spreads from the three genotypes, with no true pachytene cell observed in the *Taasy1* mutants. (C) Metaphase I chromosome spreads reveal signs of homoeologous chromosome interactions in the *Taasy1* mutants, *via* detection of multivalents, and a higher incidence of rod bivalents, similar to that seen in the *ph1b* mutant. Univalents were also detected in *Taasy1* and *ph1b* mutants. (D) At anaphase I, chromosome segregation occurs normally in the *Taasy1* and *ph1b* mutants, with near-equal distribution of chromosomes to each pole. Scale bars, 25 μm.

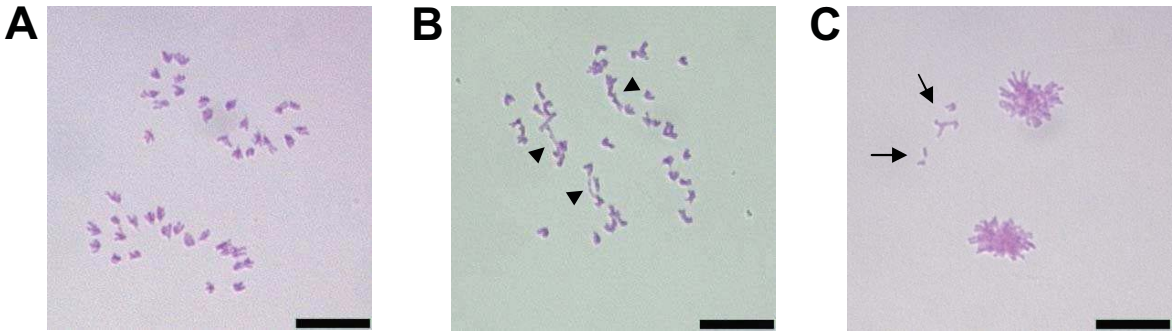

Figure 4.9 – Feulgen's–stained chromosome spreads of *Taasy1* mutants displaying various anaphase I phenotypes. Anaphase I chromosome spreads displaying: (A) Equal segregation of chromosomes to opposite poles of the cell. (B) Chromosome "stickiness". (C) The presence of "lagging" chromosomes. The arrows in (B) indicate signs of chromosome "stickiness", and the arrows in (C) indicate "lagging" chromosomes. The phenotype observed in (A) was observed in the majority of cases. Scale bar, 25 μm.

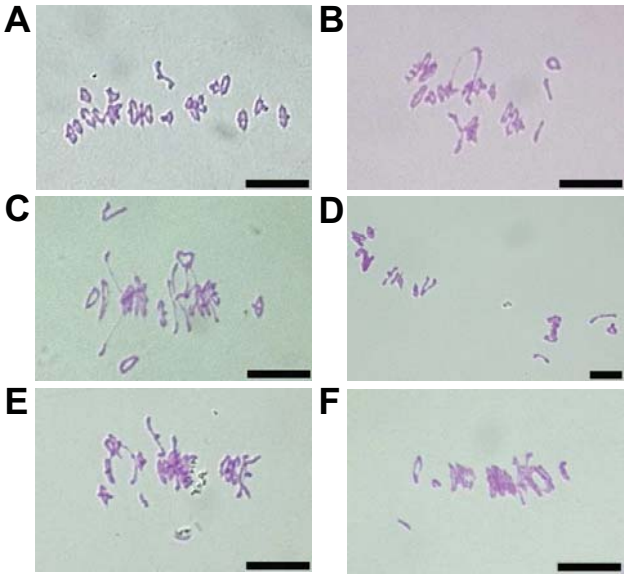

Figure 4.10 – Feulgen's-stained metaphase I chromosome spreads of independent transgenic lines (T_2 generation). (A) Control transformed Bob White MPB26 plant displaying a normal metaphase I (typical ring bivalents). (B-D) Metaphase I spreads from different plants within lines *Taasy1-1.9*. (E-F) Metaphase I spreads from different plants within lines *Taasy1-2.2*. Scale bar, 25 μm.

4.3.2.5 – *Ta*ASY1 localisation in the *Taasy1* mutants

Immuno-fluorescence microscopy was used to determine whether the localisation of the remaining *Ta*ASY1 protein was disrupted in the *Taasy1* mutants. The temporal localisation of ASY1 in the mutants appeared very similar to observations in wild-type wheat, with the protein first appearing during pre-meiotic interphase, becoming more abundant during leptotene and zygotene, before disappearing during diplotene and diakinesis (Figure 4.11A-G). However, there were clear structural differences detected when comparing the ASY1 signal of

Taasy1 mutants to that of wild-type wheat (Figure 4.11A-G). Firstly, while ASY1 was still found to load onto chromatin in a pattern similar to wild-type, the signal was less continuous and more diffuse. This resulted in the axial elements not being as well defined and the chromatin appearing less organised (Figure 4.11B-E). Furthermore, no signs of synapsis were observed in the mutants, with the ASY1 signal adopting a less-linear conformation rather then forming synapsis forks or a thickened ASY1 signal, as was observed during late zygotene and early pachytene in wild-type wheat (Figure 4.11D, E).

In association with the altered structures observed with the ASY1 signal in *Taasy1* plants, the ASY1 signal did not appear as intense in the mutants as it did in wild-type wheat. In addition, there were numerous *Taasy1* cells at leptotene and zygotene that did not contain an ASY1 signal (Figure 4.12A-C). Therefore immuno-fluorescence microscopy supported the Q-PCR analysis, displaying reduced *Ta*ASY1 protein levels in the *Taasy1* mutants.

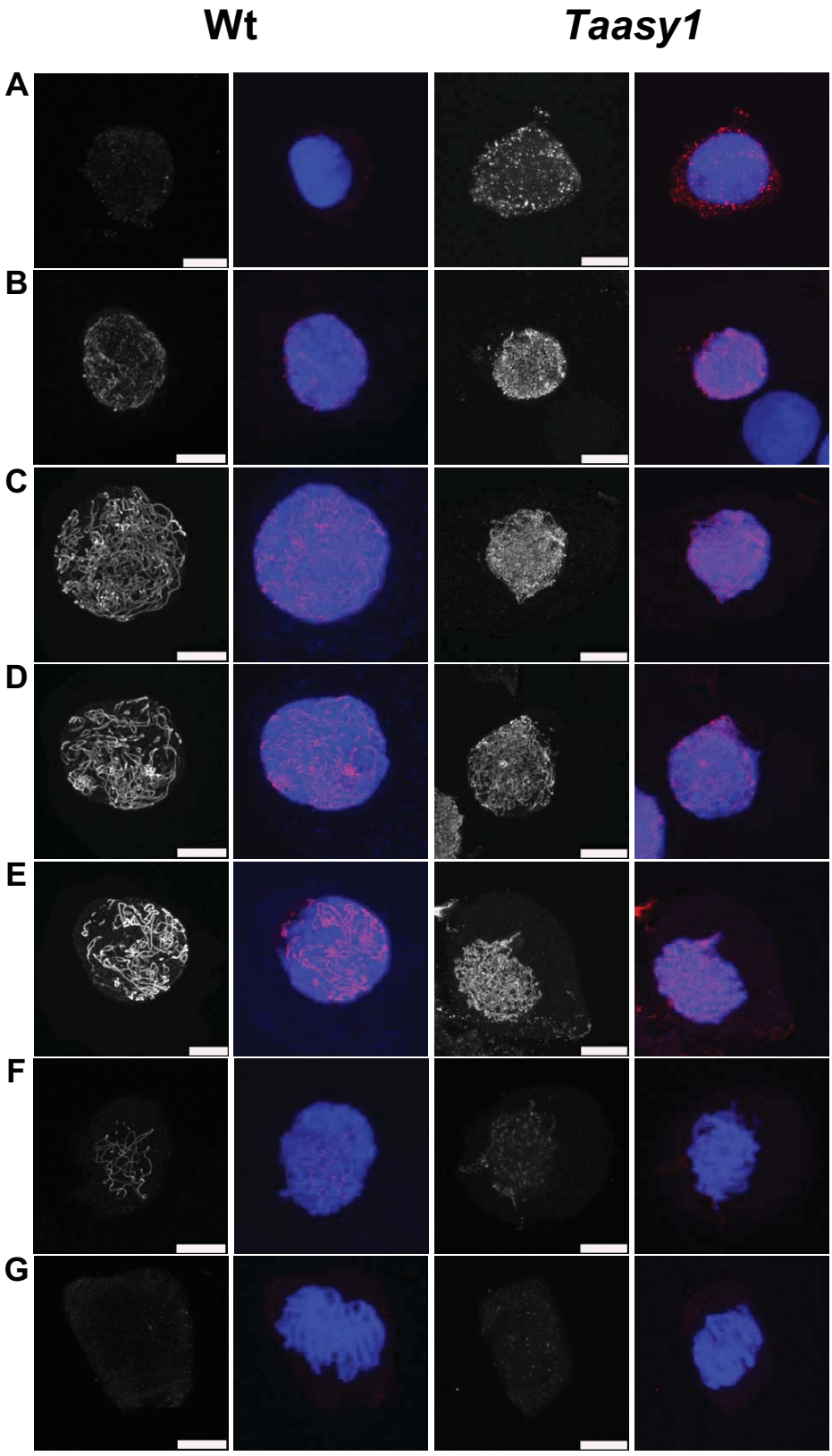
Wt
Taasy1
A
B
C
D
E
F
G

Figure 4.11 – Immuno-fluorescence localisation of *Ta*ASY1 during prophase I of *Taasy1* mutants. Localisation of *Ta*ASY1 and chromatin conformation is disrupted in the *Taasy1* mutants. (A) Pre-meiotic interphase, (B) leptotene, (C) early-zygotene, (D) late-zygotene, (E) pachytene, (F) diplotene, (G) diakinesis. For each genotype, panels on the left display ASY1 in white, while panels on the right show merged ASY1 (red) with DAPI (blue). Scale bars, 10 μm.

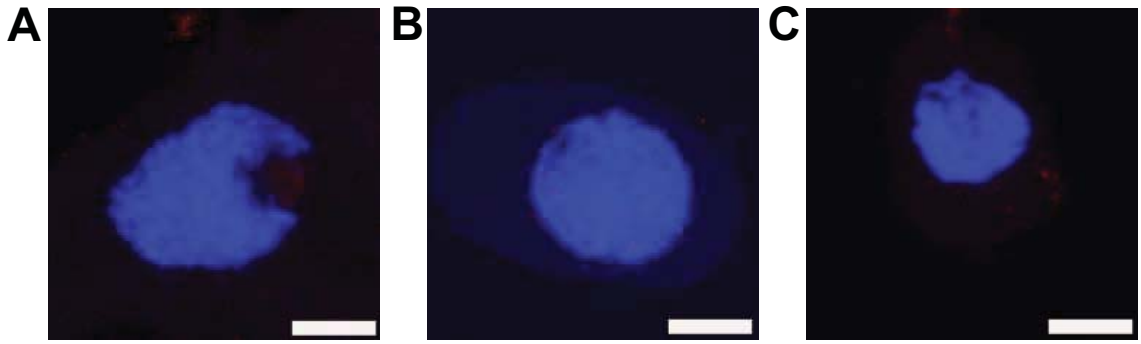

Figure 4.12 – Merged images of *Taasy1* cells lacking any detectable ASY1 protein. Numerous *Taasy1* cells progressing through early prophase I were found to be devoid of ASY1 signal, with examples found in all three lines analysed: (A) *asy1-1.9*, (B) *asy1-1.12* and (C) *asy1-2.2*. Blue represents DAPI, while small traces of red represent ASY1. Scale bars, 10 μm.

4.3.3 – Investigation of *TaASY1* in *ph1b*

Given the similarities in chromosome interactions that were observed at metaphase I in the *Taasy1* and *ph1b* mutants (see Figure 4.8), it was speculated that deletion of the *Ph1* locus may have been affecting the function of *Ta*ASY1. This hypothesis was investigated by: 1) comparing the levels of *TaASY1* transcripts in *ph1b* relative to wild-type plants, and 2) determining whether the localisation of *Ta*ASY1 was affected in *ph1b* when compared to wild-type.

4.3.3.1 – Q-PCR analysis of meiotic candidate genes in *ph1b*

Q-PCR analysis was used to determine whether the levels of *TaASY1* transcripts in *ph1b* were altered across a series of meiotic stages, relative to wild-type. This analysis showed that there was a significant increase in the level of *TaASY1* transcripts in *ph1b* during the meiotic stages

analysed, with a 20-fold increase during pre-meiotic interphase and leptotene to pachytene, relative to wild-type (Figure 4.13A). Despite the increase in transcript copy number detected in *ph1b*, the profile of *TaASY1* expression across the *ph1b* meiotic time-course remained identical to that of wild-type wheat (that is, it decreased).

To determine whether the increase in *TaASY1* transcript in *ph1b* is representative of a global up-regulation of meiotic genes in this mutant, Q-PCR analysis using the *ph1b* and wild-type meiotic time-course was performed for other meiotic candidate genes including *RAD51A*, *RAD51B* and *MSH4*. This analysis showed no significant change in transcript levels of these genes, either in relation to transcript copy number or expression profile across the meiotic time-course (Figure 4.13B-D).

Figure 4.13 – Q-PCR analysis of *TaASY1* and meiotic candidate genes during meiosis in *ph1b*. (A) Q-PCR reveals a 20-fold increase in *TaASY1* transcripts in *ph1b* compared to wild-type wheat, while no such increase was detected in transcript levels for (B) *RAD51A*, (C) *RAD51B*, or (D) *MSH4*. In each graph, the solid line represents transcripts from *ph1b*, while the broken line represents wild-type. PM = pre-meiotic interphase, LP = leptotene to pachytene, DA = diplotene to anaphase I and IP = immature pollen. Error bars represent the standard deviation of three replicates.

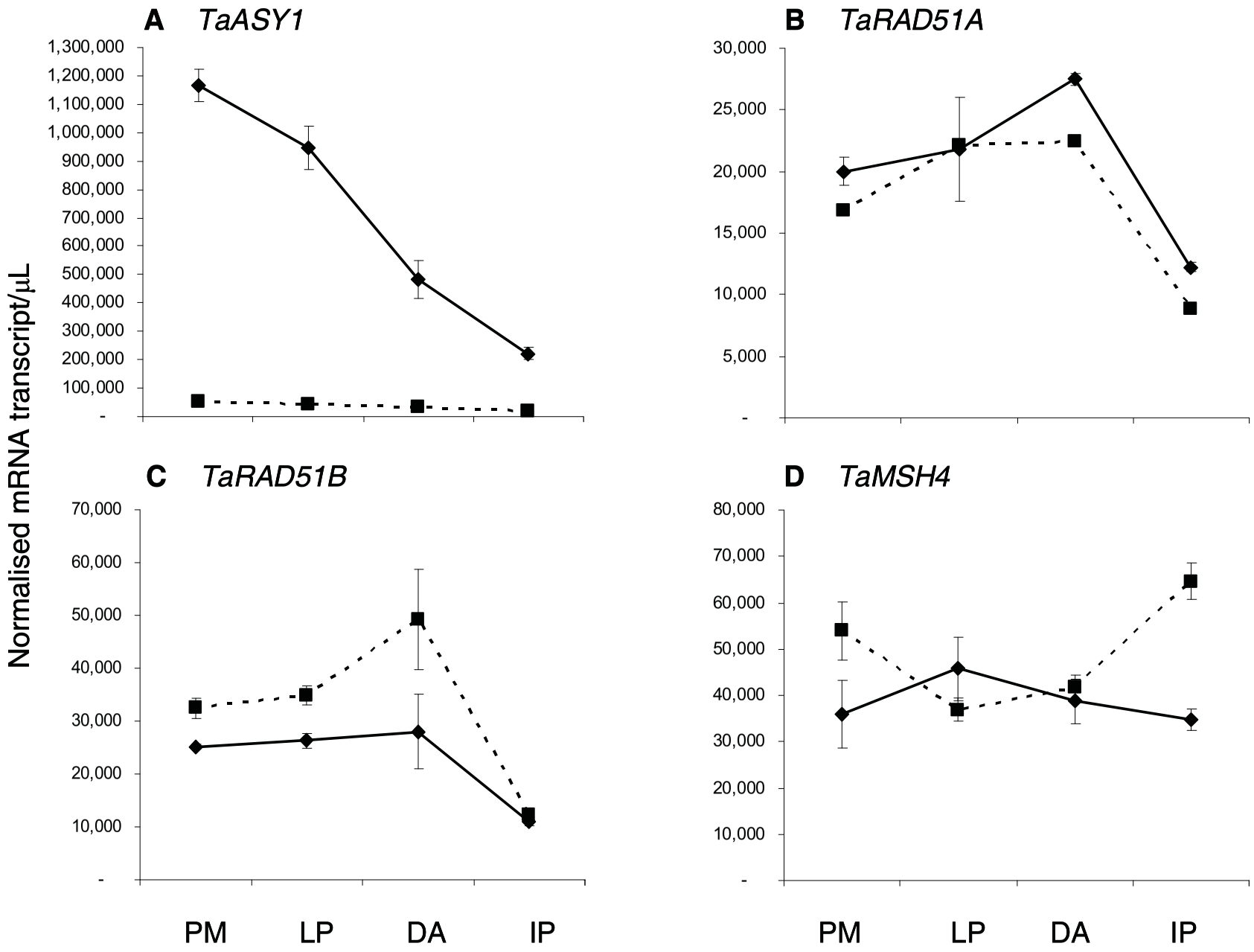
A TaASY1
B TaRAD51A
C TaRAD51B
D TaMSH4
Normalised mRNA transcript/µL
1,300,000
1,200,000
1,100,000
1,000,000
900,000
800,000
700,000
600,000
500,000
400,000
300,000
200,000
100,000
-
30,000
25,000
20,000
15,000
10,000
5,000
70,000
60,000
50,000
40,000
30,000
20,000
10,000
80,000
PM
LP
DA
IP

4.3.3.2 – Western blot analysis of *Ta*ASY1 in *ph1b*

Western blot analysis was performed using the anti-*Ta*ASY1 antibody to determine whether the levels of *Ta*ASY1 protein were higher during the meiotic time-course of *ph1b* than that of wild-type wheat (Figure 4.14). While this assay is less quantitative than Q-PCR, it provided evidence for increased levels of *Ta*ASY1 protein in *ph1b* during pre-meiotic interphase and diplotene to anaphase I, relative to wild-type. Similar levels of *Ta*ASY1 were detected during leptotene to pachytene and immature pollen from each genotype.

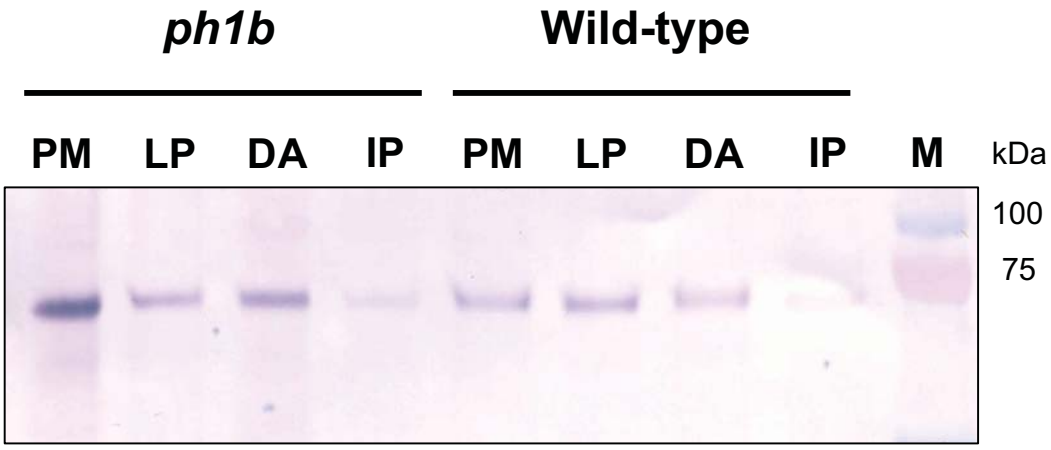

Figure 4.14 – Western blot analysis of *Ta*ASY1 protein during meiosis in *ph1b* and wild-type wheat (cv. Chinese Spring). *Ta*ASY1 protein during meiosis in *ph1b* and wild-type wheat indicates that higher levels of *Ta*ASY1 protein are present in *ph1b* than in wild-type wheat (this is particularly pronounced in the stage PM). PM = pre-meiotic interphase, LP = leptotene to pachytene, DA = diplotene to anaphase I, IP = immature pollen. The marker (M) is the PrecisionPlus Dual Color Marker (Bio-Rad, Victoria, Australia).

4.3.3.3 – Localisation of *Ta*ASY1 in *ph1b*

Given the elevated level of *TaASY1* transcript detected in *ph1b* relative to wild-type wheat, immuno-fluorescence microscopy was used to investigate whether the localisation of *Ta*ASY1 protein was also different in *ph1b*. As was observed in wild-type wheat, *Ta*ASY1 first

appeared in *ph1b* during pre-meiotic interphase, and persisted through prophase I until it was removed during diplotene and diakinesis (Figure 4.15A-G). This analysis indicated that the temporal localisation of *Ta*ASY1 was very similar in the two genotypes. However, there were clear structural differences observed when comparing the ASY1 signal of *ph1b* and wild-type wheat (Figure 4.15A-G).

Firstly, while the ASY1 signal still appeared to localise to chromosome axes during leptotene and early zygotene, there were clear signs of disorder observed during zygotene, as shown by the spiral-like conformation adopted by ASY1 during this stage (Figure 4.15B-D). The spiral-like conformation of ASY1 persisted until pachytene and early diplotene (Figure 4.15E-F). In addition, ASY1 'clusters' that are thought to represent polycomplexes, were found in the nucleolar region of *ph1b* meiocytes (Figure 4.15C-G). These ASY1 polycomplexes were only found in *ph1b*, and may represent elevated levels of *Ta*ASY1 protein in this mutant. Further support for there being elevated levels of *Ta*ASY1 protein in meiocytes of *ph1b* can be observed at leptotene, where the ASY1 signal was much stronger then that detected in wild-type wheat (Figure 4.15B).

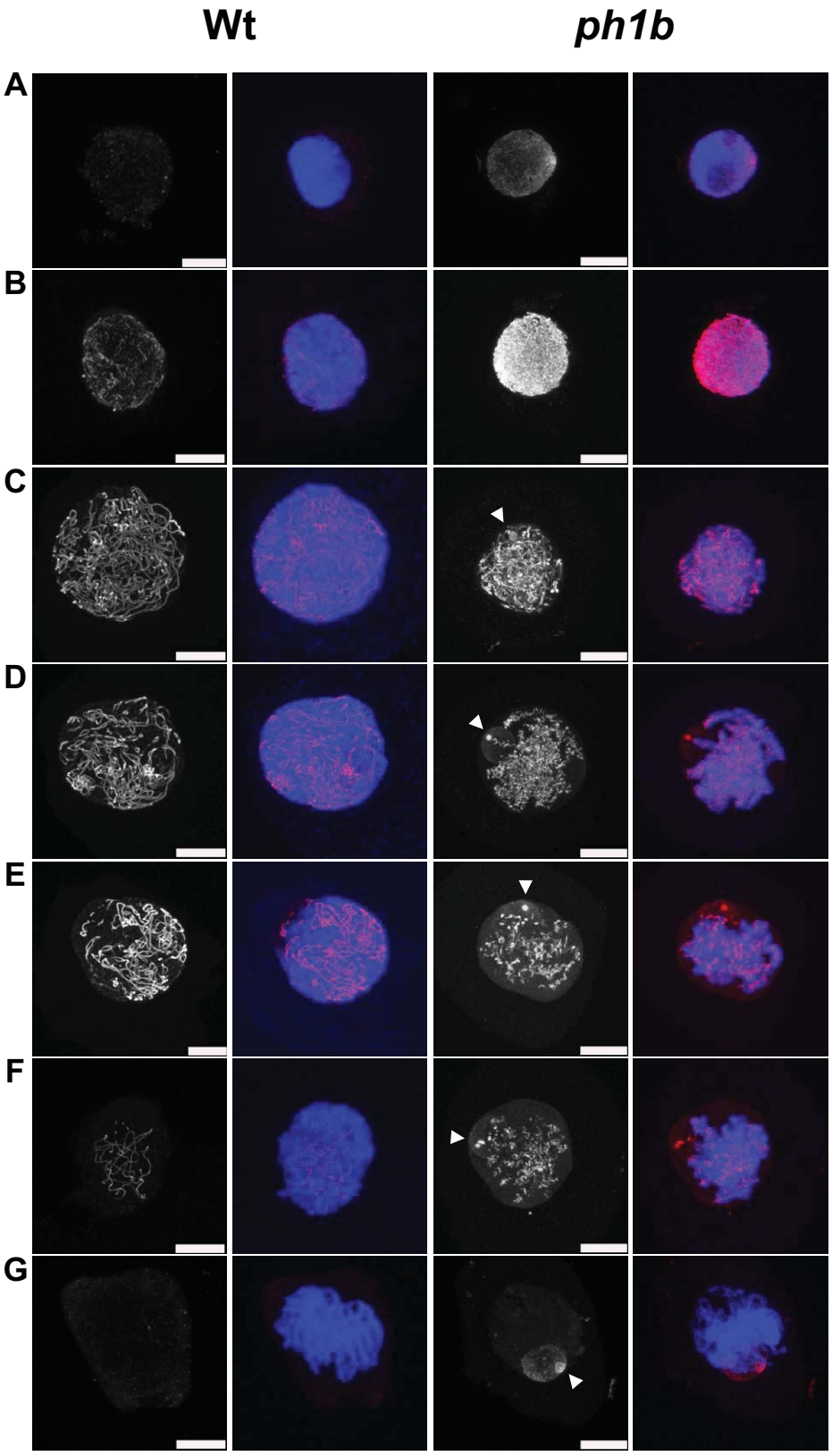
Wt
ph1b
A
B
C
D
E
F
G

Figure 4.15 – Immuno-fluorescence localisation of *Ta*ASY1 during prophase I of *ph1b*. Localisation of *Ta*ASY1 and chromatin conformation is disrupted in the *ph1b* mutant. (A) Pre-meiotic interphase, (B) leptotene, (C) early zygotene, (D) late zygotene, (E) pachytene, (F) diplotene, (G) diakinesis. For each genotype, panels on the left display ASY1 in white, while panels on the right show merged ASY1 (red) with DAPI (blue). White arrow-heads in the *ph1b* panel indicate ASY1 polycomplexes. Scale bars, 10 μm.

4.4 – Discussion

The aim of the work presented in this chapter was to provide a greater understanding for the role of *Ta*ASY1 during meiosis in bread wheat, and by doing so, provide further insight into the mechanism that regulates homologous chromosome interactions. In the first instance, this involved analysis of bread wheat plants that had reduced activity of *TaASY1* through the use of RNA interference (RNAi). The meiotic phenotype of these plants then led to an investigation of *TaASY1* in the *ph1b* mutant, to determine whether the function of *Ta*ASY1 is affected upon deletion of the *Ph1* locus.

A major component of this chapter involved analysis of *TaASY1* RNAi mutants, which were generated to observe the effect that reduced activity of *TaASY1* would have on meiosis in bread wheat. Practically, RNAi represents the most logical method to generate a mutant with reduced function of a gene in bread wheat, as it is the most likely of the gene-silencing techniques to suppress the activity of a gene across all three genomes. However, confidence in this technique providing a phenotype that is attributable to only one gene being affected is reliant on the specificity of the sequence used to induce the RNAi silencing effect. In this case, as *TaASY1* and its homologues in Arabidopsis, rice and *B. oleracea* (Caryl et al., 2000; Nonomura et al., 2004; Armstrong et al., 2002) share no homology to any other known sequence within their respective genomes (not including pseudo-genes), it was proposed that *TaASY1* would be the only gene affected in these bread wheat mutants.

Previous to this report, analysis of ASY1/PAIR2 had been performed in the diploids, Arabidopsis and rice, using mutants that had the activity of *ASY1*/*PAIR2* silenced by insertion of transfer DNA (T-DNA) and a retrotransposon, respectively (Ross et al., 1997; Nonomura et al., 2004). While much research has been conducted to determine the processes affected by the deletion of this gene, little evidence was available to conclude whether the aberrant synapsis of homologous chromosomes in these mutants represented a role for ASY1/PAIR2 in either chromosome pairing or synapsis (Caryl et al., 2000; Armstrong et al., 2001; 2002; Nonomura et al., 2004; Nonomura et al., 2006; Sanchez-Moran et al., 2007). Hence, in using the RNAi mutants to determine the role of *Ta*ASY1 during meiosis in bread wheat, it was thought that the reduced versus silenced activity of *TaASY1* in these mutants, and the fact that bread wheat is a polyploid rather than diploid, could provide novel information about the role for ASY1 in plant meiosis.

4.4.1 – Genetic analysis of the *Taasy1* mutants

Genotype analysis identified positive transgenic plants in both the T_1 and T_2 generation, thus confirming that the transgene had stably integrated into the bread wheat genome, and could be genetically inherited. Southern blot hybridisation showed that while one line contained a single copy of the transgene, most lines contained multiple copies. This result is expected of plants that have been transformed *via* particle bombardment given that it is a process that incorporates foreign DNA randomly throughout the genome. Several studies whereby wheat transformation have been reported, document that multiple insertions are more common than single insertion events when using bombardment (for example Wright et al., 2000; Pellegrineschi et al., 2002). Furthermore, as all positive plants of a given individual line with multiple copies of the transgene displayed an identical Southern blot banding pattern, it is likely that the multiple copies were co-segregating. A possible explanation for the co-

segregation of multiple copies is that there may have been numerous transgene insertion events at one particular locus.

PCR analysis was performed to identify positive and negative transgenic plants of both the T_1 and T_2 generations. Typically, studies of transgenic plants would use the ratio of positive to negative transgenics to perform chi-squared tests. This would enable statistical comparisons to be made, determining whether the expected versus observed segregation ratios were upheld. However, reduced fertility of the *Taasy1* mutants prevented this analysis to be conducted due to the low sample size of plants within each line. Nonetheless, segregation ratios of positive to negative plants were determined for both the T_1 and T_2 generation. In the T_1 generation, it was expected that the segregation ratio of positive to negative plants would be 3:1, given that it is most likely that the T_0 plant would be heterozygous for the transgene. However, none of the T_1 lines displayed this ratio. While it is possible that the observed ratios would approach the expected value with an increased sample size, it is also possible that these distorted ratios are the result of unexplained pollen abortion that has been observed previously in RNAi transgenic plants (Xing and Zachgo, 2007). While this result may also be explained by unequal segregation of the transgene in lines that contain multiple copies, it is unlikely that this occurred, as all the positive T_1 plants within a given line displayed identical banding in the Southern blot analysis. Lines analysed in the T_2 generation did tend to display segregation ratios that would be expected of lines that originated from parents that were either heterozygous or homozygous for the transgene. Through this analysis, two T_1 plants (*asy1-1.9* and *asy1-2.2*) were identified as being homozygous for the transgene, with all 10 T_2 offspring being positive. It is worth noting that the identification of these two lines was critical to this study, as the destructive nature of the meiotic phenotype analysis required a large collection of plants to ensure that there would be seed for future work. In addition, the identification of two homozygous lines originating from independent transgenic events ensured that the observed

phenotype could be solely explained by reduced activity of *TaASY1* and not through the position in which the transgene may have inserted within the genome.

4.4.2 – Expression analysis of *Taaasy1* mutants

Following the identification of positive transgenic plants, Q-PCR analysis was performed to determine whether the RNAi transgene did indeed cause reduced levels of *TaASY1* transcripts in meiotic tissue. In both the T_1 and T_2 generation, a number of positive transgenic plants displayed reduced levels of *TaASY1* transcripts. However, in the T_1 generation especially, it was noted that positive transgenic plants displayed varying levels of *TaASY1* transcripts. There are several possible explanations for this observation. Firstly, such variation has been observed previously in wheat RNAi transgenic plants, with differences even observed between different tillers of the one plant (Anand et al., 2003). Secondly, as RNA was extracted from whole spike tissue rather then staged anthers, variations in meiotic stages of the anthers within a whole spike might have been sufficient to distort the Q-PCR readings given the sensitivity of this assay. This is particularly true for the T_1 generation, as more attention was given to the precise stage of the meiotic material collected from the T_2 generation than for the T_1 generation. It is also possible that transcript variation between positive transgenic plants of different lines was attributable to the different number of transgene copies within each line. Similarly, in the analysis of the T_1 positive transgenic plants, it is possible that the observed variation within a given line reflects the difference in silencing ability of plants that are heterozygous for the transgene, versus those that are homozygous. This would explain why less variation was observed within each of the T_2 lines, which were likely to have been homozygous for the transgene. Importantly, the similar reduction in *TaASY1* transcripts of the T_2 generation ensured that plants could be equally considered for phenotype analysis.

4.4.3 – Whole plant morphology of *Taasy1* mutants

Taasy1 mutants were compared to wild-type wheat during stages of vegetative and reproductive development to identify changes in whole plant morphology caused by reduced activity of *TaASY1*. As has been observed in many Arabidopsis meiotic mutants, no changes were noted in the vegetative development of the *Taasy1* plants (Schommer et al., 2003; Higgins et al., 2004; 2005; Li et al., 2004; Kerzendorfer et al., 2006; Jackson et al., 2006; De Muyt et al., 2007; Uanschou et al., 2007). However, the *Taasy1* mutants did display clear signs of infertility, with empty spikelets often observed towards the top half of a spike within each individual. The reduced fertility of these plants was further confirmed upon analysis of pollen viability and seed set, with the mutants displaying significantly reduced levels of viable pollen and seed counts, relative to wild-type wheat. This supports observations of the *asy1* and *pair2* mutants, which both displayed significantly reduced fertility (Ross et al., 1997; Nonomura et al., 2004).

Interestingly however, the decrease in fertility of the *Taasy1* mutants was not as severe as that observed in *asy1* or *pair2*, which displayed 10% of wild-type fertility and complete sterility, respectively (Caryl et al., 2000; Nonomura et al., 2004). One possible explanation for this difference is based on the methodology used to produce the mutants. The use of RNAi rather then a gene disruption event (as occurred in the *asy1* and *pair2* mutants), appears to have not totally knocked-out the expression of the transgene, and has therefore allowed for the production of more viable gametes due to partial but not complete silencing of *TaASY1*, when compared to the other studies mentioned. Furthermore, it is possible that the polyploid genome of bread wheat was able to buffer the effect of losing one or two copies through compensation from either of the two homoeologous genomes, when compared to the diploids Arabidopsis and rice.

While there are few wheat meiotic mutants to compare the phenotype of the *Taasy1* plants with, there are two particular reports that provide some evidence for *Ta*ASY1 having a role in chromosome pairing, rather than synapsis. Firstly, Martini and Bozzini (1966) reported on two tetraploid wheat mutants that had been generated using fast-neutron irradiation, which were completely sterile. These mutants were found to be asynaptic, displaying a lack of chromosome pairing and equatorial chromosome segregation at anaphase I, which was later shown to be caused by a lack of synaptonemal complex formation (Martini and Bozzini, 1966; La Cour and Wells, 1970). Furthermore, it was reported that the gene affected in these mutants was distinct and epistatic to the mutated gene of the *ph1b* mutant (Martini and Bozzini, 1966). Unlike these two asynaptic mutants, the *ph1b* mutant (which was also generated by irradiation), displayed reduced fertility rather than complete sterility (Sears, 1977). This reduced fertility is the result of a chromosome pairing defect, whereby the strict regulation of pairing is lost so that homoeologous as well as homologous chromosome pairing is observed (Okamoto, 1957; Riley and Chapman, 1958; Sears, 1977). Therefore, it is possible based on these two previous reports, that the reduced fertility rather than the complete sterility that is observed in the *Taasy1* mutants is the result of a chromosome pairing defect instead of a loss of chromosome synapsis. This possibility was further investigated by analysis of chromosome morphology during meiosis in the *Taasy1* mutants.

4.4.4 – Investigating meiosis of the *Taasy1* mutants

Chromosome preparations of *Taasy1* mutants were examined to determine whether chromosome pairing and/or synapsis were altered in these plants (Ross et al., 1997; Nonomura et al., 2004). Feulgen's-stained preparations of cells at prophase I showed that chromosomes of the *Taasy1* mutants displayed similar characteristics to chromosomes of the *asy1* and *pair2* mutants, with an obvious reduction in synapsis that included the absence of true pachytene

cells (Ross et al., 1997; Nonomura et al., 2004). These observations were supported by the immuno-fluorescence analysis of *Taasy1* mutants during prophase I. The ASY1 signal in these cells indicated that the chromatin and axial elements were not as well organised in *Taasy1* as they were in wild-type wheat. In addition, no synapsis forks or thickening of the ASY1 signal were observed in *Taasy1* cells, thus explaining why no true pachytene cells were observed in the Feulgen's stain analysis. While the appearance of chromosomes during prophase I of *Taasy1* plants was similar to those of *asy1* and *pair2*, differences were observed when comparing metaphase I chromosome preparations.

In contrast to the univalents that were observed during metaphase I of *asy1* and *pair2* (Ross et al., 1997; Nonomura et al., 2004), metaphase I chromosome preparations from the *Taasy1* mutants displayed multivalents, as well as bivalents and a number of univalents. In addition there was an increase in the number of rod-like bivalents, compared to wild-type metaphase, which mainly consisted of ring-bivalents. These observations (multivalents and more rod-like bivalents) both support an increase in homoeologous chromosome interactions, as they have previously been used to score for new *ph1* deletion lines (Roberts et al., 1999). Indeed, the metaphase I phenotype of the *Taasy1* mutants was similar to those previously observed in *ph1b*, thus providing evidence that *Ta*ASY1 has a role in the correct pairing of homologous chromosomes during meiosis in bread wheat (Riley and Chapman, 1958; Sears 1977; Holm, 1988). Examination of anaphase I preparations also supported a role in pairing, with most cells displaying equal segregation of homologous chromosomes to each pole of the cell, which is similar to observations of *ph1b* cells, but in contrast to anaphase I cells of the asynaptic wheat mutants discussed previously (Martini and Bozzini, 1966).

The evidence for homoeologous chromosome interactions occurring in *Taasy1* mutants raises an interesting question: Does *Ta*ASY1 suppress homoeologous chromosome interactions, or does it promote homologous chromosome interactions? Evidence from studies

in Arabidopsis, *C. elegans* and budding yeast suggest that ASY1 has a role in promoting homologous chromosome interactions, rather than suppressing homoeologous interactions (Couteau et al., 2004; Nabeshima et al., 2004; Sanchez-Moran et al., 2007; Carballo et al., 2008). In *asy1* Arabidopsis lines, it was noted that some metaphase I cells contain bivalents that are the result of DMC-dependent recombination events, which occur in chromosomal regions proximal to the telomeres. It was proposed that these recombination events were aided by the pre-alignment of homologous chromosomes *via* the telomeres (Sanchez-Moran et al., 2007). Similarly, the non-null HIM-3 mutant, *him3(me80)* (*CeHIM3* is the gene that encodes the HORMA domain containing protein of *C. elegans*), displays reduced, but not abolished pairing of homologous chromosomes (Couteau et al., 2004; Nabeshima et al., 2004). Interestingly, chromosome pairing in this mutant was found to occur at near normal levels for the X chromosomes, and to a reduced level for the autosomal chromosomes (Couteau et al., 2004; Nabeshima et al., 2004). The chromosome pairing that occurs in the *him3(me80)* is thought to be facilitated by pairing centres, which are chromosome structures that have been shown to mediate pairing, recognition and synapsis of homologous chromosomes in *C. elegans* (Nabeshima et al., 2004; MacQueen et al., 2005).

These two sets of results suggest that chromosome interactions can still occur in regions where chromosome structures facilitate the close juxtaposition of homologues, but that without ASY1/HIM-3, homologous chromosomes cannot interact along their entire length. Therefore, it is possible that ASY1/HIM-3 represents an axial element protein that promotes the complete pairing of homologous chromosomes, either by initiating the juxtaposition of homologues, or by stabilising their initial interactions (Jordan, 2006). This suggestion is supported by a study in yeast that showed *Sc*HOP1 is a critical component of a pathway that promotes inter-homologue recombination (Carballo et al., 2008). Thus, while there are definitely many more critical components of the chromosome pairing machinery, these three

independent studies indicate that ASY1/HIM-3/HOP1 has a significant role in chromosome pairing.

The results presented in this chapter therefore support a role for *Ta*ASY1 in bread wheat chromosome pairing, especially when placed in context of the abovementioned studies and previous analyses of wheat meiosis (Holm, 1988; Holm and Wang, 1988; Martinez-Perez, 2001; 2003). It has been shown that during early meiosis of bread wheat, homoeologous chromosomes interact *via* their centromeres to form seven homoeologous groups (Martinez-Perez et al., 2003). These seven homoeologous groups are then resolved into 21 homologous chromosome pairs (Martinez-Perez et al., 2003). This clustering of homoeologous chromosomes *via* their centromeres is analogous to the pre-alignment of homologous chromosomes *via* their telomeres and pairing centres that occur in Arabidopsis and *C. elegans*, respectively. However, in contrast to the associations being between two chromosomes as it is in Arabidopsis and *C. elegans*, the early meiotic interactions in bread wheat involve six chromosomes. Therefore, it is likely that the multivalents observed in the *Taasy1* mutants are the result of the early homoeologous chromosome interactions not being resolved into homologous chromosome pairs, leaving a chromosome just as likely to interact with a homoeologue as with its true homologue. Furthermore, this implies that *Ta*ASY1 is required to correctly resolve homoeologous chromosome interactions into homologous chromosome pairs.

Interestingly, it has been previously shown that deletion of *Ph1* causes a very similar, if not identical effect, by reducing the specificity of centromere interactions to homologues (Martinez-Perez et al., 2001). In addition, *ph1b* displays a similar phenotype to the *Taasy1* mutants during prophase I, with synapsis found to arrest during zygotene in *ph1b* and other chromosome 5B genotypes (reviewed in Holm and Wang, 1988). The similarities in

phenotype between the *Taasy1* and *ph1b* mutants led to investigating the activity and localisation of *TaASY1* and its protein during meiosis in the absence of *Ph1*.

4.4.5 – Investigation of *TaASY1* in the *ph1b* mutant

The similarities in the metaphase I phenotype of the *Taasy1* and the *ph1b* mutants suggested that deletion of *Ph1* may affect the function of *Ta*ASY1. Over the last decade, substantial genetic work has been performed to delineate the original 70 Mbp deletion of the *ph1b* mutant, which has led to the identification of a 2.5 Mbp region that contains seven *Cdk*-like genes and a segment of heterochromatin (Roberts et al., 1999; Griffiths et al., 2006). In the absence of *Ph1*, the corresponding *Cdk*-like genes on the A and D genome, which are not normally transcribed, compensate for the loss of expression from the B genome (Al-Kaff et al., 2007). However, this compensation of transcription occurs at a higher level than that normally produced from the B genome *Cdk*-like genes, suggesting that *Ph1* regulates the overall activity of these *Cdk*-like genes (Al-Kaff et al., 2007).

It was therefore hypothesised that the similarities in metaphase I phenotypes of *ph1b* and *Taasy1* mutants represented a flow on effect of the over-compensatory expression of the 5A and 5D *Cdk*-like genes following deletion of *Ph1*, causing a change in expression of *TaASY1*. Indeed, Q-PCR provided evidence that *ASY1* is up-regulated in *ph1b* with a significant 20-fold increase during pre-meiotic interphase and leptotene to pachytene, when compared to the wild-type. This result suggests that *TaASY1* is a downstream transcriptional target of a pathway involving the *Cdk*-like genes, and that *Ph1* represents a regulatory mechanism that controls the expression of *TaASY1*. This mechanism appears to only regulate the amplitude of *TaASY1* expression, as the transcript profile of *TaASY1* across the *ph1b* meiotic time-course remained identical to that of wild-type wheat. While it is premature to conclude that *TaASY1* is the only gene whose activity is affected in *ph1b*, transcriptional

analysis of two recombination candidates, *RAD51A* and *RAD51B*, as well as the mismatch repair gene, *MSH4*, indicate that deletion of *Ph1* does not cause a global up-regulation of meiotic genes.

On first appearances, the phenotype of the *Taasy1* mutants and the expression analysis of *TaASY1* in *ph1b* appear contradictory, as one would not expect that both reduced, as well as increased expression of *TaASY1*, would cause homoeologous chromosome interactions. However, upon referring back to the explanation of the homoeologous chromosome interactions that occur in *Taasy1* meiosis, and the discussion of results from other species that support a role for ASY1 in promoting homologous chromosome interactions, it becomes clear why the activity of *TaASY1* needs to be controlled during bread wheat meiosis. The regulation of chromosome pairing that occurs in bread wheat is essential for maintaining the genetic integrity of this polyploid organism, as it ensures that there is a balanced segregation of homologues and homoeologues at anaphase I. This process is quite complex, as it needs to promote interactions between homologues, while preventing associations between genetically similar homoeologues. The complexity is evident by the number of loci in the bread wheat genome that have been shown to control this process, by either promoting homologous interactions or suppressing homoeologous associations (reviewed in Sears, 1976). As homoeologous interactions occur in the absence of *Ph1*, it has been described as a locus that suppresses homoeologous chromosome interactions (Sears, 1976). Based on the elevated expression of *TaASY1* in the absence of *Ph1*, it is likely that one of the roles for this locus is to suppress the activity of *TaASY1*. By suppressing the activity of *TaASY1*, *Ph1* ensures that associations occur between the genetically identical homologous chromosomes, and not between the genetically similar homoeologous chromosomes. Thus, it appears that *Ph1* controls a gene regulatory mechanism that ensures the genetic integrity of chromosome pairing in hexaploid wheat is maintained.

Given the elevated expression of *TaASY1* detected in the *ph1b* mutant, ASY1 localisation in the *ph1b* mutant was then investigated. Localisation of ASY1 in *ph1b* revealed strong evidence for disruption of the protein's activity in this mutant. While ASY1 still appeared to localise to chromosome axes during leptotene and early zygotene, there were signs of disorder during zygotene, as shown by the spiral-like conformation adopted by ASY1 during this stage. These results are consistent with previous observations of abnormalities in synapsis and chromatin remodelling that occurs in *ph1* mutants during prophase I (Prieto et al., 2004; Holm and Wang, 1988). This spiral-like conformation of ASY1, which persisted through pachytene, might result from the inability of *ph1b* to resolve multiple axial element associations that have been observed in this mutant, and that are thought to lead to multivalents at metaphase I (Holm and Wang, 1988). In addition to the altered structure of ASY1 in *ph1b*, immuno-fluorescence microscopy also provided evidence for increased levels of *Ta*ASY1 protein in the absence of *Ph1*. Firstly, ASY1 'clusters' that are thought to be polycomplexes, were found in the nucleolar region of *ph1b* meiocytes. Polycomplexes are aggregates of synaptonemal complex proteins that have been found in mutants with abnormalities in chromosome morphology, synapsis and recombination (Zickler and Kleckner, 1999). Given that the ASY1 polycomplexes were only found in *ph1b*, it is likely that they represent excess *Ta*ASY1 protein caused by the elevated up-regulation of *TaASY1* gene activity in this mutant. Secondly, the ASY1 signal appeared much more intense during leptotene in *ph1b* than it did in wild-type wheat, thus supporting an increase in *Ta*ASY1 expression in *ph1b*.

Interestingly, despite the anti-ASY1 antibody having been used to study many meiotic mutants in Arabidopsis, the only mutants reported thus far to cause disruption of ASY1 localisation have been *swi1* and *rec8* (Mercier et al., 2003; Chelysheva et al., 2005). Activation of REC8 has been shown to represent an early marker for the commitment to the

meiotic cycle, and thus the disrupted localisation of *Ta*ASY1 in *ph1b* supports the proposal that *Ph1* affects pre-meiotic as well as meiotic processes (Roberts et al., 1999; Hamant et al., 2006).

The main objective of the work presented in this chapter was to improve our understanding of the role for *Ta*ASY1 during meiosis in bread wheat, which would then provide further insight into the mechanism that controls homologous chromosome pairing in this polyploid. This has been achieved with the investigation and analysis of *TaASY1* RNAi mutants and the behaviour of *TaASY1* in the bread wheat pairing mutant, *ph1b*. The results imply that *TaASY1* has a definite role in chromosome pairing. Even so, chromosome pairing is a very complex process, which includes the equally complex events of chromosome synapsis and recombination. Hence it is premature to conclude that *TaASY1* has a single unique role during meiosis in bread wheat. In summary, the results of this chapter have enabled a more complete understanding of key events and the roles of specific proteins crucial to plant meiosis through the detailed investigation of *Ta*ASY1.

Chapter 5 - General Discussion and Future Directions

5.1 – General discussion

The primary objective of this project was to investigate the function of *TaASY1* and its encoded protein during prophase I of meiosis in hexaploid wheat. In addition there was a broader objective, which was to gain further understanding on how chromosome pairing is regulated during meiosis in this polyploid. As such, comparisons were continually being made between the findings of this project and those from studies of ASY1 homologues in diploid species, to identify possible areas in which the function of this gene could have diverged to mediate the strict pairing of homologous chromosomes that occurs in bread wheat.

5.1.1 – Investigating *TaASY1* in wild-type wheat

The initial stages of this project involved isolating the cDNA and genomic DNA sequences for *TaASY1*, and determining its position within the wheat genome. The cDNA sequence of *TaASY1* and the deduced amino acid sequence of the encoded protein were found to be significantly similar to sequences in other plants, including Arabidopsis (*AtASY1*; *Arabidopsis thaliana*), rice *(OsPAIRS2*; *Oryza sativa*) and *Brassica oleracea* (*BoASY1*). In addition, sequence similarities were found in other organisms such as budding yeast (*ScHOP1*; *Saccharomyces cerevisiae*) and *Caenorhabditis elegans* (*CeHIM-3*), albeit at low levels. Interestingly, the sequence similarity shared between *TaASY1* and homologues from budding yeast and *C. elegans* is not as significant as one might expect, given that chromosome pairing and synapsis represent two well conserved meiotic processes across the vast majority of sexually reproducing organisms. However, this observation is not unique to *Ta*ASY1 and has been observed previously between homologues of proteins that localise to the synaptonemal complex (SC) (Meuwissen et al., 1992; Sym et al., 1993; Heyting, 1996; Zickler and Kleckner,

1999; Page and Hawley, 2001; MacQueen et al., 2002; Higgins et al., 2005). While an explanation for this phenomenon is beyond the scope of this project, evidence from emerging studies in Arabidopsis indicate that conservation in the tertiary structures of proteins rather than amino acid sequences are important for the function of proteins that form a component of the SC (Bogdanov et al., 2003; Higgins et al., 2005). This suggests that to completely understand the function of ASY1, it will be important to investigate the biochemistry of this protein, and especially the well conserved HORMA domain, which is the most similar region within the ASY1 homologues (Hollingsworth and Byers, 1990; Aravind and Koonin, 1998; Caryl et al., 2000; Armstrong et al., 2002; Nonomura et al., 2004).

Investigation of the gene structure and location within the wheat genome revealed further levels of conservation between *TaASY1* and its plant homologues. The gene structure of *TaASY1* was found to be identical to that of *AtASY1* and *OsPAIR2*, with all three genes containing 22 exons and 21 introns (Caryl et al., 2000; Nonomura et al., 2004). Furthermore, the similarity in gene structure of *TaASY1* and *OsPAIR2* was supported upon determining that *TaASY1* is located on chromosome group 5, which shares a high level of gene order conservation with rice chromosome 9, on which *OsPAIR2* resides (Nonomura et al., 2004).

By locating *TaASY1* on chromosome group 5, and more specifically on the long arm, it was then hypothesised that *TaASY1* might have a role in association with previously identified regions of the bread wheat genome that control chromosome pairing. These previous studies had identified a number of loci that affect chromosome pairing by either suppressing homoeologous associations or promoting homologous interactions. Suppressing loci were found on 5BL (*Ph1*), 3DS (*Ph2*), 3AS, 3AL, 3DL and 4A, with *Ph1* representing the locus with the strongest effect, while pairing promoters have been identified on 5BS, 5D, 5AL, 3BL, 3DL and 3AL (reviewed in Sears, 1976). It was confirmed through this study, as well as through previous reports, that *TaASY1* does not represent *Ph1* (Roberts et al., 1999; Griffiths

et al., 2006). However, it is possible that *TaASY1* represents one of the minor pairing promoters on 5D and/or 5AL (Feldmann, 1966; Riley et al., 1966). So far, attempts to obtain these lines have not been successful. Future work with the *TaASY1* mutants (discussed in 5.2) and analysis of other meiotic candidate genes that have been found to reside on chromosome group 5 (J.A. Able, *personal communication*) may yet allow for the genetic basis of these loci to be resolved.

The expression of *TaASY1* was analysed using three different platforms, including northern blot, microarray and quantitative real-time PCR (Q-PCR). All three platforms showed that *TaASY1* is highly expressed in meiotic tissue, with only basal levels of expression detected in vegetative tissue. Stage specific analysis during meiosis showed that *TaASY1* is most highly expressed during pre-meiotic interphase and leptotene to pachytene, before reducing through meiosis until it is almost silenced in immature pollen and mature anthers. These results provided evidence for *TaASY1* being a gene that has an important role during early meiosis, as the expression profile was very similar to that of other wheat transcripts that are homologous to genes with key roles during prophase I (Crismani et al., 2006). The data from *OsPAIR2* supports these results, where expression of that gene is also predominantly detected during the early stages of meiosis (Nonomura et al., 2004). Interestingly, while *AtASY1* displays a very similar expression profile during meiosis, it was found to be equally expressed in vegetative tissue as in meiotic/reproductive tissue (Caryl et al., 2000). Therefore, it is possible that the regulatory mechanism that controls the expression of *ASY1* has changed since the divergence of monocotyledons from dicotyledons.

Immuno-fluorescence and immuno-gold microscopy were used to investigate the localisation of *Ta*ASY1 during meiosis I of bread wheat. The experiments showed that *Ta*ASY1 localises to chromatin associated with axial and lateral elements as homologous chromosomes are pairing and synapsing. Both temporal and spatial localisation of *Ta*ASY1

was similar to that of ASY1 homologues in Arabidopsis, *B. oleracea*, rice, maize (*Zea mays*) and rye (*Secale cereale*), as well as in budding yeast and *C. elegans* (Zetka et al., 1999; Armstrong et al., 2002; Golubovskaya et al., 2006; Mikhailova et al., 2006; Nonomura et al., 2006). This indicates that while the amino acid sequence of these homologous proteins may not be as well conserved as one would expect; the localisation is well conserved. One point of note is that there are minor discrepancies in the reported temporal localisation of ASY1 homologues in different plant species. In rice, the ASY1/PAIR2 signal arrives before the onset of meiosis, in contrast to Arabidopsis, where the signal first appears at the onset of meiosis (Armstrong et al., 2002; Nonomura et al., 2006). Furthermore, the rice protein was reported to disassociate from the chromosomes during synapsis, which is different from reports in Arabidopsis and rye that suggest the protein is not removed from the chromatin until after synapsis is complete (Armstrong et al., 2002; Mikhailova et al., 2006; Nonomura et al., 2006). The later observation was also shown to occur in maize, and appears to be similar to the localisation of *Ta*ASY1 (Hamant et al., 2006). There are numerous possible explanations for these discrepancies. Firstly, they may be the result of technical differences that were used in each case, including tissue fixation and chromosome preparation as well as personal considerations for the stage of a particular cell (Hamant et al., 2006). Secondly, it is possible that they represent the different strategies that each organism has adopted to assemble meiotic bivalents (Mikhailova et al., 2006). In either case, it is possible that while the localisation of ASY1 with respect to the particular stage of pre-meiotic interphase and prophase I is slightly different in each organism, the "temporal localisation" in terms of the state and progression of chromatin remodelling, especially during pre-meiotic interphase and early leptotene, is functionally identical.

The results of the immuno-localisation analysis were also used to consider the function of this protein, with particular attention given to its possible involvement in recombination,

synapsis and/or chromosome pairing. It had previously been shown that ASY1 is unlikely to have a direct role in recombination, as DMC-dependent recombination events have been shown to occur in the absence of ASY1, with an average of 1.39 chiasmata per cell (Ross et al., 1997; Sanchez-Moran et al., 2007). This conclusion was supported by the immuno-localisation of *Ta*ASY1, which did not display the distinct punctate foci that are typical of recombination proteins, such as RAD51, MSH4 or MLH3 (Franklin et al., 1999; Pawlowski et al., 2003; Higgins et al., 2004; Jackson et al., 2006). Indeed, the localisation pattern of *Ta*ASY1 was most similar to proteins that have previously been shown to have a role in synapsis and/or pairing of homologous chromosomes (Higgins et al., 2005).

One role that has been suggested for ASY1 is to initiate and stabilise the juxtaposition of homologous chromosomes (Armstrong et al., 2002). This suggestion was supported by the temporal and spatial localisation of *Ta*ASY1, which was found to form a progressively continuous signal through leptotene and zygotene that reflected the advancement of chromosome pairing that has been shown to occur in bread wheat (Martinez-Perez et al., 1999). This suggestion is further supported by the observation that synapsis does not progress beyond the pairing of telomeres at leptotene in Arabidopsis *asy1* lines, and similarly, that the residual cross-overs that occur in the absence of *ASY1* all occur at sub-terminal regions of the chromosome (Armstrong et al., 2001; Sanchez-Moran et al., 2007). Thus, these two results indicate that ASY1 is likely to have a role in confirming the interactions of homologues along their entire length following the initial association at telomeres. Again, this theory is supported by the localisation of *Ta*ASY1 detected in this study, especially through the clear detection of *Ta*ASY1 at synapsis forks that represent active sites of homologue interactions.

An additional role that has been suggested for ASY1 is to facilitate the development of axial elements (Armstrong et al., 2002). While the methodology used in this study cannot refute a role in this process, the immuno-gold based localisation of *Ta*ASY1 was not the same

as the linear signal that is typical of proteins that form a structural component of the axial or lateral elements (Anderson et al., 1994; Higgins et al., 2005). Furthermore, it has been subsequently shown that chromosome axis formation is relatively normal in *asy1* and *pair2* plants, indicating that ASY1 is unlikely to be required for the formation of axial elements (Nonomura et al., 2006; Sanchez-Moran et al., 2007).

Finally, it is also possible that the localisation of *Ta*ASY1 may represent a role in synapsis, such as recruiting proteins that form components of the SC. However, due to limitations in the effectiveness of Arabidopsis-based antibodies in bread wheat (to date), it was not possible to thoroughly investigate this putative function. Nonetheless, the role of *Ta*ASY1 during pairing and synapsis of homologous chromosomes was further investigated using bread wheat mutants with reduced activity of *TaASY1*.

5.1.2 – Using *TaASY1* RNA interference mutants to define the role of *TaASY1*

TaASY1 RNA interference (RNAi) mutants were generated to investigate what effect reduced *TaASY1* expression would have on chromosome pairing and/or synapsis in bread wheat. Importantly, the directed gene silencing strategy used in this study is different to what has previously been used to investigate meiotic mutants in wheat, which have typically relied upon fast-neutron irradiation to generate mutant lines (for example, Sears, 1977; Roberts et al., 1999). In addition, the use of RNAi made it possible to investigate the effect that reduced, rather than silenced activity of *ASY1* would have on meiosis, which is in contrast to the studies that had previously been performed in Arabidopsis and rice where gene function has been completely abolished (Ross et al., 1997; Caryl et al., 2000; Nonomura et al., 2004; 2006).

In this study, a number of independent *Taasy1* RNAi lines were identified that had reduced levels of *TaASY1* transcripts. Two particular lines of the T_2 generation were selected

for phenotype analysis. The whole plant phenotype of these *Taasy1* mutants indicated that meiosis was being affected in these plants, as they displayed clear signs of infertility relative to wild-type plants. Interestingly, the fertility of these plants was not as severely affected as Arabidopsis *asy1* and rice *pair2* mutant lines (Ross et al., 1997; Caryl et al., 2000; Nonomura et al., 2004). It is possible that this difference is due to the expression of *ASY1* being reduced rather than completely silenced, as occurred in the Arabidopsis and rice mutants. However, following analysis of meiosis in the *Taasy1* plants, it became clear that a more likely explanation for this difference concerned the polyploid nature of bread wheat, compared to the diploid genomes of Arabidopsis and rice.

During prophase I, the phenotype of the *Taasy1* plants was very similar to that of Arabidopsis *asy1* and rice *pair2* mutants, with reduced levels of synapsis and a lack of true pachytene cells typical of all three genotypes (Ross et al., 1997; Nonomura et al., 2004). However, rather than displaying univalents and unequal segregation of chromosomes that were typical of *asy1* and *pair2*, *Taasy1* cells displayed multivalents and bivalents at metaphase I as well as relatively equal segregation of chromosomes at anaphase I (Ross et al., 1997; Nonomura et al., 2004). The similarity in the early meiosis phenotype of the three mutants indicates that the immediate effect of reduced or silenced activity of *ASY1* is identical in each of the three organisms. However, the different metaphase I phenotype of the *Taasy1* mutants implies that the polyploid nature of bread wheat affects the downstream outcome of the reduced expression of *ASY1*. This difference can be explained by the fact that prior to the formation of 21 bivalents, the homoeologous chromosomes of bread wheat cluster to form 7 groups (Martinez-Perez et al., 2003). Therefore, it is likely that the higher order chromosome arrangements that occur in the *Taasy1* mutants are a remnant of these early homoeologous chromosome associations. Conversely, as no homoeologous chromosome clustering occurs in Arabidopsis or rice, chromosomes of *asy1* and *pair2* exist as univalents because there is no

opportunity to pair with another chromosome (assuming that interactions between telomeres are not sufficient to stabilise chromosome interactions). This conclusion suggests that the multivalents that were observed in the *Taasy1* mutants represent interactions between homoeologous chromosomes. Indeed, the presence of multivalents as well as the increased number of rod-like bivalents that also occurred in the *Taasy1* mutants, have been used as a marker for homoeologous interactions and are typical of metaphase I preparations of the *ph1b* mutant (Sears, 1977; Holm, 1988; Roberts et al., 1999). Importantly, the homoeologous chromosome interactions that occur when the activity of *TaASY1* is reduced imply that this gene is required to promote the pairing of homologous chromosomes.

5.1.3 – Using *TaASY1* to solve the mystery of *Ph1*

Given the similarities in the metaphase I phenotype of the *Taasy1* mutants to that of the *ph1b* mutant (see Sears, 1977), it was hypothesised that *Ph1* may affect the function of *TaASY1*. This was confirmed upon analysis of *TaASY1* transcriptional activity and localisation of the *Ta*ASY1 protein in the *ph1b* mutant. Q-PCR showed that there was a significant increase in the number of *TaASY1* transcripts in *ph1b* meiosis, relative to wild-type, and immuno-fluorescence microscopy showed that the localisation of ASY1 was severely affected in the absence of *Ph1*. In isolation, these results are quite significant, as they imply that *TaASY1* is involved in the molecular mechanism of *Ph1* that prevents the association of homoeologous chromosomes during meiosis. However, perhaps more remarkable is that these results complement numerous observations of previous reports on *ph1* mutants, and provide an explanation on how *Ph1* may directly coordinate its effect with meiotic chromosomes.

The significant increase in *TaASY1* transcripts that was observed during meiosis in the *ph1b* mutant, relative to wild-type, implies that *Ph1* has a gene regulatory role. Previously, it has been shown that the mechanism of *Ph1* is likely to have arisen following polyploidisation,

with this locus found to be present in both hexaploid wheat and numerous tetraploid wheats, but not in the diploid progenitors (Griffiths et al., 2006). Similarly, it has been shown that the activity of a number of genes has been affected following the hybridisation of two or more genomes, with numerous examples of genetic and epigenetic mechanisms being used to suppress the expression of particular wheat genes following the event of polyploidisation (reviewed in Feldmann and Levy, 2005). This control of gene activity ensures that there is a well-balanced relationship between the genomes that exist within the one nucleus, such that there is not an abundance of transcripts caused by the extra doses of each gene. In this particular case, the idea of *Ph1* regulating the overall level of *TaASY1* transcription is supported by the observation that absence of *Ph1* appears to only affect the amplitude of *TaASY1* transcripts during meiosis, rather than affecting the pattern of *TaASY1* expression during the meiotic time-course.

Recent delineation of the *Ph1* locus has shown that it consists of seven *Cdk*-like genes as well as a segment of sub-telomeric heterochromatin, with the *Cdk*-like genes displaying homology to the human checkpoint kinase, *Cdk2* (Griffiths et al., 2006; Al-Kaff et al., 2007). Interestingly, *Cdk2* has been shown to act in partnership with cyclins to regulate the expression of genes involved in cell-cycle progression, thus indicating that the *Cdk*-like genes of the *Ph1* locus are indeed part of a gene regulatory mechanism (Ma et al., 2000; Morris et al., 2000; Zhao et al., 2000). If for a moment we consider the results of Al-Kaff et al. (2007), who showed that the absence of the B genome *Cdk*-like genes causes an overall up-regulation in the expression of the bread wheat *Cdk*-like genes; it becomes apparent how the *Ph1* locus may suppress homoeologous chromosome interactions. Given that an increase in *Cdk*-like activity (absence of *Ph1*) causes an increase in the level *TaASY1* transcripts, it is plausible that the *Cdk*-like genes are required for promoting the expression of *TaASY1*. If we now consider evidence from the analysis of the *Taasy1* mutants that ASY1 promotes the association of

homologous chromosomes, it is reasonable to assume that an abundance of *Ta*ASY1 would promote interactions between genetically similar homoeologues as well as genetically identical homologues. Therefore, these results suggest that a function of *Ph1* is to suppress the overall activity of the wheat *Cdk*-like genes, which in turn, regulates the activity of *TaASY1*.

Comparisons in the progression of chromosome pairing in the presence and absence of *Ph1* do indeed suggest that an increase in the activity of the *Cdk*-like genes results in promotion of homoeologous as well as homologous chromosome interactions. For example, analysis of centromere and telomere pairing behaviour during early meiosis has shown that absence of *Ph1* leads to a reduced specificity of chromosome interactions (Martinez-Perez et al., 2001; Prieto et al., 2004). In addition, it has been shown that the absence of *Ph1* results in pairing and recombination between homoeologous chromosome regions that does not occur when *Ph1* is present (Luo et al., 1996; Dvorak and Lukaszewski, 2000). Taken together, these reports indicate that the activity of the wheat *Cdk*-like genes needs to be tightly regulated to ensure that pairing occurs between homologues, but not between homoeologues. Based on the results of this report, it is possible that this role is being directed through regulation of *TaASY1*.

Given the elevated expression of *TaASY1* detected in the absence of *Ph1*, we decided to investigate ASY1 localisation in *ph1b*. Importantly, this analysis showed that the localisation of ASY1 is disrupted in *ph1b*, and further supported the transcription analysis which showed that *TaASY1* expression is up-regulated in *ph1b*. The disrupted localisation of ASY1 is consistent with previous observations of chromosome behaviour during prophase I in *ph1* mutants. For example, the lack of synapsis forks and the absence of a thickened ASY1 signal in the *ph1b* mutant support findings of Holm and Wang (1988), who showed that synapsis is arrested at zygotene when *Ph1* is absent. Also, the spiral like conformation of the ASY1 signal during zygotene is consistent with findings of abnormalities in chromatin

remodelling that has been shown to occur in the absence of *Ph1* (Prieto et al., 2004; Colas et al., 2008). The spiral-like conformation of the ASY1 signal was found to persist through pachytene and diplotene, which is consistent with observations that multiple axial element associations remain unresolved up until diplotene in the absence of *Ph1* (Holm and Wang, 1988). Interestingly, immunisation of *ph1b* meiocytes with the anti-*Ta*ASY1 antibody showed that ASY1 polycomplexes are present within the nucleolar region of cells throughout prophase I. Polycomplexes are often found in mutants that display abnormalities in chromosome morphology, synapsis and recombination (reviewed in Zickler and Kleckner, 1999). Hence, the polycomplexes provide further support for involvement of *Ta*ASY1 in the molecular function of *Ph1*, and are suggestive of there being excess *Ta*ASY1 protein in the meiocytes of *ph1b*.

Finally, there are two aspects of discussion in the field of *Ph1* and chromosome pairing in bread wheat that these results help to resolve. Firstly, while it has definitively been shown that the absence of *Ph1* affects the interactions between chromosomes at their centromeres and telomeres, Dvorak and colleagues have suggested that the action of *Ph1* is not unique to these sites, and that it actually examines the homology of a given chromosome along its entire length (Luo et al., 1996; Dvorak and Lukaszewski, 2000; Martinez-Perez et al., 2001; Prieto et al., 2004). This hypothesis, as well as the suggestion that ASY1 is associated with promoting homologous chromosome interactions, is supported by the localisation of *Ta*ASY1 in wild-type wheat, which showed that the protein localises along the entire length of the chromosomes during zygotene and pachytene. Furthermore, its disrupted localisation in *ph1b* is consistent with the idea that loss of *Ph1* affects pairing along the entire length of the chromosome (Dvorak and Lukaszewski, 2000). Secondly, since the discovery of *Ph1*, there have been a number of suggestions made about when *Ph1* is having its effect, either during pre-meiotic interphase or during the 1 or 2 stages immediately prior to metaphase I (discussed

in Dvorak and Lukaszewski, 2000). The disruption in *TaASY1* gene expression and protein localisation in *ph1b* suggest that *Ph1* is affecting processes during both stages. For example, it was shown that deletion of *Ph1* affects the expression of *TaASY1* during pre-meiotic interphase as well as later stages of meiosis, and that the localisation of *Ta*ASY1 is subsequently affected during prophase I. Therefore, it seems inaccurate to limit the activity of *Ph1* to one particular stage of meiosis; instead it appears more likely that *Ph1* and the *Cdk*-like genes are co-ordinating a number of affects up until late prophase I. This is supported by the suggestion that *Ph1* has an affect on pre-meiotic replication (Colas et al., 2008).

5.1.4 – A model for the involvement of chromosome pairing in bread wheat

The analysis of *TaASY1* in wild-type wheat and *ph1b*, as well as the metaphase I phenotype of the *Taasy1* mutants, indicate that this gene has a critical role during meiosis. A summary of the role for *TaASY1*, and the consequences of its altered expression in the *Taasy1* and *ph1b* mutants, is provided in Figure 5.1. This model suggests that the critical role of *TaASY1* is to promote interactions between homologous chromosomes, and that altered levels of *TaASY1* expression can cause disruptions in chromosome pairing so that homoeologues as well as homologues interact with each-other. This model is supported by previous reports of bread wheat meiosis (which are referenced within the figure).

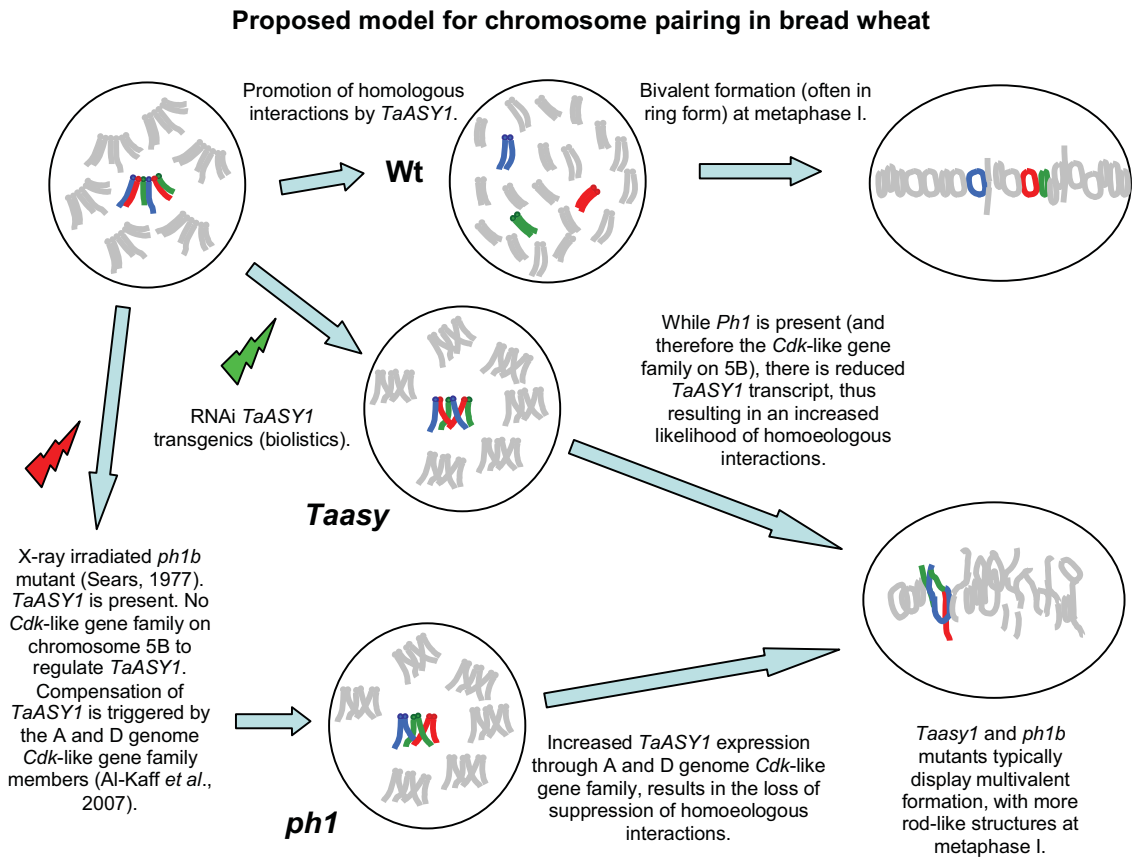

Figure 5.1 - A proposed model for the control of homologous chromosome pairing in bread wheat developed using the results from this study. Included is a definition of the role for *TaASY1* in chromosome pairing during meiosis (Wt), as well as an explanation on how disrupted expression in the *Taasy1* RNAi mutants (*Taasy1*), and increased expression in the *ph1b* mutant could lead to homoeologous chromosome interactions. For simplicity in each image, one of the homoeologous chromosome groups is shown in colour (red, blue, green), while the remaining homoeologous groups are grey.

5.2 – Future directions

5.2.1 – Further investigations of *Ta*ASY1 in bread wheat

This report has provided comprehensive analysis of *TaASY1* and its encoded protein in wild-type wheat. However, there are still a number of areas which could be investigated to provide further information about the function of this gene during meiosis.

Firstly, while immuno-fluorescence and immuno-gold microscopy have provided stage-wise information about the localisation of *Ta*ASY1, many previous studies of meiosis in wheat have investigated the process of chromosome pairing using probes that target centromeres and telomeres (Aragon-Alcaide et al., 1997; Martinez-Perez et al., 2001; Prieto et al., 2004; Colas et al., 2008). Therefore, it would be useful to determine the pattern of *Ta*ASY1 localisation during the stages of meiosis when the telomere bouquet is forming and the centromeres of homoeologous chromosomes are associated, in order to accurately determine when *Ta*ASY1 is coordinating its effect on chromosome pairing.

Secondly, research in budding yeast has shown that *Sc*HOP1 coordinates its effect on chromosome pairing in partnership with a number of proteins, including *Sc*RED1 as well as *Sc*MEC1 and *Sc*TEL1, which phosphorylate *Sc*HOP1 so that it can promote inter-homologue recombination (de los Santos and Hollingsworth, 1999; Woltering et al., 2000; Carballo et al., 2008). However, as yet, no homologue of RED1 has been identified in a higher eukaryote, and furthermore, no ASY1 interacting proteins have been identified in Arabidopsis or rice (Armstrong et al., 2002). During this project, a yeast-two-hybrid library that contained cDNA clones from pre-meiotic interphase and leptotene to pachytene of bread wheat was generated (results not presented in the thesis given the preliminary findings ultimately obtained to this point). Screens using both full-length and partial-length versions of *TaASY1* as bait were completed with a small number of interacting sequences identified. Whether these sequences

are true interacting proteins of *Ta*ASY1 will be the focus of future research within the Able laboratory. In addition, it is expected that analysis using cDNA sequence of the HORMA domain may allow for further ASY1 interacting proteins to be detected. It is known that similar analyses have been performed using *AtASY1* sequence as bait; however, this yielded limited success (F.C.H. Franklin, *personal communication*). Recent analysis has shown that there are a number of [S/T]Q motifs and zinc finger motifs that are essential for the function of *Sc*HOP1 (Hollingsworth et al., 1990; Carballo et al., 2008). However, these motifs have not been identified in the plant ASY1 homologues (Caryl et al., 2000). Hence, through further biochemical analysis of the plant ASY1 homologues, and further investigation of the HORMA domain, it may be possible to define regions of ASY1 that are involved in protein interactions.

Finally, despite a 2.3 kb sequence having been identified upstream of the *TaASY1* gene, no results have yet been obtained to suggest that this sequence promotes gene activity in meiotic tissue. Nonetheless, stable transformed wheat plants that contain the isolated *TaASY1* promoter sequence fused to the green fluorescent protein are currently being generated. It is anticipated that these plants will be ready for analysis late-2008. This sequence is also being compared to other isolated promoter sequences of key meiotic genes to identify *cis*-elements that are common to promoters of meiotic genes (J.A. Able, *personal communication*). Such analysis might enable the identification and study of transcription factors that promotes *TaASY1* transcription, which in turn could provide further information for the gene regulatory role of *Ph1* and *TaASY1* expression.

5.2.2 – Analysis of *Taasy1* mutants

Analysis of the *Taasy1* mutants has shown that reduced expression of *TaASY1* results in reduced synapsis during prophase I, and the development of multivalents during metaphase I, which suggest that homoeologous chromosome interactions occur in these plants. However

while this suggestion is supported by previous analysis of *ph1* mutants, it has not been definitively shown that the multivalents are only comprised of homoeologous chromosomes, and not non-homologous chromosomes also. Therefore, one possible area of future work would be to investigate the composition of these multivalents by performing fluorescence *in-situ* hybridisation (FISH) using probes that are specific to syntenous regions of each genome on a particular chromosome group. This would help identify the chromosomal composition of the multivalents that occur in *Taasy1* mutants.

In addition, while this study showed that there were reduced levels of synapsis in the mutant plants, no quantification of the level of synapsis was performed. This was partly due to time constraints. However, experimentation performed to identify the level of synapsis through ZYP1 localisation (a central element protein) was not successful due to the limited effectiveness of the antibody designed against the Arabidopsis ZYP1 antibody (Higgins et al., 2005). Following the development of a protocol that would enable localisation of ZYP1 during meiosis in bread wheat, it would definitely be interesting to investigate the level of synapsis and synaptonemal complex formation in these mutants.

Similarly, while the observation of multivalents and bivalents (either rod-like or ring in conformation) indicates that recombination does occur in the *Taasy1* mutants, no analysis was performed to determine whether there are altered levels of recombination in these mutants, relative to wild-type. Therefore, investigating the comparative levels of recombination, to determine whether expression of *TaASY1* in bread wheat influences the frequency of recombination events is an avenue that could also be pursued. One possible method to perform this analysis would involve localisation of proteins such as MLH1 or MLH3, which mark sites of chiasmata through their role in cross-over resolution (Jackson et al., 2006; Lhuissier et al., 2007).

Given the results of this thesis suggest homoeologous chromosome interactions that occur in the absence of *Ph1* are at least partially the result of increased expression of *TaASY1*, would transgenic wheat plants that over-express *TaASY1* also display homoeologous chromosome interactions? If indeed over-expression of *TaASY1* does promote interactions between homoeologues as well as homologues, it would be reasonable to assume that a major function of *Ph1* is to control the activity of *TaASY1*.

5.2.3 – Further analysis of *Ph1*

Based on the elevated expression of *TaASY1* in *ph1b*, it was concluded that *Ph1* has a gene regulatory role. Analysis of three other meiotic candidate genes, *RAD51A*, *RAD51B* and *MSH4* indicated that the increased levels of *TaASY1* transcripts are not representative of a global up-regulation of meiotic genes in *ph1b*. Having said this, it is too premature to conclude *TaASY1* is the only gene whose activity is affected by the absence of *Ph1*. Therefore, one area of future work with *Ph1* is to investigate the expression of a whole suite of meiotic candidate genes in *ph1b* to determine whether this locus regulates the activity of other candidates (particularly those that a have role in chromosome pairing). Similarly, it would also be interesting to investigate the localisation of other meiotic proteins in *ph1b*. One protein to target is ZYP1, as it has been shown that ZYP1 closely aligns with ASY1 along meiotic chromosomes (Higgins et al., 2005; Mikhailova et al., 2006). Furthermore, it has been shown that while there is a reduction in recombination in Arabidopsis plants that are deficient for ZYP1, there are a number of crossovers that occur between non-homologous chromosomes, indicating that ZYP1 may also have a role in homology searching (Higgins et al., 2005; Martinez-Perez and Moore, 2008).

Recently it has been shown that deletion of *Ph1* causes an increase in the activity of the wheat *Cdk*-like genes, which suggests that an immediate function of this locus is to control the

expression of the *Cdk*-like genes (Al Kaff et al., 2007). However, while it has been shown through studies in mice that deletion of *Cdk2* causes defects in chromosome pairing and synapsis, no studies have yet been performed in plants to observe the effect that deletion of the *Cdk*-like genes would have on meiosis (Ortega et al., 2003). It would therefore be interesting, if even in a diploid plant such as Arabidopsis or *Brachypodium*, to investigate the effect that deletion of the *Cdk2* homologue would have on chromosome pairing and synapsis.

5.2.4 – The bigger picture

The long term objective of meiotic research in bread wheat is to understand the molecular mechanisms that control homologous chromosome pairing. While this research may appear purely fundamental, it has some very practical outcomes. It has been well documented that our modern cultivars of tetraploid and hexaploid wheat would benefit from the ability to capture genetic diversity that exists amongst wild-relatives of wheat (Able et al., 2007; Martinez-Perez and Moore, 2008). An ability to access this genetic variation would help advance the performance of our modern cultivars by improving their ability to diversify and adapt to adverse conditions. This has important implications as it would ensure that there would be a growing food supply for the continually increasing world population (Able and Langridge, 2006; Able et al., 2007). At present, there are a number of reproductive barriers that prevent this genetic variation from being accessed, and one of the biggest barriers is the suppression of interactions between closely related homoeologous chromosomes (Sears, 1977).

Fundamentally, the method in which wheat breeders could tap into the genetic diversity that exists within the *Triticum* genus is through recombination. However, inter-specific hybrids that contain a haploid set of wheat and wild-relative chromosomes display low levels of pairing and recombination between the two sets of chromosomes (Martinez-Perez and Moore, 2008). Hence, there is a limited capacity to introduce genes that infer

beneficial traits into the bread wheat genome. It has been suggested that the factors that limit the interactions between homoeologous chromosomes in the inter-specific hybrids are also those which suppress interactions between homoeologues during meiosis in wild-type bread wheat (Riley and Chapman, 1958; Sears, 1976; Martinez-Perez and Moore, 2008). Therefore, by identifying the mechanism that controls chromosome pairing in bread wheat, it may be possible to manipulate this process so that homoeologues can interact in inter-specific hybrids to facilitate more frequent introgression of beneficial genes. Importantly, the results from this study suggest that *TaASY1* in involved in this process, and furthermore, that by altering the levels of *TaASY1* expression, it may be possible to manipulate the extent of homoeologous chromosome interactions.